M Ű E G Y E T E M 1 7 8 2

Queueing problems for IP networks

PhD dissertation

Department of Computer Science and Information Theory,
Faculty of Electrical Engineering and Informatics,
Budapest University of Technology and Economics

Supervisor: László Győrfi

Tamás Éltető

Budapest, 2006

Katának kitartásáért

Contents

Chapter 1

Introduction

Queueing theory has been attracting research interest for a long time. The first paper in queueing theory was written by A. K. Erlang in 1909 on the traffic in a telephone exchange. The term ”queueing system“ was probably first used by Kendall in 1951. The field has begun an enormous development in the second half of the 20^{th} century. It is difficult to give a detailed history of queueing theory and it is even demanding to collect a short summary of the main achievements. Let us mention some milestones with the lack of completeness.

Lindley [36] formulated in 1952 the basic relation describing the queue length and waiting time in single server queues. Kendall [30] in 1953 introduced the notation A/B/C for queueing systems. An interesing result by Smith [57] from 1953 is that exponential tail exists both for the queue length and the waiting time for the G/G/1 using some weak conditions on the service-time distribution. The knowledge of the asymptotical behaviour of a queueing system might be insufficient in case of practical problems where measure of interest is e.g. the average. Little [37] in 1961 showed a suprisingly simple and general relation between the average waiting time, the average arrival rate and the average number of customers in a queueing system known today as Little's law. Benes [8] in 1963 gave a formula relating the probability distribution of the queue length to the arrival process. Takács [59] in 1969 showed that in a stationary M/G/∞ system the number of customers in the system has Poisson distribution that depends on the average arrival rate and average holding time of the calls, but it does not depend on higher moments of the holding time distribution. This result explains the robustness of Erlang's result. Reiser and Lavenberg [51] in 1980 published the Mean Value Analysis (MVA) algorithm for treating closed-queueing networks. The nice numerical features of MVA made it a popular tool. Neuts [42] in 1981 introduced the matrix analytic methods that have been proven to be extremely useful for the numerical treatment of queueing systems. Wolff [63] in 1982 popularised the principle that the state of a stationary queueing system sampled according to a Poisson process is the same as the state of the queueing system at an arbitrary time (PASTA).

The results of queueing theory find straightforward applications in the telecommunication industry. In this work the main object of interest is the application of queueing theory and statistics to the traffic analysis and modelling of the Internet. As we know, the history of the Internet began in 1969 when four unversities were connected into a packet switched network called ARPANET. This was originally a military initiative and its early development was influenced by defence requirements leading to a robust design. Since then, the Internet has been a success story thanks to its fortunate principles from the origin. The most important of these might be the end-to-end principle. In simple words this states, that the communicating hosts should be intelligent and the transport network has to provide only the basic service of delivering the packets to the receivers.

Although the service that the transport network provides is simple, the design and effective operation of it is not. This is because the traffic is the result of a complex interaction of intelligent protocols and user behaviour. The significance of understanding the network is underlined by the constant need for more efficient design and operation. The cognition of the Internet traffic began together with the Internet itself (Jackson and Stubbs [27] 1969). On one hand, the statistical description of the Internet traffic by measurement analysis has been a popular research topic. On the other hand, a lot of attempts were made to develop models leading to methods that predict the network performance.

Recently a consensus has been reached concerning the statistical properties of the Internet traffic. Long-range dependence and self-similarity were found in the time series of the traffic performance descriptors. Borella and Brewster [13], Borella et al. [12] investigate packet delay but there are many other similar conclusions regarding the traffic volume and others. However, all of these results implicitly assume that the time series are stationary. Though attempts were made to inspect the validity of this assumption, the methods that were used for this can be improved and this work contributes to these attempts.

The TCP (Transmission Control Protocol, see Stevens [56]) is one of the core protocols of the Internet Protocol suite. TCP defines two way, connection oriented data transfer between two communicating parties. TCP guarantees reliable, in order packet delivery to the sender application. When a TCP implementation sends packets, it constantly measures the network conditions and adapts its traffic in order to maximise its bandwidth share in the network.

Numerous models have been established with the goal of predicting the performance of TCP data transfers in various network scenarios (to mention a few: Mathis et al. [40], Padhye et al. [45], Alessio et al. [1], Ben Fredj et al. [21], Heyman et al. [25]). All models have their assumptions on the network topology and traffic conditions. An issue that can be raised regarding traffic modelling is the tradeoff between the complexity and possibly narrow scope of a model that might lead to very good predictions versus simpler models with broader scope together with larger error tolerance. This work contributes to the second direction of modelling efforts because this way has the promise of widening the comprehension of TCP traffic in practical situations using as few restrictions as possible.

The network performance is characterised by e.g. the queue length, queueing delay, connection throughput. These are the main descriptors of interest in this work. My goal is to predict either their averages or the probability distributions using effective numerical methods. For this reason, I follow Markovian approaches. In fact, I mostly use matrix-analytic methods, which are concerned about the numerical computation of stationary and transient distributions of structured Markov chains. Thanks to the fact that issues on computational complexity often rise in matrix-analytic theory, this goal can be achieved for many practical problems. Moreover, tools of Markovian traffic modelling can represent remarkably complex traffic behaviour that is greatly exploited in this work.

1.1 Overview of the Theses

Stationarity is an important assumption in measurement analysis and traffic modelling. In simple words, a data series is regarded to be stationary if the characteristics of the series do not change over time. The traffic in today's telecommunication networks has strong daily pattern implying non stationarity on a daily basis. Partly because of this, most models attempt to describe the traffic in the busy period, that is, the period of time when the network utilisation is the highest. This way the daily periodicity does not play a role in the measurement analysis and the busy period is usually considered to be stationary.

Previous studies on IP packet delay (Sanghi et al. in [55], Andrén et al. in [2] or Borella et al. in [12]) have found high variability and long-range dependence in the round-trip delay[1]. However, these conclusions heavily depend on the assumption of stationarity that should be validated. There is a lot of results available on the statistical analysis of time series with long-range dependent correlations. This is because such issues arise e.g. for the water level of rivers or other environmental factors in order to predict and prevent chatastrophes. A typical approach is to look for points where the characteristics of the time series suddenly change. For example, change-point detection methods were used to detect the change in the level of the river Nile around the construction of the first Aswan dam in 1898 (e.g. Csörgő and Horváth [18]). In Thesis 1, I propose a change-point detection method motivated partly by the method of Csörgő and Horváth [18]. I apply my proposed method for validating stationarity in round-trip delay measurements and in Thesis 1 I perform and present further statistical analysis of the time series.

Although both the asymptotics (Smith [57]) and the average behaviour (Little [37]) of an M/G/1 queueing system are known for a long time, considerable research efforts have been made on more detailed system analysis. The numerical solution of M/G/1 systems using matrix geometric methods has already been presented (e.g. Baum [6], Meini [41] or Riska and Smirni [52]) but its applicability is hampered by possible existence of slowly decaying service time distributions. The problem of these approaches is that if the service time distribution is not bounded then the numerical solutions involve infinite summation at some point. The infinite summation should be truncated but this can lead to significant errors if the service time distribution has e.g. polynomial decay as an example shows it in Thesis 2. For this reason, the computational complexity of the existing solutions does not scale well in such cases. However with some restrictions on the service time distribution, Thesis 2 proposes a solution method involving finite summation and nice scalability even for slowly decaying queue lengths.

Thesis 2 proposes a numerical analysis method for solving a particular M/G/1 queueing problem: the BMAP/PH/1 (BMAP - Batch Markovian Arrival Process, PH - Phase-type service) queue. The scope of the BMAP/PH/1 queue is considerably wide since it covers correlated arrival patterns allowing for batch arrivals, and the class of the service time distributions is quite flexible as well. For this reason, the results of Thesis 2 can be applied for building traffic models of the Internet.

The first paper in queueing theory dealt with the modelling of calls in a telephone exchange. The original problem was leading to the stationary distribution of an infinite

[1] The time it takes for an echo request to travel from a sender to a receiver and for a reply to travel in the reverse direction.

server queue with Poisson arrival and exponential holding time, that is an M/M/∞ system. Takács [59] showed that the stationary distribution of an M/G/∞ system is the same as of an M/M/∞ queue with the same arrival rate and average holding time. However, there are practical examples where the arrival is not a Poisson process. The MAP (and BMAP) can handle considerably general point processes (Asmussen [5]). Interestingly, the average number of customers in a MAP/G/∞ system is still insensitive – i.e. it depends solely on the average arrival rate and average holding time according to Little's result [37] – but the distribution is not.

Effective analytical formulae have been developed for the moments in a BMAP/PH/∞ system (see Masuyama and Takine [39]), but it is difficult to obtain the distribution from the moments (Rácz et al. [49]). Thesis 3 shows that the distribution of MAP/G/∞ system can also be obtained effectively using numerical methods. Furthermore, Thesis 3 shows that the analytical tractability of the moments of a MAP/PH/∞ system can be extended to a wider class of holding time distributions, expanding in this way the existing result of Masuyama and Takine [39]. As an application of the methodology, I explore the sensitivity of the distribution of the number of customers when the arrival model changes.

The performance of TCP/IP networks has been studied by the analysis of measurements in real networks and by theoretical models. A major effort was put in describing the TCP traffic by theoretical tools. Since the TCP adapts its sending rate to the network conditions it is a fascinating research task to find formulae that calculate the throughput given different network scenarios (just a few examples are Cardwell [17], Arvidsson and Krzesinski [4], Roughan et al. [53], Heyman et al. [25] or Ben Fredj et al. [21]). A common feature of the avaliable models is that their performance predictions are good in one case, but the goodness of the predictions is unknown in other cases. In my view, there is a need to have an understanding of the important factors that contribute in the network performance. This way, the quaility of the various predictions can be evaluated in a broader sense. One step towards this understanding is to establish a traffic modelling framework that is free of restrictions on the network conditions as much as possible.

The intention of Thesis 4 on one hand is to find simple approximate predictions instead of having a complex but exact calculation. I show an example where some performance descriptors of a simulated TCP/IP network are predicted using simplifications and the predictions are compared to the exact results. The proposed modelling framework collects ideas from different previous works, to particularly mention the model of Heyman et al. [25]. On the other hand, the modelling structure is motivated by the recognition of important factors of the TCP traffic, therefore Thesis 4 bestows a small piece to the understanding of the Internet traffic.

1.2 Research objectives

The main research objective was to find general models for single server and infinite server queueing systems. The results were applied in the analysis of the Internet traffic, putting special emphasis on the dynamics of the TCP/IP traffic.

The following four bullets summarise the objectives of the Theses.

- Measure and analyse the round-trip delay in IP networks. Establish and validate a model that describe the measurement results. (**Thesis 1**)

- Develop analytic results on finite server queueing systems with batch arrivals. Apply the analytic results in the case of TCP/IP traffic. (**Thesis 2**)
- Develop results on infinite server queueing systems with non-Poissonian arrivals and general holding times. (**Thesis 3**)
- Investigate the behaviour of the TCP protocol, and give a framework that takes into account the adaptivity of the TCP traffic in the case when the number of TCP connections is changing in the system. (**Thesis 4**)

1.3 Methodology

During the measurement analysis I used statistical tools for distribution fitting and checking the goodness of fit. I used the theory of matrix-analytic methods in the description of finite and infinite server queueing systems. The proposed models are validated numerically and by simulations.

1.4 List of abbreviations

ACF Autocorrelation Function

ATM Asyncronous Transfer Mode

BCMP Basket, Chandy, Muntaz, and Palacios

BMAP Batch Markov Arrival Process

CTMC Continuous-Time Markov Process

DPH Discrete Phase-type

FIFO First-In First-Out

GSM Global System for Mobile communications

HLR Home Location Register

HTTP Hypertext Transfer Protocol

IP Internet Protocol

LAN Local Area Network

MAP Markov Arrival Process

MBAC Measurement-Based Admission Control

MMPP Markov-Modulated Poisson Process

MVA Mean-Value Analysis

MTU Maximum Transmission Unit

PH Phase-type distribution

QBD Quasi Birth-Death

RTT Round-Trip Time

TCP Transmission Control Protocol

VBR Variable Bit Rate

WAN Wide Area Network

WWW World-Wide Web

Chapter 2

Thesis 1: Measurement analysis of TCP traffic

2.1 Problem statement

As it was pointed out in the Introduction, the traffic modelling of IP networks should consider TCP because of its dominant role today. Indeed, we can observe the expanding application of the TCP/IP protocol suite in the last decade and the success of Internet can partly be explained by the excellent philosophy of this protocol suite (see e.g. Stevens [56]). The TCP provides a reliable transport layer service for many Internet applications including WWW, e-mail, news, etc. However, many drawbacks of this protocol suite have also arisen and several modifications have been developed in the recent years, just to mention some: TCP Tahoe, Reno, Vegas and Fast TCP (a summary is given by Fall et al. in [20]). In spite of the fact that there are many issues on the effective operation and management of TCP/IP networks, it seems to be one of the main technologies for the future. Therefore, there is a constant need for understanding the traffic produced by the TCP/IP protocols for teletraffic engineering of that type of networks as it is expressed by Paxson and Floyd in [48] or Thompson et al. in [60].

Thesis 1 is devoted to the measurement analysis of TCP traffic. More specifically, round-trip delay measurements are analysed and modelled. There are two major aspects mentioned below about why the round-trip delay characteristics are important for traffic modelling.

- The TCP protocol defines a feedback mechanism that determines the rate at which the sender emits new packets in the network. The mechanism is based on the packet loss and the round-trip delay measured by the connection. The understanding of the round-trip delay characteristics lead to a better understanding of TCP.

- Since the round-trip delay is strongly related to the queueing that develops in the network, its modelling can be useful in inferring knowledge on the current or expected status of the network.

Previous studies on IP packet delay like Sanghi et al. in [55], Andrén et al. in [2] or Borella et al. in [12] have found high variability of the delay process. Borella [12] measures round-trip delay in wide area networks, and using different empirical estimators finds that the measurements possess self-similar nature. In an early paper on round-trip delay, Sanghi et al. [55] present a high level analysis of round-trip delay and only a few details are presented on the statistical properties of the measurements. Andrén et al. [2] analyse one way delay with some emphasis taken on dealing with the clock skew of the measurer computers and esitmate the distribution and autocorrelation function of the packet losses and delays. The delay is modelled by a gamma distribution and the autocorrelation function is claimed to have polynomial decrease and therefore the self similar property of the round trip delay is also observed.

All of these results heavily rely on the assumed stationarity of their time series. However, for example in Borella [12], there cannot be found details concerning the analysis of stationarity and there is a lack of hypothesis tests giving a firm support for the conclusions of the paper. Andrén et al. [2] checked whether their measurements were stationary or not but the paper does not provide any details on this issue. Therefore, the first question addressed by Thesis 1 is that to what extent a round-trip delay is stationary.

There is a lot of results available on the statistical analysis of time series with long-range dependent correlations. A popular example of long-range dependent time series is the "Noah effect", that is the water level increases significantly and the new level remains for long time. Indeed, a frequent subject in times series analyses is the water level of the river Nile around the construction of the first Aswan dam in 1898. Csörgő and Horváth [18] proposes a change-point detection technique for analysing this time series. In Thesis 1, I propose a change-point detection method motivated partly by the method of Csörgő and Horváth [18]. An important difference between the two methods is that Csörgő's method is designed to find one change-point in a relatively short interval while my goal is to find many change points in a long time series. I apply my proposed method for validating stationarity in round-trip delay measurements.

Since the use of round-trip delay measurements as indicators of the network congestion was pointed out above, the next step is to perform further statistical analysis of the delay series provided that the stationarity assumption holds. The second objective of Thesis 1 is to fit a parametric model to the stationary distribution of the round-trip delay. Besides the possibility of having a compact description of the delay series offered by a parametric model, it also helps to answer the third question of Thesis 1, whether it is possible to classify the network state based on the distribution analysis.

2.2 Results

The results are published in [C1].

Thesis 1

In Thesis 1 I show that the round-trip delay measurements I made consist of a series of stationary intervals. I construct an algorithm for detecting the endpoints of these intervals. I find a parametric model for the round-trip delay measurement and characterise the measured data using the parametric model. I evaluate the model's goodness of fit with statistical hypothesis tests. I model the round-trip delay distribution within a *stationary interval with a truncated normal distribution. I identify three main types of empirical distributions that I can fit the same parametric distribution family to.*

Thesis 1.1

The measurements (Figure 2.1) are modelled as a series of disjoint intervals, within which the delay series can be regarded as stationary. When an interval ends and a new interval starts the characteristics of the data change. I constructed an algorithm that detects the endpoints of the stationary intervals.

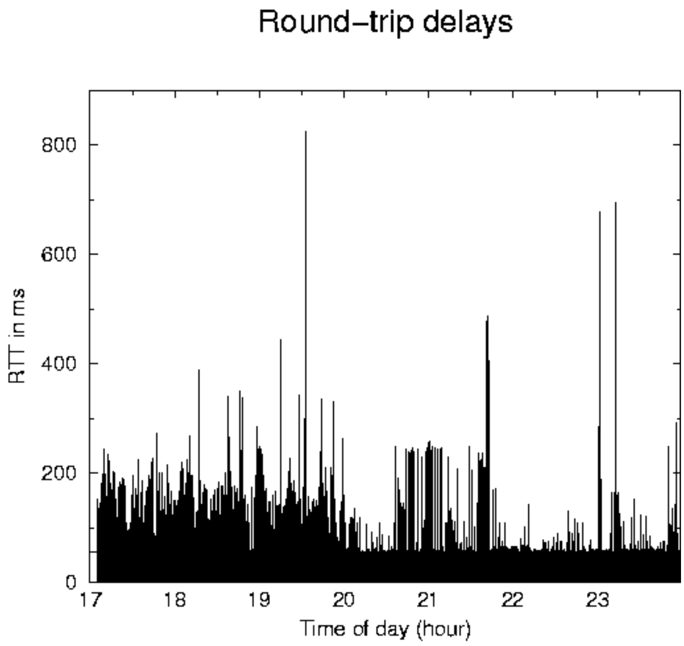

Figure 2.1: A measurement period of round-trip delays (ms/hours)

The stationary intervals are detected by a three-step method:

1. A change-point detection analysis is performed on a pair of two joint intervals of equal length of the delay series. The two intervals slide over the whole series resulting in an output series. This way, the edges of the stationary intervals can be determined. An example is shown in Figure 2.2.

2. A moving average is applied in order to discover trends within the intervals that are not highlighted by the change-point detection analysis.

3. The autocorrelation function (ACF) is investigated for discovering possible periodicities. Figure 2.3 shows an example ACF.

There were intervals where neither trends nor periodicities could be found. These were the subject of further analysis for parametric distribution fitting.

The input of the alogirthm is the series of the measured round-trip delays. An intermediate output of the algorithm is a series of values – I call it test series – that is used to

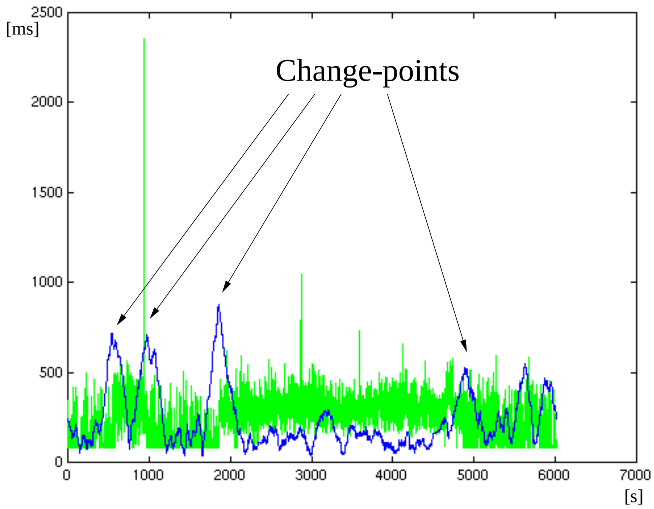

Figure 2.2: Result of the test (black) and the original data (grey) for a 6000 seconds period

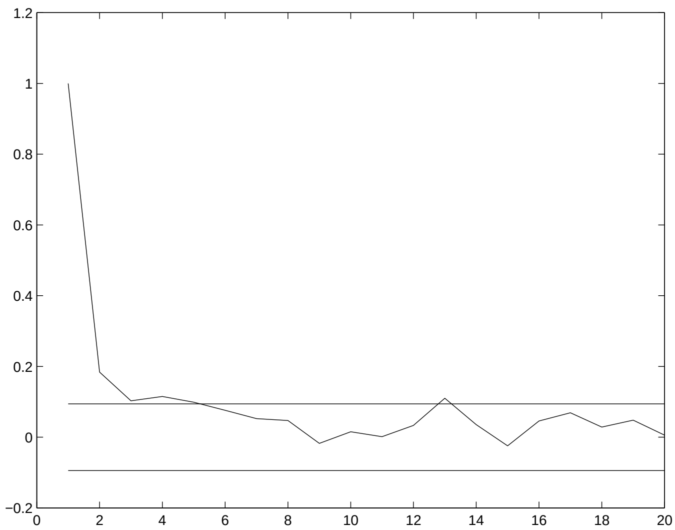

Figure 2.3: The estimated autocorrelation function of a calm period

detect the end points of a stationary interval. The values of the test series are calculated for every window position by the two sample Kolmogorov-Smirnov test comparing the empirical distribution of the first and second intervals. The final output of the algorithm is a set of intervals that are assumed to be stationary in the further analysis.

Thesis 1.2

I approximate the round-trip delay distribution within the stationary periods by a truncated normal distribution. I validate this by examining the quantile-quantile plot and by the Kolmogorov-Smirnov hypothesis test. I develop a parameter fitting procedure based on three sample statistics.

I formally define the truncated normal distribution in my model as follows. Assume a normally distributed random variable

$$Y \sim N(\mu, \sigma^2).$$

I generate a new random variable X from Y by setting

$$X = \begin{cases} c, & Y \le c \\ Y, & Y > c \end{cases},$$

with a constant c.

I estimate the parameters of the truncated normal distribution using the following parameter fitting procedure. c is the minimum of the measured samples. I estimate the quantile α of the truncation level by $\hat{\alpha}$ as the number of samples taking the minimum:

$$\hat{\alpha} = \sum_{i=1}^{N} \chi(X_i \le c). \tag{2.1}$$

I estimate the mean of the sample not taking the minimum $\mathrm{E}(X|X > c)$ by the censored sample average:

$$\mathrm{E}(X|X > c) \approx \frac{1}{|\{1 \le i \le N : X_i > c\}|} \sum_{i=1}^{N} X_i \chi(X_i > c). \tag{2.2}$$

The estimators for the mean and variance of the normal distribution before truncation are $\hat{\mu}$, and $\hat{\sigma}$.

$$\hat{\mu} = c - \hat{\sigma}\Phi^{-1}(\hat{\alpha}), \tag{2.3}$$

and

$$\hat{\sigma} = \frac{\mathrm{E}(X|X > c) - c}{a - \Phi^{-1}(\hat{\alpha})}, \tag{2.4}$$

where a is defined as

$$a = \frac{1}{\sqrt{2\pi}(1 - \hat{\alpha})} e^{-\frac{(c-\mu)^2}{2\sigma^2}} = \frac{1}{\sqrt{2\pi}(1 - \hat{\alpha})} e^{-\frac{\left(\Phi^{-1}(\hat{\alpha})\right)^2}{2}}, \tag{2.5}$$

depending on $\hat{\alpha}$ only and $\Phi(\cdot)$ function denotes the standard normal cumulative distribution function.

Thesis 1.3

By investigating the quantile functions of the data in different intervals, I use the delay measurements as indicators of network congestion. I identify three main types of quantile functions related to the rare, medium and busy traffic activities (Figures 2.4,2.5,2.6).

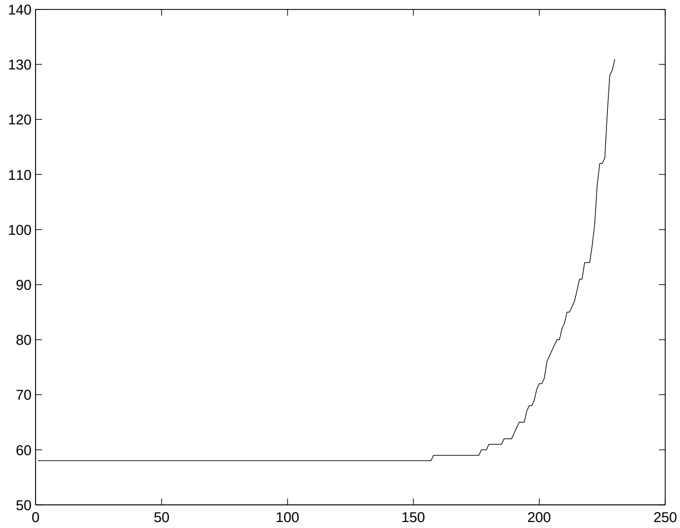

Figure 2.4: The quantile functions of the rare periods

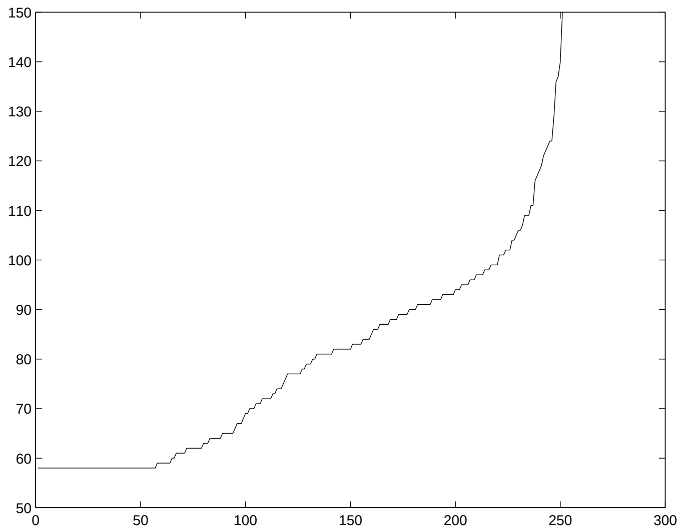

Figure 2.5: The quantile functions of the medium periods

2.3 Discussion

The change-point detection methods investigate time series for locations where the statistical properties of the data suddenly change. A change-point can be a sudden change in the mean or the variance of the measured data. In these cases it might be enough to check e.g. the moving average and locate the change-point according to the increase in the mean. However, a moving average is in fact a lowpass filter, that is, a sudden change turns into a gradual increase. There are two important requirements for a change-point detection method:

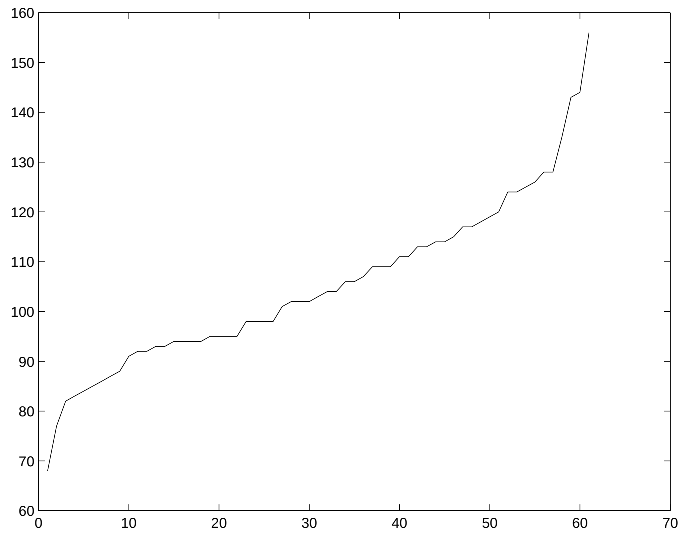

Figure 2.6: The quantile functions of the busy periods

- It should not work like a lowpass filter,
- the form of change in the data is unknown therefore it should be sensitive to any change in the distribution.

Since the goal is to study the statistical properties of the round-trip delay it is desirable not to affect the study with a-priori assumptions. The change is not necessarily occur in the form of shift in mean or variance. The tool satisfying these requirements in my change-point detection analysis is based on the (two sample) Kolmogorov-Smirnov test (a detailed description can be found e.g. in the famous book of Kendall and Stewart [31]).

Let

$$X_1,\ X_2,\ \dots X_N$$

be the first sample (of length N), and

$$Y_1,\ Y_2,\ \dots Y_M$$

be the second sample and let $F_N(x)$ and $G_M(x)$ be the corresponding empirical distributions. Then the statistics is

$$D_{N,M} = \max_x |F_N(x) - G_M(x)|$$

According to the limit distribution theorem we have

$$\lim_{N,M\to\infty} P\left(\sqrt{\frac{NM}{N+M}} D_{N,M} < y\right) = K(y), \quad 0 < y < \infty,$$

where $K(y)$ is the Kolmogorov distribution.

Assume that $N = M$. In this case $D_{N,N}$ is computed practically in the following way. Denote $Z_i^{(2N)}$ the merged and ordered series:

$$Z_1^{(2N)} \leq Z_2^{(2N)} \leq \ldots \leq Z_{2N}^{(2N)}.$$

Let

$$\delta_i = \begin{cases} 1, \text{if } Z_i^{(2N)} \text{ comes from the series of } X_k \\ -1, \text{otherwise} \end{cases}$$

and

$$S_j = \delta_1 + \delta_2 + \ldots + \delta_j.$$

Here $D_{N,N}$ is obtained,

$$D_{N,N} = \frac{1}{2N} \max_{1 \leq j \leq 2N} |S_j|.$$

This method computes a distance between two empirical distributions. The value of $D_{N,N}$ is related to the difference between the originating distributions, that is, the larger its value is, the larger the difference is.

The goal is to find the intervals where the distribution does not change (Csörgő and Horváth [18]). In order to determine these intervals the empirical distribution of two neighbouring time windows is compared and these two windows slide together along the series. In this way another series is defined that is referred to as test-series. (The comparison was done by Kolmogorov-Smirnov test of the subsamples.) The edges of an interval are marked by values in the test-series, which are much more significant than their neighbourhood.

Since the inverse distribution function is monotone, it is enough to use the test series directly for determining the change-points.

The data was collected in the Ericsson Corporate Network between Budapest and Stockholm. The route contains a WAN X25 link and high speed LAN's. The destination addresses were at a distance of 5-7 hops. Practically, I had two LANs (10 Mbit/s Ethernet and 155 Mbit/s ATM) connected by a relatively slow link (768 Kbit/s). The buffer of the slow link could store approx. 100-150 packets while the packet size was 1500 bytes.

I used the PING program for measuring the packet round-trip time. The PING program sends echo requests to a computer in equal time intervals. In my measurements it was set to one second. The reliability of the measurements depends on the reliability of the computer's system clock. The range of the measurements was in the order of hundreds of milliseconds, the system clock provided enough accuracy for further analysis.

Figure 2.2 shows periods that can be candidates for fitting parametric distributions. The scale in Figure 2.2 is valid for the measured data. In this case the length of the sampling intervals was 250 samples. (Note, that the resulting test-series was rescaled in order to be able to depict the two series in the same plot.)

Figure 2.7 shows a shorter interval, which is less than twice as long as the sampling window. Figure 2.8 shows another case where when the window size equals the interval length.

Fortunately, the sharp edges can be recognised here as well. This is perhaps because the distribution changes suddenly, and the distributions remain approximately constant on

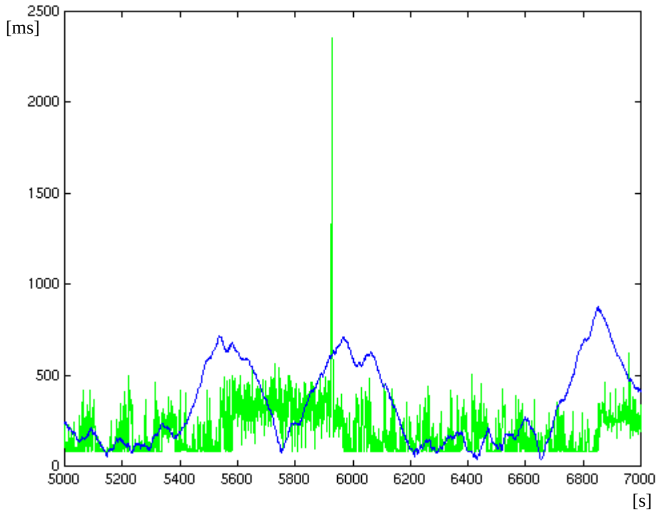

Figure 2.7: Result of the test and the original data for a 5000-seconds period

both sides of the edges. Of course, if a period is much longer than the sampling length one can observe the edges quite clearly.

With the assumptions mentioned above, a possible change-point detection method is quite straightforward as it is based on detecting local maxima. Two change-points may bound an interval if the length of the interval is greater or equal to the length of the window.

This algorithm was applied to find a model with parametric probability distribution. A trend analysis was performed based on the method of moving averages to reveal the presence of long trends in the intervals which may ruin the stationarity assumption.

In the following, the methods being used to fit parametric distributions to the data in the identified intervals are presented.

Parzen in [46] advises to use the quantile functions and density quantile functions in addition to the empirical distribution function.

The quantile function

$$Q(u),\ 0 \leq u \leq 1$$

is defined as follows: for a general distribution function $F(x)$ which is continuous from right,

$$Q(u) = F^{-1}(u) = \inf\,(x:\ F(x) \geq u).$$

For $-\infty < x < \infty$ and $0 < u < 1$

$$F(x) \geq u \quad \leftrightarrow \quad Q(u) \leq x.$$

Denote by $\hat{F}(\cdot)$ the empirical distribution function. Then denote by $\hat{Q}(\cdot)$ the empirical quantile function, which is:

$$\hat{Q}(u) = \inf\,(x:\ \hat{F}(x) \geq u).$$

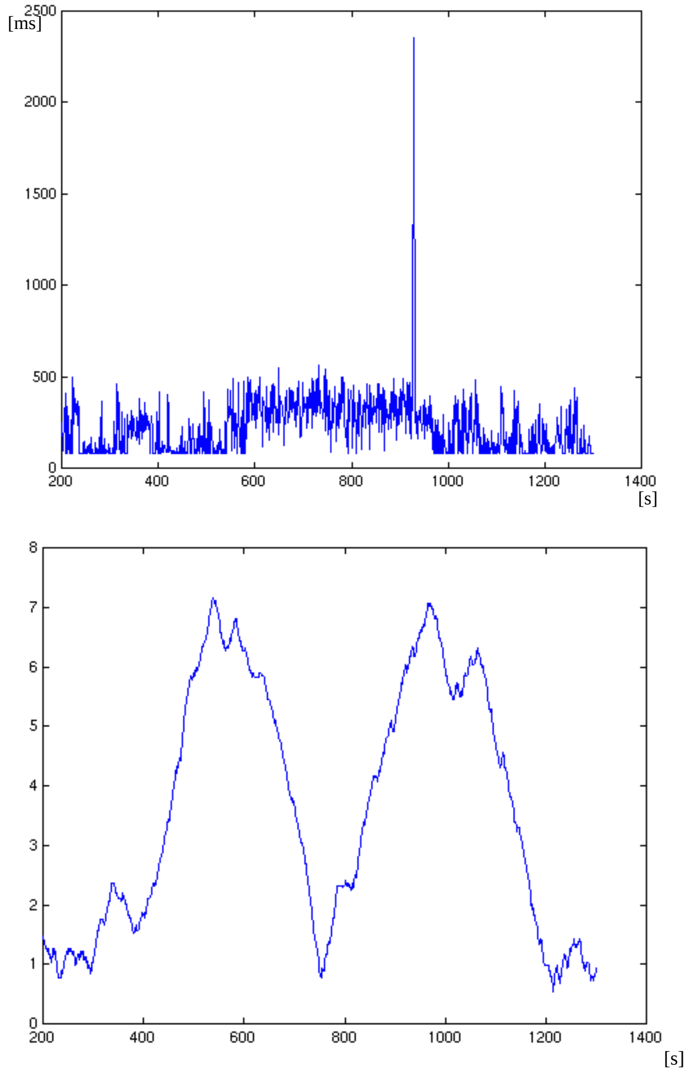

Figure 2.8: Result of the test and the original data for a 1000-seconds period

This is a piecewise constant function whose values are the ordered statistics:

$$\hat{Q}(u) = X_{(j)} \quad \text{for}$$

$$(j-1)/n < u \leq j/n, j = 1, \ldots, n$$

where $X_{(i)}$ is the i^{th} value of the ordered sample:

$$X_{(1)} < X_{(2)} < \ldots < X_{(n)}.$$

Of course, $\hat{Q}(0)$ is the sample minimum.

The minimum of the a daily series was 64 ms. In fact, it is the propagation delay, that is, it takes 64 milliseconds to have the packet sent, for it to arrive, and delivered back to us without any queueing. Three main types of histograms could have been identified, that are outlined in Figure 2.9.

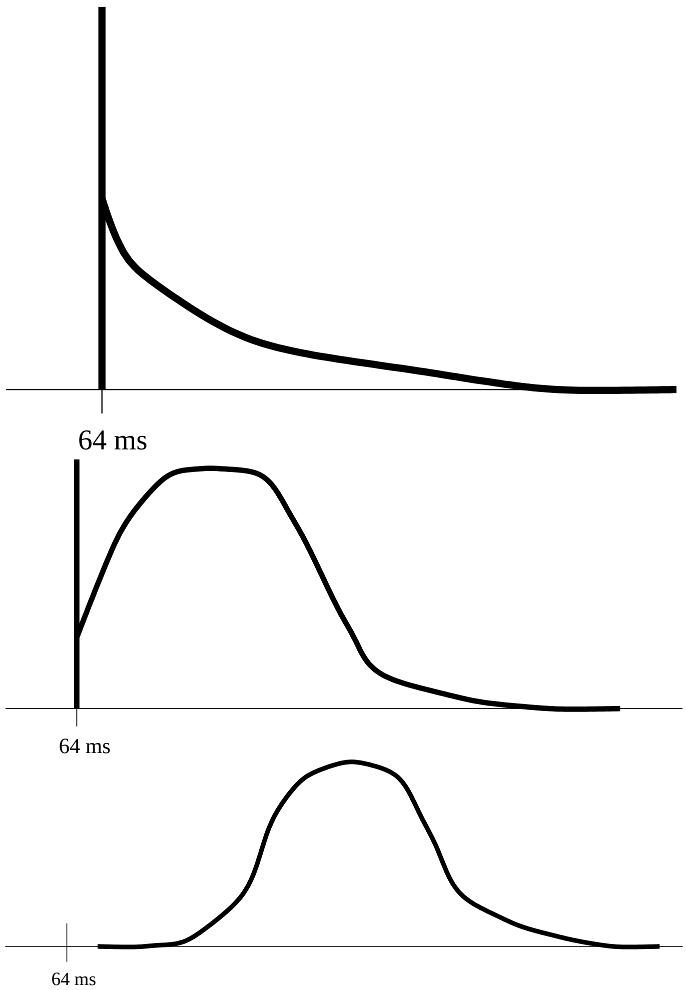

Figure 2.9: Roughly outlined histograms of the rare, medium, and busy periods

As Figure 2.9 shows, the all three distributions are bounded below at the propagation delay. In the rare periods, there is a strong weight at this point and there is a fast decay above 64 ms. For the medium period, there is also a weight at the minimum, but comparable number of samples fall in the above regions as well. The range of the distribution in busy periods is well above 64 ms, that is, the lower bound is practically not observable.

The symmetric, bell-shaped appearance of the histogram in busy periods suggests normality in Figure 2.10.

My opinion is that these shapes arise as a result of the central limit theorem applied to the sum of TCP flows which can cause normally distributed queueing delays in network buffers.

Next, the estimation procedure obtaining the parameters of a truncated normal distribution is presented together with its validation.

I estimate the parameters μ, σ and c. Obviously c would be the lowest measured value, and μ and σ are obtained in the following way.

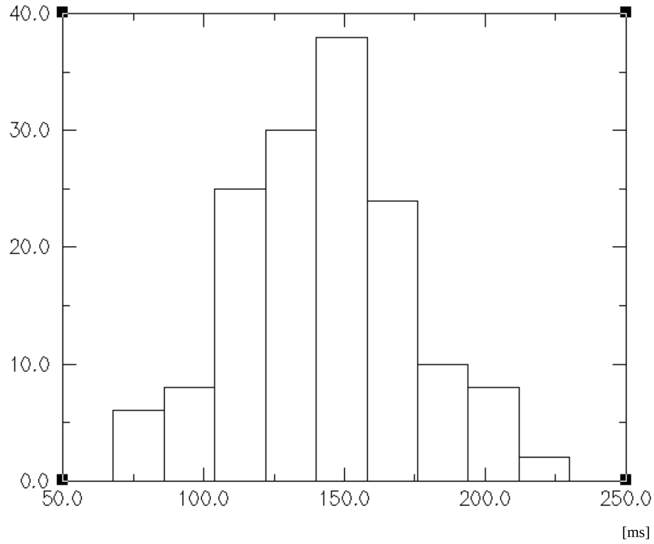

Figure 2.10: The histogram of the busy period

Let the quantile be α such that

$$\alpha = \Phi(\frac{c-\mu}{\sigma}), \tag{2.6}$$

here the function $\Phi(\cdot)$ denotes the standard normal distribution function.

Again I assume that the originating distribution is $\mathrm{Normal}(\mu, \sigma^2)$.

$$\mathrm{E}(X|X>c) = \int_c^{+\infty} t\frac{1}{\sqrt{2\pi}\sigma(1-\alpha)}e^{-\frac{(t-\mu)^2}{2\sigma^2}}\,dt = \frac{1}{1-\alpha}\int_{\frac{c-\mu}{\sigma}}^{+\infty}(\sigma u+\mu)\frac{1}{\sqrt{2\pi}}e^{-\frac{u^2}{2}}\,du$$

$$= \frac{\sigma}{1-\alpha}\int_{\frac{c-\mu}{\sigma}}^{+\infty} u\frac{1}{\sqrt{2\pi}}e^{-\frac{u^2}{2}}\,du \;+\frac{\mu}{1-\alpha}\int_{\frac{c-\mu}{\sigma}}^{+\infty}\frac{1}{\sqrt{2\pi}}e^{-\frac{u^2}{2}}\,du = \frac{\sigma}{1-\alpha}\frac{1}{\sqrt{2\pi}}e^{-\frac{(c-\mu)^2}{2\sigma^2}}$$

$$+\frac{\mu}{1-\alpha}\left(1-\Phi(\frac{c-\mu}{\sigma})\right). \tag{2.7}$$

From (2.5) and (2.7) I get (2.3).

For the validation of my model I used two statistical tools.

- Quantile-quantile plot,
- Kolmogorov-Smirnov test.

In the following I give a short outline of both methods.

Q-Q plot is a clear graphic but not that exact way of comparing the empirical distributions of two samples. There is a function $q_{(X_1,\ldots),(Y_1,\ldots)}(\cdot)$ such that

$$q_{(X_1,\ldots),(Y_1,\ldots)} : \mathbb{R} \to \mathbb{R}.$$

If the graph of this function fits the graph of the $u(x) = x$ function well, then the two distributions are quite similar. Define the $q(\cdot)$ function as follows.

Consider $Q_X(u)$ the estimated quantile function from the sample

$$X_1,\, X_2,\, \ldots\, X_m$$

and $Q_Y(u)$ from the sample

$$Y_1,\, Y_2,\, \ldots\, Y_n.$$

Now let $q(\cdot)$ be the following

$$q(Q_X(u)) = Q_Y(u),$$

that is

$$q(x) = Q_Y(F_X^*(x)), \tag{2.8}$$

where

$$F_X^*(x) = \frac{1}{m}\sum_{i=1}^{m}\chi(X_i \leq x).$$

For the sake of good visibility, one should evaluate less or an equal number of α's than the minimum of m and n, and use rather identical increments of α.

In order to show that the assumptions about the quantile functions and the histograms of the periods hold, I plot the quantile-quantile plot of the measured data and the fitted distributions. The results for the busy and medium periods are shown in Figure 2.11. Since both case fits well to the $y = x$ function one can conclude that the visual validation accepts the proposed parametric models.

The one-sample Kolmogorov-Smirnov test with normal distribution is a very sensitive and reliable hypothesis test. The method is almost the same as it was outlined in the change-point analysis part.

Since the goal here is to test a sample for normal distribution, a period had to be choosen with busy traffic activities in the network because only stationary intervals during this time miss the observation of a lower bound (the propagation delay).

The results are given in Table 2.3. The meaning of the value for the asymptotical significance could be understood as follows. A random sample gives a random value for the asymptotical significance in the Kolmogorov-Smirnov test. If the null hypothesis is true then the asymptotical significance has uniform distribution in [0,1). Therefore, my acceptance or rejection of the null hypothesis depends on the decision I make whether a random sample from uniform distribution could be e.g. 0.198 (Table 2.3) or not. However, the Kolmogorov-Smirnov test is very sensitive to small deviations in the distribution given $N = 543$ samples, therefore I think the hypothesis of normality of the sample providing such test result can be accepted.

The autocorrelation function of the "calm" intervals was also estimated. As it can be seen in Figure 2.3 the estimation shows independence at longer lags, but suggests dependence within four or five lags, that is, the packet delays are correlated within five seconds. I believe that this correlation is an artifact of the nonstationarity because of two reasons:

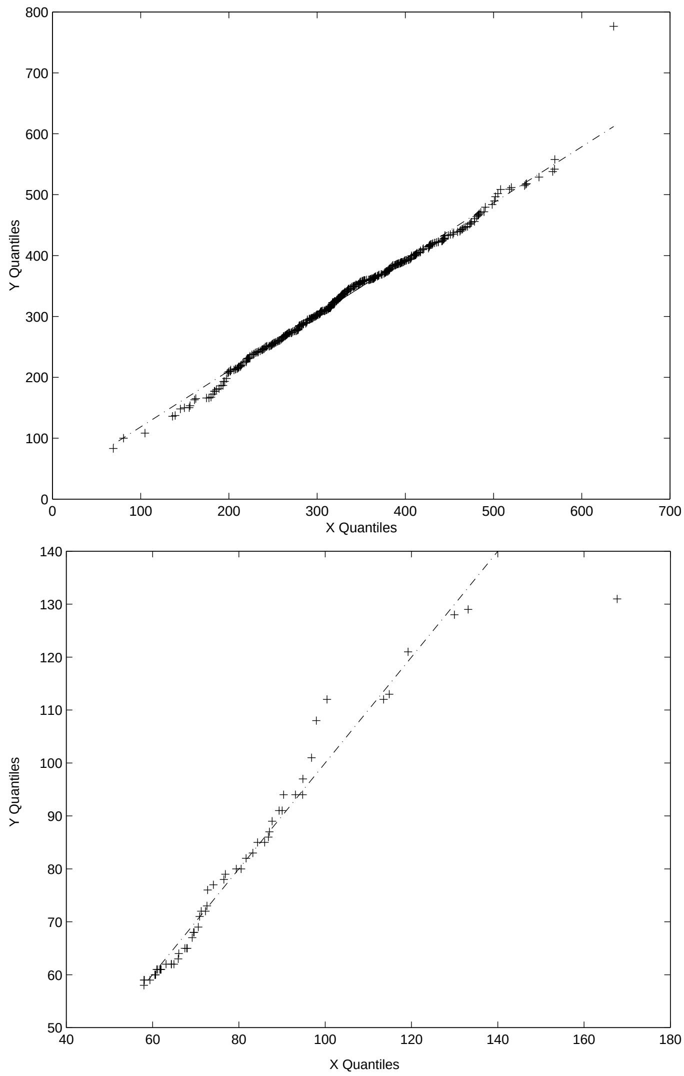

Figure 2.11: Q-Q plot with an estimated normal, and truncated normal distribution

- There must be no recognizable dependence between samples of queue length on a rate of several seconds, because the queues in the network change very quickly, and they may depend at most on 100-200ms past.
- If the series were stationary, the autocorrelation function of a smaller period of data would be the same and for example in Figure 2.12 this is not the case.

The estimated autocorrelation function of a series where the parameters have small changes or where the series has small trend may exhibit similar phenomena. I think that the problem is that I cannot find “entirely clear” periods.

Descriptive Statistics

	N	Average	Standard Deviation	Minimum	Maximum
X	543	332.94	91.12	83.00	1042.00

One-sample Kolmogorov-Smirnov test against normal distribution

Number of observations		543
Estimated Parameters	Mean	332.94
	Standard Deviation	91.12
Most Extreme Differences	Absolute	.046
	Positive	.046
	Negative	-.036
Kolmogorov-Smirnov Z		1.075
Asymptotic Significance	(2-tailed)	.198

Table 2.1: Results of Kolmogorov-Smirnov test

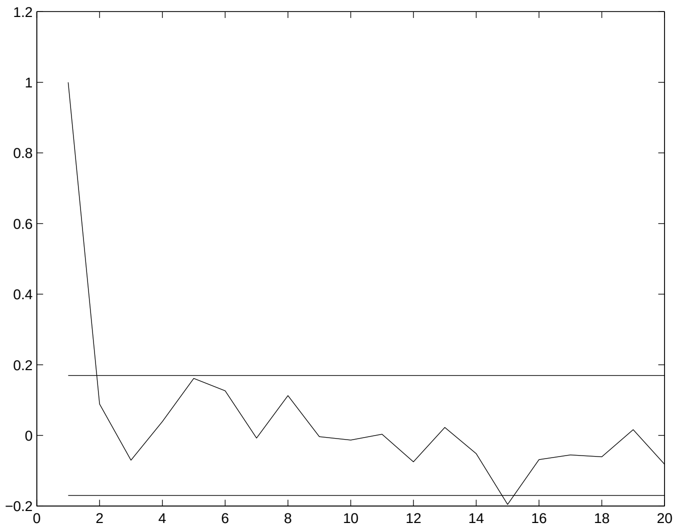

Figure 2.12: The estimated autocorrelation function of a short interval of a calm period

Chapter 3

Thesis 2: Solution of BMAP/PH/1 type queues

3.1 Problem statement

M/G/1 type Markov chains are studied for a long time (e.g. Neuts [43]). Many finite server queueing problems have been shown to lead to an M/G/1 type Markov chain (Neuts [43], Latouche and Ramaswami [34]). Such problems also arise in Thesis 4 because there is a need for analysing FIFO queues with correlated batch arrival process. Also, the need for solving a finite server queueing system leading to M/G/1 type problems is mentioned in Thesis 4.

The asymptotical behaviour of M/G/1 queues can be inferred using e.g. the result of Smith [57]. If one is more interested in the averages than in the asymptotics then a simple formula by Little [37] is available. However, when neither the knowledge of the asymptotics nor the average is satisfactory more in depth analysis of the queueing system is neccessary. Consider a finite queue where the probability of packet loss due to insufficient storage space is important. If the queue length is too short to reach the asymptotical region then the solution of the queueing system is needed.

Various solution methods were developed for the effective numerical computation of the steady state distribution of M/G/1 queues (e.g. Baum [6], Meini [41] or Riska and Smirni [52]). For an interested reader there is a survey of available methods, which can be found in a book by Bini et al. [10]. These methods evaluate the solution of an infinite order matrix equation or use infinite matrix summation. The main problem of the available solution methods is that there are cases when the solution is numerically infeasible. The reason for this is that the infinite order matrix equation or summation should be truncated in order to have it implemented in practice. If there are slowly varying components in the series then the truncation can introduce significant error in the final solution like for example to the numerical problems of approximating the mean of a Pareto distribution by finite summation (provided that mean is finite at all).

When there are existing but difficult solutions for a general problem it is quite natural to look for particular cases where the complex general solution can be simplified. One particular M/G/1 type queueing system is the BMAP/PH/1 queue (BMAP - Batch Markovian Arrival Process, PH - Phase-type distribution) because of its ”skip-free to the left“

property (Neuts [43]). The above mentioned methods handle arbitrary batch size distribution in the arrival process of a BMAP/PH/1 queue. An infinite order matrix equation occurs because the batch size distribution introduces a non-Markovian property to the system. However, there is always a hope that the equation becomes finite and the whole problem will be better tractable if a Markovian structure of the batch size distribution is assumed.

The main contribution of Thesis 2 is that it proposes to restrict the batch size distribution to the class of discrete PH distributions. The discrete PH distribution is defined as the number of steps until absorption in a discrete time Markov chain with an absorbing state. The Markovian structure of the PH distributions is obvious from their definition. Thesis 2 proves that the matrix equation describing the solution of the PHBMAP/PH/1 queue has indeed finite order thanks to this restriction. Moreover, Thesis 2 shows that a PHBMAP/PH/1 queue is in fact a QBD (Quasi Birth-Death) system therefore a huge set of effective numerical methods becomes available to handle the problem. There is an application example presented showing that restrictions like this also make it possible to study cases that cannot be explored by existing tools because of numerical difficulties.

I note that the restriction I propose is not necessarily a strong limitation. A general batch size distribution can be approximated arbitrarily well by a discrete PH distribution and in this way the proposed solution can provide estimates for general but so far practically intractable problems.

3.2 Results

The results are published in [J2, O1].

Thesis 2

In Thesis 2 I define the Batch Markov Arrival Processes (BMAP) with parametric batch size distribution. I give a solution for the stationary distribution of the BMAP/PH/1 queue by substituting an infinite order matrix equation with a finite one. I also show that the state space of the investigated Markov chain can be extended in order to obtain a simpler structure that can be analysed by traditional methods. I show an application example, where my proposed approach provides the only numerically feasible solution method.

Consider a discrete time Markov chain with $n+1$ states. Let 1 state be an absorbing state, that is, there is no transition leaving this state and let the other n states be transient states called phases. For the transient states, there is at least one outgoing transition from a transient state to another transient state and at a transition from at least one transient state to the absorbing state. An order n discrete Phase-type distribution is defined as the number of steps until this Markov process enters into the absorbing state.

I assume that the probability of start in the absorbing state is 0, that is, I define the initial probability vector over the transient states. Denote the initial probability vector by α and the transition probability matrix (between the transient states) by $\mathbf{T}$. The probabilities of a discrete Phase-type distribution can be determined by the following expression:

$$p(i) = Pr(\text{time to absorption} = i) = \alpha \mathbf{T}^{i-1} t = \alpha(\mathbf{T}^{i-1} - \mathbf{T}^{i})\mathbb{1},\ i \geq 1, \qquad (3.1)$$

where $\mathbb{1}$ is the row vector of ones, and the row vector t contains the transition probabilities from the phases to the absorbing state ($t = \mathbb{1} - \mathbf{T}\mathbb{1}$).

The BMAP (Batch Markovian Arrival Process) is a point process determined by a Markov chain. The states of the Markov chain are referred to as phases like in the case of the Phase-type distribution. The point process generates batch Poisson arrivals during the holding time of a phase. When the phase changes then the arrival process might generate batches too.

A Batch Markov Arrival Process is defined by the matrices $\mathbf{D_0}, \mathbf{D_1}, \mathbf{D_2}, \ldots$, which describe the phase transitions associated with $0, 1, 2, \ldots$ arrivals, respectively. The off-diagonal elements of matrices $\mathbf{D_0}, \mathbf{D_1}, \mathbf{D_2}, \ldots$ refer to the rates of phase changes. For matrices $\mathbf{D_1}, \mathbf{D_2}, \ldots$ these elements also refer to the rate of $1, 2, \ldots$ arrivals associated with phase change. On the other hand, the diagonal elements in $\mathbf{D_1}, \mathbf{D_2}, \ldots$ refer to the rates of $1, 2, \ldots$ arrivals when the phase does not change at an arrival instant. The diagonal of the $\mathbf{D_0}$ matrix contains negative elements so that the generator matrix of the phases, which is in fact $\mathbf{D} = \sum_{i \geq 0} \mathbf{D_i}$, is a stochastic matrix and the negative diagonals of $\mathbf{D_0}$ lead to zero row sums. Note, that the stochastical meaning of the diagonals of $\mathbf{D_0}$ is the negative reciprocal of the average time between arrivals and/or phase transitions.

Alternatively, the $\mathbf{D_1}, \mathbf{D_2}, \ldots$ matrices can be represented by a $\mathbf{D}_A$ matrix describing the occurrence of arrivals together with the associated phase transitions and a $\mathbf{P}(i)$ matrix whose elements define the distribution of the number of arrivals in an arrival instance:

$$\mathbf{D_A} = \sum_{i=1}^{\infty} \mathbf{D_i}, \quad P_{k\ell}(i) = \frac{[\mathbf{D_i}]_{k\ell}}{[\mathbf{D_A}]_{k\ell}} \quad \Longleftrightarrow \quad \mathbf{D_i} = \mathbf{D_A} \circ \mathbf{P}(i) \;,$$

where $\circ$ denotes the element-wise matrix multiplication (Hadamard or Schur product). I say that the BMAP has Phase-type distributed batch size (PHBMAP), if the $\mathbf{D}_i, i \geq 1$ matrices can be composed as

$$\mathbf{D_i} = \sum_{k=1}^{K} \mathbf{M_k} \, p_k(i), \tag{3.2}$$

where K is finite, $\mathbf{M_k}$ ($1 \leq k \leq K$) are non-negative matrices and $p_k(i)$ ($1 \leq k \leq K$) are probability mass functions of discrete Phase-type distributions. The alternative definition of BMAPs with matrices $\mathbf{D_A}$ and $\mathbf{P}(i)$ indicates that any general BMAP can be approximated with PHBMAP using an element-wise discrete Phase-type approximation of $\mathbf{P}(i)$. In the worst case, this approximation contains $K = |\mathbf{D_i}|^2$ Phase-type distributions, where $|\mathbf{D_i}|$ is the cardinality of the BMAP. Usually, the sparse structures of real life models result far smaller PHBMAP representations in practical applications (i.e., $K << |\mathbf{D_i}|^2$).

The generator of M/G/1 type Markov chains has the following regular block structure (for details see Neuts [43] or Latouche and Ramaswami [34]):

$$\mathbf{Q} = \begin{array}{|c|c|c|c|c|c|} \hline \mathbf{C'_0} & \mathbf{C'_1} & \mathbf{C'_2} & \mathbf{C'_3} & \mathbf{C'_4} & \dots \\ \hline \mathbf{C_0} & \mathbf{C_1} & \mathbf{C_2} & \mathbf{C_3} & \mathbf{C_4} & \dots \\ \hline & \mathbf{C_0} & \mathbf{C_1} & \mathbf{C_2} & \mathbf{C_3} & \dots \\ \hline & & \mathbf{C_0} & \mathbf{C_1} & \mathbf{C_2} & \dots \\ \hline & & & \ddots & \ddots & \ddots \\ \hline \end{array} . \tag{3.3}$$

$\mathbf{C_0}$ are the backward transitions, while $\mathbf{C_1}$ and $\mathbf{C'_0}$ are the local transitions.

An M/G/1 type Markov chain said to have PH distributed jumps if

$$\mathbf{C'_i} = \sum_{k=1}^{K'} \mathbf{M'_k}\, p'_k(i), i \geq 1$$

and

$$\mathbf{C_i} = \sum_{k=1}^{K} \mathbf{M_k}\, p_k(i-1), i \geq 2,$$

where K' and K are finite integers, $\mathbf{M'_k}$ $(1 \leq k \leq K')$ and $\mathbf{M_k}$ $(1 \leq k \leq K)$ are non-negative matrices of size $|\mathbf{C'_0}|\times|\mathbf{C'_0}|$ and $|\mathbf{C_0}|\times|\mathbf{C_0}|$, respectively, and $p'_k(i)$ $(1 \leq k \leq K')$ and $p_k(i)$ $(1 \leq k \leq K)$ are probability mass functions of discrete Phase-type distributions.

E.g., an infinite buffer, finite server queue with PHBMAP arrival and PH or MAP service results in an M/G/1 type Markov chain with PH distributed jumps.

Based on the same argument as for BMAPs, any general M/G/1 type Markov chain can be approximated with another M/G/1 type Markov chain with PH distributed jumps.

Consider matrix $\mathbf{G}$ satisfying the following matrix equation

$$0 = \mathbf{C_0} + \mathbf{C_1 G} + \mathbf{C_2 G}^2 + \ldots = \sum_{i=0}^{\infty} \mathbf{C_i G}^i . \tag{3.4}$$

The solution matrix $\mathbf{G}$ of this equation is used in the calculation of the stationary distribution of the Markov chain (3.3). However, this equation involves an infinite summation that can make the solution impossible. Moreover, the stationary distribution of the M/G/1 type Markov chain can also be calculated using infinite sums only.

Thesis 2.1

I show that an underlying structure in the coefficient matrices $\mathbf{C_0}$, $\mathbf{C_1}$, *etc. makes it possible to define an equivalent finite equation as I state in Theorem 1 below. I also show in Theorem 2 that introducing a PH structure for the* $\mathbf{C_i}$ *matrices makes it is possible to calculate the stationary distribution in a finite number of steps.*

Theorem 1. *If the M/G/1 type Markov chain has PH distributed jumps then (3.4) is eqivalent with the following finite order matrix equation:*

$$\mathbf{0} = \sum_{i=0}^{c} \mathbf{W_i}\, \mathbf{G}^i, \tag{3.5}$$

where $\mathbf{W_i}$ is a matrix of size $|\mathbf{C_0'}| \times |\mathbf{C_0'}|$ and it is calculated using the PH structure of the $\mathbf{C_i}$ matrices. A comparison of (3.4) and (3.5) shows that the presence of PH distributed jumps allows to reduce the infinite order matrix equation to a finite one.

Theorem 2. *The stationary distribution of the M/G/1 type process with PH distributed jumps can be calculated in a finite number of steps as*

$$\pi_i\Big(- \mathbf{C_1} - \mathbf{Z}(0)\, \mathbf{G}\Big) = \pi_0\, \mathbf{Z}'(i-1) + \sum_{\ell=1}^{i-1} \pi_\ell\, \mathbf{Z}(i-1-\ell)\ , \tag{3.6}$$

where

$$\pi_0 = \frac{1}{\pi_0^* \left(\mathbb{1} + \overline{\mathbf{Z}'}\, g\right)}\, \pi_0^*, \tag{3.7}$$

π_0^* is the solution of

$$\pi_0^*\Big(\mathbf{C_0'} + \mathbf{Z}'(0)\, \mathbf{G}\Big) = 0, \tag{3.8}$$

the column vector g is

$$g = \Big(- \mathbf{C_1} - \mathbf{Z}(0)\mathbf{G} - \overline{\mathbf{Z}}\Big)^{-1} \mathbb{1}\ , \tag{3.9}$$

$\mathbf{G}$ is given in (3.5) and matrices $\mathbf{Z}(n)$, $\mathbf{Z}'(n)$ and $\overline{\mathbf{Z}'}$ are defined as

$$\mathbf{Z}(n) = \sum_{j=0}^{\infty} \widehat{\alpha}\widehat{\mathbf{T}}^{n+j}\, \widehat{\mathbf{t}}\, \mathbf{G}^j = \sum_{j=0}^{\infty} \mathbf{C_{n+j+2}}\, \mathbf{G}^j\ ,$$

$$\mathbf{Z}'(n) = \sum_{j=0}^{\infty} \widehat{\alpha'}\widehat{\mathbf{T}'}^{n+j}\, \widehat{\mathbf{t}'}\, \mathbf{G}^j = \sum_{j=0}^{\infty} \mathbf{C'_{n+j+1}}\, \mathbf{G}^j\ ,$$

$$\overline{\mathbf{Z}} = \sum_{n=0}^{\infty} \mathbf{Z}(n), \text{ and } \overline{\mathbf{Z}'} = \sum_{n=0}^{\infty} \mathbf{Z}'(n).$$

The calculation of $\mathbf{Z}(n)$, $\mathbf{Z}'(n)$, $\overline{\mathbf{Z}}$ and $\overline{\mathbf{Z}'}$ in a finite number of steps is provided in the Discussion in Corollary 4. $\widehat{T}$ and $\widehat{T'}$ are the generator matrices of the PH jumps defined in (3.18).

Thesis 2.2

In Thesis 2.2 I show that by introducing additional states to the M/G/1 type Markov chain with Phase-type structure I obtain a considerably simpler block tridiagonal structure where the blocks around the diagonal are repeated in each block row as it is shown in (3.10). In Theorem 3 I give the relation between the solution of the extended state QBD *process and the original M/G/1 type Markov chain. I show an efficient way of introducing additional states that further improves the numerical performance of the method.*

The Markov chains with structure (3.10) are called QBD (Quasi Birth-Death) processes. The advantage of this structure is that it makes possible to use a number of numerically effective methods solving QBD processes to find a solution to the structured M/G/1 type Markov chain.

I define the state extension as follows. The phase process of the extended QBD is composed by 3 blocks see Figure 3.1 and Figure 3.2. Block 0 represents the phases of the original M/G/1 type process, block 1 and 2 are for describing the PH distributed upward transitions of the M/G/1 type process starting from level 0 and level i, $i > 0$, respectively.

The block structure of the extended QBD process is

$$\mathbf{Q}' = \begin{array}{|c|c|c|c|c|c|} \hline \mathbb{B} & \mathbb{A}_0 & & & & \\ \hline \mathbb{A}_2 & \mathbb{A}_1 & \mathbb{A}_0 & & & \\ \hline & \mathbb{A}_2 & \mathbb{A}_1 & \mathbb{A}_0 & & \\ \hline & & \mathbb{A}_2 & \mathbb{A}_1 & \mathbb{A}_0 & \\ \hline & & & \ddots & \ddots & \ddots \\ \hline \end{array} \quad , \tag{3.10}$$

where the definition of $\mathbb{B}$, $\mathbb{A}_0$, $\mathbb{A}_1$ and $\mathbb{A}_2$ is given in (3.16)-(3.17).

Let matrix $\mathbb{G}$ be the solution of the matrix equation

$$0 = \mathbb{A}_2 + \mathbb{A}_1\mathbb{G} + \mathbb{A}_0\mathbb{G}^2. \tag{3.11}$$

The stationary solution of the QBD (3.10) can be obtained as

$$0 = \pi'_{i-1}\mathbb{A}_0 + \pi'_i(\mathbb{A}_1 + \mathbb{A}_0\mathbb{G}),\ i \geq 1, \quad \text{and} \quad 0 = \pi'_0\mathbb{B} + \pi'_1\mathbb{A}_2. \tag{3.12}$$

Theorem 3. *The stationary distribution of the M/G/1 type Markov chain with PH distributed jumps (3.3) can be calculated from the stationary distribution of the enlarged, but finite phase QBD process (3.10) and Figure 3.1,3.2 as*

$$\pi_i = \frac{\pi'_{i,0}}{\sum_{k=0}^{\infty} \pi'_{k,0}}, \tag{3.13}$$

where π_i is the stationary distribution of the M/G/1 type Markov chain with PH distributed jumps (with generator $\mathbf{Q}$), π'_i is the stationary distribution of the enlarged QBD process (with generator $\mathbf{Q}'$) and $\pi'_{i,0}$ denotes the block 0 part of the π'_i vector.

Block 1 and 2 of the extended QBD process, defined in (3.18), is very redundant in practice since $\mathbf{M_k}$ and $\mathbf{M'_k}$ contain only some non-zero elements. For an effective implementation of the analysis method a compact representation is required.

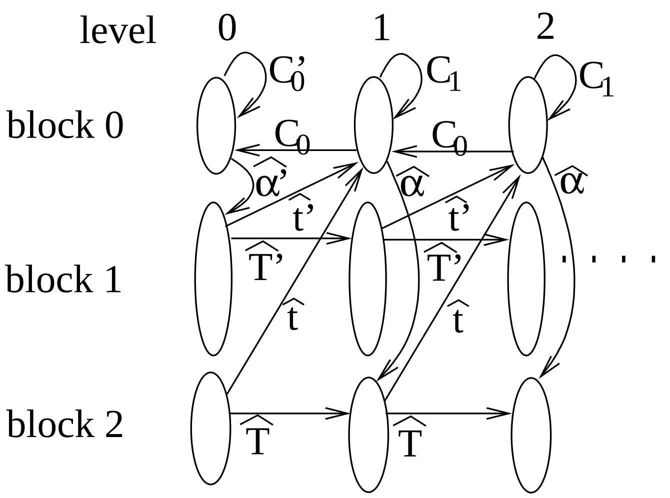

Figure 3.1: The transition structure of the expanded QBD process

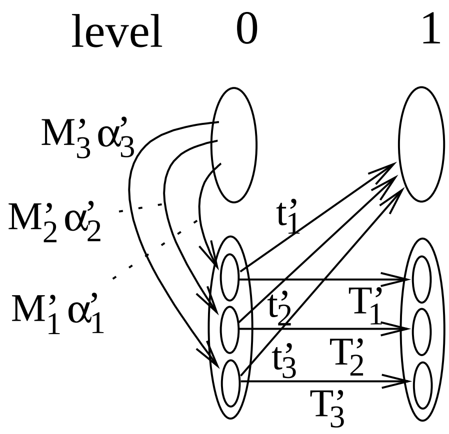

Figure 3.2: The sub-block structure of $\widehat{\alpha'}$, $\widehat{\mathbf{T}'}$ and $\widehat{\mathbf{t}'}$

In the Discussion in (3.33) I show that it is not necessary to enlarge the state space by the sum of the sizes of the $\mathbf{M_k}$ matrices for $k = 1, \ldots, K$. Instead, it is enough to grow the state space by $\sum_{k=1}^{K} \text{rank}(\mathbf{M_k})$, where $\text{rank}(\mathbf{M_k})$ is the rank of matrix $\mathbf{M_k}$.

Thesis 2.3

I show that the results of Thesis 2.1 and Thesis 2.2 are indispensable to calculate the moments and the probability distribution of a PHBMAP/PH/1 system. I show an example, where a finite truncation in Equation 3.4 leads to significant deviation from the queue length distribution.

Figure 3.3 shows the queue length distribution obtained by Thesis 2.1.

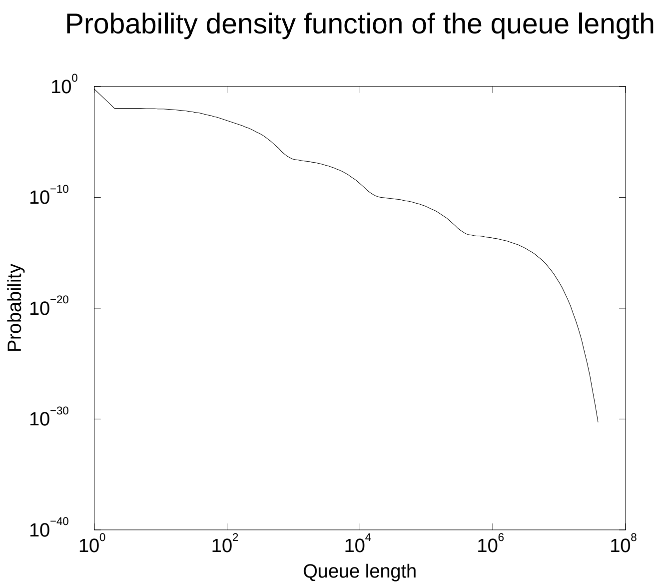

Figure 3.3: The pdf of the queue length in log-log scale

N	100	1000	100000
$1-\varrho$	0.03	$1.10 \cdot 10^{-2}$	$1.82 \cdot 10^{-4}$
q	30	300	16000

Table 3.1: The asymptotic decay rate ϱ and the queue q length at which this decay is reached as a function of the truncation (N)

Figure 3.4 shows how the exact queue length distribution can be approximated by the method of Latouche and Ramaswami [34], Equation (13.12) using different truncation points. Different numerical methods were tested and the iterative substitution on the original state space converges with the least number of multiplications to the solution as it can be seen in Table 3.6.

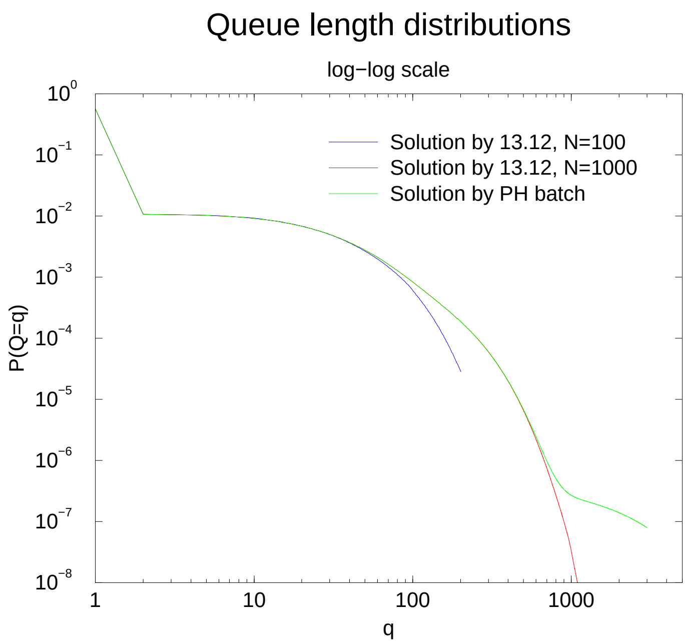

Figure 3.4: Comparison of the various solutions for the queue length distribution and the exact distribution

It can be seen in Figure 3.4 that the approximate solutions with different truncation points follow the exact solution for a while but the approximate distributions deviate from the exact even for relatively small quantiles. I can approximate these break points of the numerical solution (q) as a function of the truncation point (N) using the approach presented in Section 3.5. Table 3.1 shows the value of the geometric decay parameter as a function of N and the minimal queue length, after which the $\frac{p_n \mathbf{1}}{p_{n+1}\mathbf{1}}$ ratio is above ϱ.

One of the most important consequences of the evaluated examples is apparent from the comparison of Figure 3.3 and 3.4 and the table with the approximate break points. The (13.12) method of Latouche and Ramaswami [34], which is a commonly applied method for solving M/G/1 type models, cannot be used to calculate slowly decaying tail distribution. According to my knowledge, the only numerically feasible way to solve these kinds of models is the procedure of extended QBD model of Thesis 2.

Based on this experience I believe that the best numerical solution of M/G/1 type models with generally distributed heavy tailed jumps is to approximate the jump distribution with a PH distribution that follows the slow decay through the desired orders of magnitude and to use the numerical procedure with the extended QBD.

3.3 Discussion

The assumption of the Phase-type structure in the transiton matrix of the BMAP/PH/1 system makes the whole problem Markovian and therefore more easily tractable. The possibility of finite summation can partly be attributed to an alternative formulation of the probabilities of a PH distribution. In the following this alternative formulation and its explanation is presented.

Denote the matrix of the transition probabilities of the transient states (phases) of a discrete Phase-type distribution by $\mathbf{T}$. Based on the Jordan decomposition of $\mathbf{T}$, the Phase-type distribution can also be represented by the eigenvalues of $\mathbf{T}$ as follows (see Section 3.5):

$$p(i) = \sum_{j=1}^{\#\lambda} \sum_{\ell=1}^{\#\lambda_j} a_{j\ell} \binom{i-1}{\ell-1} \lambda_j^{i-\ell},\ i \geq 1, \tag{3.14}$$

where $\#\lambda$ is the number of distinct eigenvalues of $\mathbf{T}$, λ_j ($1 \leq j \leq \#\lambda$) denotes these eigenvalues and $\#\lambda_j$ is the multiplicity of the eigenvalue λ_j. Note that $\binom{i-1}{\ell-1} = 0$ when $i < \ell$.

Proof of Theorem 1: Utilising the special PH structure of the $\mathbf{C_i}$ matrices and the (3.14) representation of discrete PH distributions, I have:

$$\begin{aligned} \mathbf{0} = \quad & \mathbf{C_0} + \mathbf{C_1}\mathbf{G} + \sum_{i=2}^{\infty} \mathbf{C_i}\mathbf{G}^i \\ &= \mathbf{C_0} + \mathbf{C_1}\mathbf{G} + \sum_{i=1}^{\infty}\sum_{k=1}^{K} \mathbf{M_k}\, p_k(i)\mathbf{G}^{i+1} \\ &= \mathbf{C_0} + \mathbf{C_1}\mathbf{G} + \sum_{i=1}^{\infty}\sum_{k=1}^{K} \mathbf{M_k} \sum_{j=1}^{\#_k\lambda}\sum_{\ell=1}^{\#_k\lambda_j} {}_k a_{j\ell} \binom{i-1}{\ell-1} {}_k\lambda_j^{i-\ell}\mathbf{G}^{i+1} \\ &= \mathbf{C_0} + \mathbf{C_1}\mathbf{G} + \sum_{k=1}^{K} \mathbf{M_k} \sum_{j=1}^{\#_k\lambda}\sum_{\ell=1}^{\#_k\lambda_j} {}_k a_{j\ell}\, \mathbf{G}^{\ell+1} \sum_{i=1}^{\infty} \binom{i-1}{\ell-1} {}_k\lambda_j^{i-\ell}\mathbf{G}^{i-\ell} \\ &= \mathbf{C_0} + \mathbf{C_1}\mathbf{G} + \sum_{k=1}^{K} \mathbf{M_k} \sum_{j=1}^{\#_k\lambda}\sum_{\ell=1}^{\#_k\lambda_j} {}_k a_{j\ell}\, \mathbf{G}^{\ell+1} \left(\mathbf{I} - {}_k\lambda_j\mathbf{G}\right)^{-\ell}, \end{aligned} \tag{3.15}$$

where the subscripts on the left refer to the specific PH distributions.

Multiplying both sides of (3.15) by $\prod_{k=1}^{K}\prod_{j=1}^{\#_k\lambda} (\mathbf{I} - {}_k\lambda_j\mathbf{G})^{\#_k\lambda_j}$ and properly commuting the $(\mathbf{I} - {}_k\lambda_j\mathbf{G})$ matrices gives an order $c = 1 + \sum_{k=1}^{K} n_k$ matrix equation for $\mathbf{G}$ in Equation 3.4. Here n_k denotes the order of the $p_k(i)$ discrete PH distribution. □

Define $\mathbb{B}$, $\mathbb{A}_0$, $\mathbb{A}_1$ and $\mathbb{A}_2$ as

$$\mathbb{B} = \begin{array}{|c|c|c|}\hline \mathbf{C}_0' & \widehat{\alpha}' & \mathbf{0} \\ \hline \mathbf{0} & -\mathbf{I} & \mathbf{0} \\ \hline \mathbf{0} & \mathbf{0} & -\mathbf{I} \\ \hline \end{array}\ , \quad \mathbb{A}_0 = \begin{array}{|c|c|c|}\hline \mathbf{0} & \mathbf{0} & \mathbf{0} \\ \hline \widehat{\mathbf{t}'} & \widehat{\mathbf{T}'} & \mathbf{0} \\ \hline \widehat{\mathbf{t}} & \mathbf{0} & \widehat{\mathbf{T}} \\ \hline \end{array}\ , \tag{3.16}$$

$$\mathbb{A}_1 = \begin{array}{|c|c|c|}\hline \mathbf{C}_1 & \mathbf{0} & \widehat{\alpha} \\ \hline \mathbf{0} & -\mathbf{I} & \mathbf{0} \\ \hline \mathbf{0} & \mathbf{0} & -\mathbf{I} \\ \hline \end{array}\ , \quad \mathbb{A}_2 = \begin{array}{|c|c|c|}\hline \mathbf{C}_0 & \mathbf{0} & \mathbf{0} \\ \hline \mathbf{0} & \mathbf{0} & \mathbf{0} \\ \hline \mathbf{0} & \mathbf{0} & \mathbf{0} \\ \hline \end{array}\ , \tag{3.17}$$

where

$$\widehat{\alpha} = \begin{array}{|c|c|c|}\hline \alpha_1 \odot \mathbf{M}_1 & \dots & \alpha_K \odot \mathbf{M}_K \\ \hline \end{array}\ ,$$

$$\widehat{\mathbf{T}} = \begin{array}{|c|c|c|}\hline \mathbf{T_1} \odot \mathbf{I} & \mathbf{0} & \mathbf{0} \\ \hline \mathbf{0} & \ddots & \mathbf{0} \\ \hline \mathbf{0} & \mathbf{0} & \mathbf{T_K} \odot \mathbf{I} \\ \hline \end{array}\ , \quad \widehat{\mathbf{t}} = \begin{array}{|c|}\hline \mathbf{t_1} \odot \mathbf{I} \\ \hline \vdots \\ \hline \mathbf{t_K} \odot \mathbf{I} \\ \hline \end{array}\ , \tag{3.18}$$

and the $\widehat{\alpha}'$, $\widehat{\mathbf{T}'}$, $\widehat{\mathbf{t}'}$ terms are defined similarly. Throughout Chapter 3 $\odot$ denotes the Kronecker product. Then (3.10)

$$\mathbf{Q}' = \begin{array}{|c|c|c|c|c|}\hline \mathbb{B} & \mathbb{A}_0 & & & \\ \hline \mathbb{A}_2 & \mathbb{A}_1 & \mathbb{A}_0 & & \\ \hline & \mathbb{A}_2 & \mathbb{A}_1 & \mathbb{A}_0 & \\ \hline & & \mathbb{A}_2 & \mathbb{A}_1 & \mathbb{A}_0 \\ \hline & & & \ddots & \ddots \\ \hline \end{array}$$

defines a QBD. The marginal distribution of this QBD that is defined in Theorem 3 is the solution of the PHBMAP/PH/1 system.

Proof of Theorem 3: The proof follows the pattern of Section 13.1 of Latouche and Ramaswami [34]. The main idea in Section 13.1 is to transform M/G/1 type models into QBD models with an extended phase process. In case of a general M/G/1 process, an infinite phase process is introduced in this transformation, but in case of PH distributed batch size, a finite extension of the phase process is sufficient as it is presented by the block structure of matrices $\mathbb{A}_0$, $\mathbb{A}_1$, $\mathbb{A}_2$ and $\mathbb{B}$ and depicted in Figure 3.1.

Here I only show that the extended Markov chain (with generator $\mathbf{Q}'$) restricted to block 0 is identical with the M/G/1 type Markov chain with generator $\mathbf{Q}$. Indeed, block 0 of the extended process represents the states of the original process. The rest of the proof is identical with the one in Latouche and Ramaswami [34] pp. 268-275.

The downward and local transitions of the process restricted to block 0 are readable, e.g. from Figure 3.1. They are identical with the downward and local transitions of $\mathbf{Q}$. The upward transitions between consecutive visits in block 0 are through block 1 (starting from level 0) or block 2 (starting from level $i \geq 1$).

First I consider the case of starting from level 0. The upward transition rate of the restricted process can be obtained as the product of the exit rate from block 0 and the probability of returning to block 0 in a given state. The exit rate of block 0 is characterized by matrix $\sum_{k=1}^{K'} \mathbf{M}'_\mathbf{k}$. Each $\mathbf{M}'_\mathbf{k}$ matrix selects one PH structure of block 1 and it remains unchanged during the visit in block 1 (see Figure 3.2). The probability of starting from block 0 of level 0 moving to block 1 and returning to block 0 at level i ($i \geq 1$) supposed that the kth PH structure is selected, equals to $\alpha_k \mathbf{T_k}^{i-1} \mathbf{t_k}$. Hence the upward transitions of the restricted process from level 0 to level i are

$$\sum_{k=1}^{K'} \mathbf{M}'_\mathbf{k} \, \alpha_k \mathbf{T_k}^{i-1} \mathbf{t_k} = \sum_{k=1}^{K'} \mathbf{M}'_\mathbf{k} \, p'_k(i) = \mathbf{C}'_\mathbf{i}.$$

The upward transitions starting from level $i \geq 1$ can be obtained similarly. □

Lemma 1 points out that the solution of (3.11), the matrix equation on the enlarged state space, has a special block structure. This block structure is used in the proof of Theorem 2 below.

Lemma 1. *The fundamental matrix of the extended QBD (3.10) is*

$$\mathbb{G} = \begin{array}{|c|c|c|} \hline \mathbf{G} & \mathbf{0} & \mathbf{0} \\ \hline \widehat{\mathbf{G}'} & \mathbf{0} & \mathbf{0} \\ \hline \widehat{\mathbf{G}} & \mathbf{0} & \mathbf{0} \\ \hline \end{array}\,, \tag{3.19}$$

where $\mathbf{G}$ *is the fundamental matrix of the M/G/1 type Markov chain (3.4) and*

$$\widehat{\mathbf{G}'} = \sum_{i=0}^{\infty} \widehat{\mathbf{T}'}^{i} \, \widehat{\mathbf{t}'} \, \mathbf{G}^{i+2} \,, \quad \widehat{\mathbf{G}} = \sum_{i=0}^{\infty} \widehat{\mathbf{T}}^{i} \, \widehat{\mathbf{t}} \, \mathbf{G}^{i+2}. \tag{3.20}$$

Proof: The structure of matrix $\mathbb{G}$ is readable from the block structure of the Markov chain presented in Figure 3.1. The second and third block column are 0 because downward transitions are not possible in block 1 and 2. A transition from block 1 level k to block 0 level $k-1$ can happen with i ($i \geq 0$) consecutive upward transitions in block 1 (characterised by $\widehat{\mathbf{T}'}^{i}$) then a transition from block 1 level $k+i$ to block 0 level $k+i+1$

(characterised by $\widehat{\mathbf{t}'}$) and then $i+2$ level decreasing transitions (characterised by $\mathbf{G}^{i+2}$). The transitions from block 2 level k to block 0 level $k-1$ can be calculated similarly. □

The stationary distribution of a QBD can be calculated in an iterative manner from $\mathbb{G}$ using (3.12). However, there is an alternative method:

$$\pi'_i = \pi'_{i-1}\mathbb{R},\ i \geq 1, \quad \text{and} \quad 0 = \pi'_0\mathbb{B} + \pi'_1\mathbb{A}_2.$$

In some cases, this alternative proves to be more useful. Like the matrix $\mathbb{G}$, $\mathbb{R}$ also has a special structure.

Lemma 2. *The extended QBD (3.10) has the following sub-block structure*

$$\mathbb{R} = \begin{array}{|c|c|c|} \hline \mathbf{0} & \mathbf{0} & \mathbf{0} \\ \hline \widetilde{\mathbf{G}'} & \widehat{\mathbf{T}'} & \widetilde{\mathbf{G}'}\widehat{\alpha} \\ \hline \widetilde{\mathbf{G}} & \mathbf{0} & \widetilde{\mathbf{G}}\widehat{\alpha} + \widehat{\mathbf{T}} \\ \hline \end{array}, \tag{3.21}$$

$$\left(\mathbb{I} - \mathbb{R}\right)^{-1} = \begin{array}{|c|c|c|} \hline \mathbf{I} & \mathbf{0} & \mathbf{0} \\ \hline (\mathbf{I} - \widehat{\mathbf{T}'})^{-1}\widetilde{\mathbf{G}'}(\mathbf{I} + \widehat{\alpha}\mathbf{X}) & (\mathbf{I} - \widehat{\mathbf{T}'})^{-1} & (\mathbf{I} - \widehat{\mathbf{T}'})^{-1}\widetilde{\mathbf{G}'}\widehat{\alpha}\mathbf{Y} \\ \hline \mathbf{X} & \mathbf{0} & \mathbf{Y} \\ \hline \end{array}, \tag{3.22}$$

where

$$\widetilde{\mathbf{G}'} = \left(\widehat{\mathbf{t}'} + \widehat{\mathbf{T}'}(\widehat{\mathbf{t}'}\mathbf{G} + \widehat{\mathbf{T}'}\widehat{\mathbf{G}'})\right)\left(-\mathbf{C_1} - \widehat{\alpha}\widehat{\mathbf{t}}\mathbf{G} - \widehat{\alpha}\widehat{\mathbf{T}}\widehat{\mathbf{G}}\right)^{-1},$$

$$\widetilde{\mathbf{G}} = \left(\widehat{\mathbf{t}} + \widehat{\mathbf{T}}(\widehat{\mathbf{t}}\mathbf{G} + \widehat{\mathbf{T}}\widehat{\mathbf{G}})\right)\left(-\mathbf{C_1} - \widehat{\alpha}\widehat{\mathbf{t}}\mathbf{G} - \widehat{\alpha}\widehat{\mathbf{T}}\widehat{\mathbf{G}}\right)^{-1},$$

$$\mathbf{X} = \left(\mathbf{I} - \widehat{\mathbf{T}} - \widetilde{\mathbf{G}}\widehat{\alpha}\right)^{-1}\widetilde{\mathbf{G}} \quad \textit{and} \quad \mathbf{Y} = \left(\mathbf{I} - \widehat{\mathbf{T}} - \widetilde{\mathbf{G}}\widehat{\alpha}\right)^{-1}.$$

Proof: Matrix $\mathbb{R}$ is obtained from $\mathbb{R} = \mathbb{A}_0(-\mathbb{A}_1 - \mathbb{A}_0\mathbb{G})^{-1}$ and $(\mathbb{I} - \mathbb{R})^{-1}$ from matrix $\mathbb{R}$ considering the block structure of the $\mathbb{A}_0$ and $\mathbb{A}_1$ matrices. □

I can use the result of Theorem 3 to calculate the stationary distribution of the M/G/1 type process directly in Theorem 2. In contrast with the case of general jump distributions, PH distributed jumps allows to calculate the stationary distribution in a finite number of steps *without any truncation of infinite sums*.

Proof of Theorem 2: Having the fundamental matrix $\mathbb{G}$, the stationary solution of the QBD (3.10) can be obtained as in (3.12) Decomposing the vectors and the matrices in (3.12) according to Lemma 1, for $i \geq 1$, results:

$$0 = \pi'_{i-1,1}\widehat{\mathbf{t}'} + \pi'_{i-1,2}\widehat{\mathbf{t}} + \pi'_{i,0}\mathbf{C_1} + \pi'_{i,1}\left(\widehat{\mathbf{t}'}\mathbf{G} + \widehat{\mathbf{T}'}\widehat{\mathbf{G}'}\right) + \pi'_{i,2}\left(\widehat{\mathbf{t}}\mathbf{G} + \widehat{\mathbf{T}}\widehat{\mathbf{G}}\right) \tag{3.23}$$

$$0 = \pi'_{i-1,1}\widehat{\mathbf{T}'} - \pi'_{i,1} \tag{3.24}$$

$$0 = \pi'_{i-1,2}\widehat{\mathbf{T}} + \pi'_{i,0}\widehat{\alpha} - \pi'_{i,2} \tag{3.25}$$

and for $i = 0$

$$
\begin{aligned}
0 &= \pi'_{0,0}\mathbf{C'_0} + \pi'_{0,1}\mathbf{C_0} && (3.26)\\
0 &= \pi'_{0,0}\widehat{\alpha'} - \pi'_{0,1} && (3.27)\\
0 &= \pi'_{0,2} && (3.28)
\end{aligned}
$$

From (3.24) and (3.25), $\pi'_{i,1} = \pi'_{i-1,1}\widehat{\mathbf{T'}}$ and $\pi'_{i,2} = \pi'_{i-1,2}\widehat{\mathbf{T}} + \pi'_{i,0}\widehat{\alpha}$. Repeatedly substituting these into (3.23) provides

$$
\begin{aligned}
&\pi'_{i,0}\Big(-\mathbf{C_1} - \widehat{\alpha}\widehat{\mathbf{t}}\mathbf{G} - \widehat{\alpha}\widehat{\mathbf{T}}\widehat{\mathbf{G}}\Big)\\
&= \pi'_{i-1,1}\Big(\widehat{\mathbf{t'}} + \widehat{\mathbf{T'}}\widehat{\mathbf{t'}}\mathbf{G} + \widehat{\mathbf{T'}}^2\widehat{\mathbf{G'}}\Big) + \pi'_{i-1,2}\Big(\widehat{\mathbf{t}} + \widehat{\mathbf{T}}\widehat{\mathbf{t}}\mathbf{G} + \widehat{\mathbf{T}}^2\widehat{\mathbf{G}}\Big)
\end{aligned} \tag{3.29}
$$

A substitution of equations (3.27), (3.28) and (3.20) and some algebra results:

$$
\pi'_{i,0}\Big(-\mathbf{C_1} - \sum_{j=0}^{\infty}\widehat{\alpha}\widehat{\mathbf{T}}^j\widehat{\mathbf{t}}\mathbf{G}^{j+1}\Big) = \pi'_{0,0}\sum_{j=0}^{\infty}\widehat{\alpha'}\widehat{\mathbf{T'}}^{i-1+j}\widehat{\mathbf{t'}}\mathbf{G}^j + \sum_{\ell=1}^{i-1}\pi'_{\ell,0}\sum_{j=0}^{\infty}\widehat{\alpha}\widehat{\mathbf{T}}^{i-1-\ell+j}\widehat{\mathbf{t}}\mathbf{G}^j\ , \tag{3.30}
$$

where

$$
\widehat{\alpha}\widehat{\mathbf{T}}^j\widehat{\mathbf{t}} = \sum_{k=1}^{K}\mathbf{M_k}\,p_k(j+1) = \mathbf{C_{j+2}}\ ,\quad \widehat{\alpha'}\widehat{\mathbf{T'}}^j\widehat{\mathbf{t'}} = \sum_{k=1}^{K'}\mathbf{M'_k}\,p'_k(j+1) = \mathbf{C'_{j+1}}\ .
$$

Based on Theorem 3, I introduce $\pi_i = \pi'_{i,0}$. With this notation (3.30) becomes (3.6).

I also prove the calculation of π_0. It is basically similar to Theorem 3.2.1 of Neuts [43] on page 137. Even though, I provide a similar proof supported with probabilistic interpretation based on the length of the idle and busy period of the M/G/1 type queue.

The mean time of the idle period is

$$
E(\text{idle}) = \overline{\pi}_0(-\mathbf{C'_0})^{-1}\mathbb{1}, \tag{3.31}
$$

where $\overline{\pi}_0$ is the phase distribution at the beginning of the idle period. The stationary distribution during the idle period is proportional to the mean time spent in various phases before moving to a higher level ($\overline{\pi}_0(-\mathbf{C'_0})^{-1}$), i.e., $\pi^*_0 = a\,\overline{\pi}_0(-\mathbf{C'_0})^{-1}$, where a is a constant coefficient ($a \in \mathbb{R}^+$). The mean time of the busy period is

$$
\begin{aligned}
E(\text{busy}) &= -\frac{d}{ds}\sum_{i=1}^{\infty}\alpha_i\mathbf{G}^i(s)\mathbb{1}\Big|_{s\to 0} = -\frac{d}{ds}\sum_{i=1}^{\infty}\overline{\pi}_0(-\mathbf{C'_0})^{-1}\mathbf{C'_i}\,\mathbf{G}^i(s)\mathbb{1}\Big|_{s\to 0}\\
&= -\sum_{i=1}^{\infty}\overline{\pi}_0(-\mathbf{C'_0})^{-1}\mathbf{C'_i}\sum_{\ell=0}^{i-1}\mathbf{G}^{\ell}(s)\mathbf{G'}(s)\mathbf{G}^{i-\ell-1}(s)\mathbb{1}\Big|_{s\to 0}\\
&= -\sum_{i=1}^{\infty}\overline{\pi}_0(-\mathbf{C'_0})^{-1}\mathbf{C'_i}\sum_{\ell=0}^{i-1}\mathbf{G}^{\ell}\mathbf{G'}(0)\mathbf{G}^{i-\ell-1}\mathbb{1}\\
&= \overline{\pi}_0(-\mathbf{C'_0})^{-1}\underbrace{\sum_{i=1}^{\infty}\mathbf{C'_i}\sum_{\ell=0}^{i-1}\mathbf{G}^{\ell}}\,g = \overline{\pi}_0(-\mathbf{C'_0})^{-1}\underbrace{\overline{\mathbf{Z'}}}\,g,
\end{aligned} \tag{3.32}
$$

where α_i is the phase distribution at the beginning of the busy period, $\mathbf{G}(s)$ is a solution of $s\mathbf{G}(s) = \sum_{i=0}^{\infty} \mathbf{C_i}\mathbf{G}^i(s)$ and $g = -\mathbf{G}'(0)\mathbb{1}$.

The column vector $g = -\mathbf{G}'(0)\mathbb{1} = -\frac{d}{ds}\mathbf{G}(s)\mathbb{1}\Big|_{s\to 0}$ is calculated from the derivative of the equation characterizing $\mathbf{G}(s)$:

$$\begin{aligned}
\frac{d}{ds}\, s\,\mathbf{G}(s)\,\mathbb{1}\Big|_{s\to 0} &= \frac{d}{ds}\sum_{i=0}^{\infty}\mathbf{C_i}\,\mathbf{G}^i(s)\,\mathbb{1}\Big|_{s\to 0} \\
\Big(\mathbf{G}(s) + s\mathbf{G}'(s)\Big)\mathbb{1}\Big|_{s\to 0} &= \sum_{i=1}^{\infty}\mathbf{C_i}\sum_{\ell=0}^{i-1}\mathbf{G}^{\ell}(s)\,\mathbf{G}'(s)\,\mathbf{G}^{i-\ell-1}(s)\,\mathbb{1}\Big|_{s\to 0} \\
\mathbf{G}\,\mathbb{1} &= \sum_{i=1}^{\infty}\mathbf{C_i}\sum_{\ell=0}^{i-1}\mathbf{G}^{\ell}\,\mathbf{G}'(0)\,\mathbf{G}^{i-\ell-1}\,\mathbb{1} \\
\mathbb{1} &= -\underbrace{\sum_{i=1}^{\infty}\mathbf{C_i}\sum_{\ell=0}^{i-1}\mathbf{G}^{\ell}}\,g = -\underbrace{\Big(\mathbf{C_1} + \mathbf{Z}(0)\mathbf{G} + \overline{\mathbf{Z}}\Big)}\,g \\
\Big(-\mathbf{C_1} - \mathbf{Z}(0)\mathbf{G} - \overline{\mathbf{Z}}\Big)^{-1}\mathbb{1} &= g\,.
\end{aligned}$$

The stationary probability of level 0 is obtained as

$$\pi_0\mathbb{1} = \frac{E(\text{idle})}{E(\text{idle}) + E(\text{busy})} = \frac{\overline{\pi}_0(-\mathbf{C'_0})^{-1}\mathbb{1}}{\overline{\pi}_0(-\mathbf{C'_0})^{-1}\mathbb{1} + \overline{\pi}_0(-\mathbf{C'_0})^{-1}\overline{\mathbf{Z}'}\,g} = \frac{\pi_0^*\mathbb{1}}{\pi_0^*\Big(\mathbb{1} + \overline{\mathbf{Z}'}g\Big)}$$

and π_0^* is calculated as the stationary distribution of the M/G/1 type process restricted to level 0:

$$\pi_0^*\sum_{i=0}^{\infty}\mathbf{C'_i}\,\mathbf{G}^i = \pi_0^*\Big(\mathbf{C'_0} + \mathbf{Z}'(0)\,\mathbf{G}\Big) = 0.$$

□

Corollary 4. *Matrices $\mathbf{Z}(n)$, $\mathbf{Z}'(n)$, $\overline{\mathbf{Z}}$ and $\overline{\mathbf{Z}'}$ can be calculated in a finite number of steps.*

Proof:

$$\begin{aligned}
\mathbf{Z}(n) &= \sum_{i=0}^{\infty}\sum_{k=1}^{K}\mathbf{M_k}\,p_k(n{+}i{+}1)\,\mathbf{G}^i \\
&= \sum_{i=0}^{\infty}\sum_{k=1}^{K}\mathbf{M_k}\sum_{j=1}^{\#_k\lambda}\sum_{\ell=1}^{\#_k\lambda_j}{}_k a_{j\ell}\binom{n{+}i}{\ell{-}1}{}_k\lambda_j^{n+i+1-\ell}\,\mathbf{G}^i \\
&= \sum_{i=0}^{\infty}\sum_{k=1}^{K}\mathbf{M_k}\sum_{j=1}^{\#_k\lambda}\sum_{\ell=1}^{\#_k\lambda_j}{}_k a_{j\ell}\sum_{m=1}^{\ell}\binom{n}{\ell{-}m}\binom{i}{m{-}1}{}_k\lambda_j^{n+i+1-\ell}\,\mathbf{G}^i \\
&= \sum_{k=1}^{K}\mathbf{M_k}\sum_{j=1}^{\#_k\lambda}\sum_{\ell=1}^{\#_k\lambda_j}{}_k a_{j\ell}\sum_{m=1}^{\ell}\binom{n}{\ell{-}m}{}_k\lambda_j^{n-\ell+m}\,\mathbf{G}^{m-1}\sum_{i=0}^{\infty}\binom{i}{m{-}1}{}_k\lambda_j^{i+1-m}\,\mathbf{G}^{i+1-m} \\
&= \sum_{k=1}^{K}\mathbf{M_k}\sum_{j=1}^{\#_k\lambda}\sum_{\ell=1}^{\#_k\lambda_j}{}_k a_{j\ell}\sum_{m=1}^{\ell}\binom{n}{\ell{-}m}{}_k\lambda_j^{n-\ell+m}\,\mathbf{G}^{m-1}\Big(\mathbf{I} - {}_k\lambda_j\,\mathbf{G}\Big)^{-m}.
\end{aligned}$$

$$\begin{aligned}\overline{\mathbf{Z}} &= \sum_{n=0}^{\infty}\mathbf{Z}(n) = \sum_{k=1}^{K}\mathbf{M_k}\sum_{j=1}^{\#_k\lambda}\sum_{\ell=1}^{\#_k\lambda_j}{}_k a_{j\ell}\sum_{m=1}^{\ell}\sum_{n=0}^{\infty}\binom{n}{\ell-m}{}_k\lambda_j^{n-\ell+m}\,\mathbf{G}^{m-1}\Big(\mathbf{I}-{}_k\lambda_j\,\mathbf{G}\Big)^{-m}\\ &= \sum_{k=1}^{K}\mathbf{M_k}\sum_{j=1}^{\#_k\lambda}\sum_{\ell=1}^{\#_k\lambda_j}{}_k a_{j\ell}\sum_{m=1}^{\ell}(1-{}_k\lambda_j)^{-\ell+m-1}\,\mathbf{G}^{m-1}\Big(\mathbf{I}-{}_k\lambda_j\,\mathbf{G}\Big)^{-m}.\end{aligned}$$

The calculation of $\mathbf{Z}'$ follows the same pattern as the one of $\mathbf{Z}$ and the calculation of $\overline{\mathbf{Z}'}$ is similar to the one of $\overline{\mathbf{Z}}$. □

There are Markovian queues which are specific cases of M/G/1 type Markov chains with PH distributed jumps. For example, the BMAP/M/1 queue with geometrically distributed batch size is a special case. A particular property of this special case is that the stationary distribution is matrix geometric as it is shown in Section 3.5.

In Thesis 2.2 I claimed that there is an effective way of representing the original M/G/1 type Markov chain by an enlarged state space. For such an efficient definition of the QBD process, $\mathrm{M}_\mathbf{k}$ and $\mathbf{I}$ (and similarly $\mathrm{M}'_\mathbf{k}$ and $\mathbf{I}$) need to be replaced by $\mathrm{M}^\mathbf{r}_\mathbf{k}$ and $\mathrm{N}^\mathbf{r}_\mathbf{k}$, respectively, in (3.18) such that $\mathrm{M}_\mathbf{k}\mathbf{I} = \mathrm{M}^\mathbf{r}_\mathbf{k}\mathrm{N}^\mathbf{r}_\mathbf{k}$, the size of $\mathrm{M}^\mathbf{r}_\mathbf{k}$ is $|\mathbf{C_0}| \times rank(\mathrm{M}_\mathbf{k})$ and the size of $\mathrm{N}^\mathbf{r}_\mathbf{k}$ is $rank(\mathrm{M}_\mathbf{k}) \times |\mathbf{C_0}|$. I.e.,

$$\widehat{\alpha} = \begin{array}{|c|c|c|}\hline \alpha_1 \odot \mathbf{M^r_1} & \dots & \alpha_K \odot \mathbf{M^r_K} \\ \hline\end{array} \quad ,$$

$$\widehat{\mathbf{T}} = \begin{array}{|c|c|c|}\hline \mathbf{T_1}\odot\mathbf{I} & \mathbf{0} & \mathbf{0}\\ \hline \mathbf{0} & \ddots & \mathbf{0}\\ \hline \mathbf{0} & \mathbf{0} & \mathbf{T_K}\odot\mathbf{I}\\ \hline\end{array} \quad , \quad \widehat{\mathbf{t}} = \begin{array}{|c|}\hline \mathbf{t_1}\odot\mathbf{N^r_1}\\ \hline \vdots \\ \hline \mathbf{t_K}\odot\mathbf{N^r_K}\\ \hline\end{array} \quad , \tag{3.33}$$

Note, that there is another obvious way to reduce the QBD representation with respect to (3.16) and (3.17) when $\widehat{\alpha} = \widehat{\alpha'}$, $\widehat{\mathbf{T}} = \widehat{\mathbf{T'}}$, $\widehat{\mathbf{t}} = \widehat{\mathbf{t}'}$. In this case

$$\mathbb{B} = \begin{array}{|c|c|}\hline \mathbf{C'_0} & \widehat{\alpha}\\ \hline \mathbf{0} & -\mathbf{I}\\ \hline\end{array} \quad , \quad \mathbb{A}_0 = \begin{array}{|c|c|}\hline \mathbf{0} & \mathbf{0}\\ \hline \widehat{\mathbf{t}} & \widehat{\mathbf{T}}\\ \hline\end{array} \quad , \quad \mathbb{A}_1 = \begin{array}{|c|c|}\hline \mathbf{C_1} & \widehat{\alpha}\\ \hline \mathbf{0} & -\mathbf{I}\\ \hline\end{array} \quad , \quad \mathbb{A}_2 = \begin{array}{|c|c|}\hline \mathbf{C_0} & \mathbf{0}\\ \hline \mathbf{0} & \mathbf{0}\\ \hline\end{array} \quad . \tag{3.34}$$

3.4 Application

First I summarise the potential numerical procedures to evaluate M/G/1 type Markov chains with PH distributed jumps.

Matrix $\mathbb{G}$ is the minimal non-negative solution of the matrix equation

$$\mathbf{0} = \mathbb{A}_2 + \mathbb{A}_1\mathbb{G} + \mathbb{A}_0\mathbb{G}^2\,. \tag{3.35}$$

Using the partitioned form of matrices $\mathbb{A}_0$, $\mathbb{A}_2$, $\mathbb{A}_2$ and $\mathbb{G}$ (3.35) become

$$\begin{aligned} \mathbf{0} &= \mathbf{C_0} + \mathbf{C_1}\mathbf{G} + \widehat{\alpha}\widehat{\mathbf{G}} & (3.36) \\ \mathbf{0} &= -\widehat{\mathbf{G}'} + \widehat{\mathbf{t}'}\mathbf{G}^2 + \widehat{\mathbf{T}'}\widehat{\mathbf{G}'}\mathbf{G} & (3.37) \\ \mathbf{0} &= -\widehat{\mathbf{G}} + \widehat{\mathbf{t}}\mathbf{G}^2 + \widehat{\mathbf{T}}\widehat{\mathbf{G}}\mathbf{G} & (3.38) \end{aligned}$$

Matrix $\mathbf{G}$ can be calculated based on (3.36) and (3.38) (independent of (3.37)). Using this property (which is also visible from the block structure of the extended Markov chain) I can generate the reduced matrices associated with block 0 and 2:

$$\mathbb{A}_0^r = \begin{array}{|c|c|}\hline \mathbf{0} & \mathbf{0} \\ \hline \widehat{\mathbf{t}} & \widehat{\mathbf{T}} \\ \hline \end{array}, \quad \mathbb{A}_1^r = \begin{array}{|c|c|}\hline \mathbf{C_1} & \widehat{\alpha} \\ \hline \mathbf{0} & -\mathbf{I} \\ \hline \end{array}, \quad \mathbb{A}_2^r = \begin{array}{|c|c|}\hline \mathbf{C_0} & \mathbf{0} \\ \hline \mathbf{0} & \mathbf{0} \\ \hline \end{array}, \quad \mathbb{G}^{\mathbf{r}} = \begin{array}{|c|c|}\hline \mathbf{G} & \mathbf{0} \\ \hline \widehat{\mathbf{G}} & \mathbf{0} \\ \hline \end{array},$$

and calculate the fundamental matrix as

$$\mathbf{0} = \mathbb{A}_2^r + \mathbb{A}_1^r\mathbb{G}^{\mathbf{r}} + \mathbb{A}_0^r\mathbb{G}^{\mathbf{r}2} \,. \tag{3.39}$$

I have four finite order matrix equations (sets of equations) to compute matrix $\mathbf{G}$:

- eq. (3.5),
- eq. (3.35),
- eq. (3.36) together with eq. (3.38) and
- eq. (3.39).

Out of these four equations (3.35) is redundant and (3.36) together with (3.38) is a partitioned form of (3.39).

Standard QBD solution methods can be applied for the solution of (3.35) and (3.39). Methods available for structured Markov chains with bounded jumps (e.g. Bini and Meini [9] or Wolfner and Telek [64]) can be used for the solution of (3.5).

The following numerical method calculates the solution of (3.36) and (3.38) :

- Initialization: $\mathbf{G}_0 = \mathbf{0}$, $\widehat{\mathbf{G}}_0 = \mathbf{0}$,
- Iteration:

$$\begin{aligned} \widehat{\mathbf{G}}_{i+1} &= \widehat{\mathbf{t}}\mathbf{G}_i^2 + \widehat{\mathbf{T}}\widehat{\mathbf{G}}_i\mathbf{G}_i \\ \mathbf{G}_{i+1} &= (-\mathbf{C_1})^{-1}\left(\mathbf{C_0} + \widehat{\alpha}\widehat{\mathbf{G}}_{i+1}\right) \end{aligned} \tag{3.40}$$

- Stopping condition: $||\mathbf{G}\mathbb{1} - \mathbb{1}|| < \epsilon$

The initialization and the stopping condition can also be replaced with $\mathbf{G}_0 = \mathbf{I}$, $\widehat{\mathbf{G}}_0 = (\mathbf{I} - \widehat{\mathbf{T}})^{-1}\widehat{\mathbf{t}}$ and $||\mathbf{G}_{i+1} - \mathbf{G}_i|| < \epsilon$, respectively.

Having the fundamental matrix, there are two possible numerical methods to calculate the stationary distribution of M/G/1 type Markov chains with PH distributed batch size.

The first method is to calculate the stationary solution of the extended QBD process based on (3.12) and to transform the results using (3.13). This method uses enlarged block size, but it allows the use of standard QBD solution methods. The second algorithm maintains the smaller block size of the original M/G/1 type process, but in this case the steps are more complex. It calculates the stationary distribution based on (3.7) and (3.6).

In the following, these methods are used to calculate the solution of an M/G/1 type process in a numerical example. Consider a queueing system, which has two states. In state 1 the server has high service rate and no customer arrival while in state 2 the server has reduced service capacity and cusomers can arrive in batches with PH batch size.

Two batch size distributions are applied. Both are 6 state PH distributions. The first one approximates a power-tailed discrete distribution for 5 orders of magnitude. (Details on the PH approximation method for power-tailed distributions can be found in Horváth and Telek [26].)The second one comes from a 6 state Erlang distribution sampled at discrete time-intervals. The two distributions are shown in Figure 3.5.

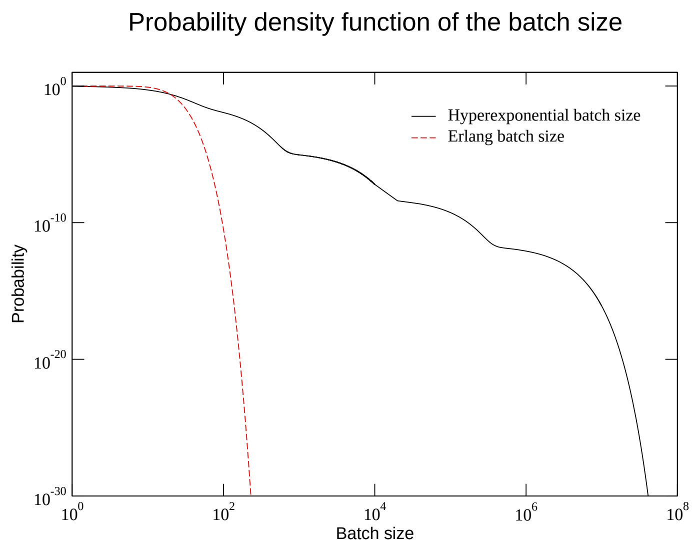

Figure 3.5: The pdf of the batch size in log-log scale

The matrix and the initial vector of the PH batch size that approximates a power-tailed distribution is

$$\mathbf{I}-\mathbf{T} \approx \begin{pmatrix} 0.170 & 0 & 0 & 0 & 0 & 0 \\ -0.076 & 0.083 & 0 & 0 & 0 & 0 \\ 0 & 0 & 1.030\cdot 10^{-6} & 0 & 0 & 0 \\ 0 & 0 & 0 & 2.417\cdot 10^{-5} & 0 & 0 \\ 0 & 0 & 0 & 0 & 5.607\cdot 10^{-4} & 0 \\ 0 & 0 & 0 & 0 & 0 & 0.013 \end{pmatrix},$$

$$\alpha \approx \begin{pmatrix} 0.300 & 0.660 & 2.33\cdot 10^{-12} & 6.100\cdot 10^{-9} & 1.583\cdot 10^{-5} & 0.041 \end{pmatrix}.$$

The representation of the discretised 6 state Erlang distribution is the following

$$\mathbf{I}-\mathbf{T} \approx \begin{pmatrix} 0.314 & -0.258 & -0.049 & -6.095 \cdot 10^{-3} & -5.733 \cdot 10^{-4} & -4.315 \cdot 10^{-5} \\ 0 & 0.314 & -0.258 & -0.049 & -6.095 \cdot 10^{-3} & -5.733 \cdot 10^{-4} \\ 0 & 0 & 0.314 & -0.258 & -0.049 & -6.095 \cdot 10^{-3} \\ 0 & 0 & 0 & 0.314 & -0.258 & -0.049 \\ 0 & 0 & 0 & 0 & 0.314 & -0.258 \\ 0 & 0 & 0 & 0 & 0 & 0.314 \end{pmatrix},$$

$$\alpha = \begin{pmatrix} 1 & 0 & 0 & 0 & 0 & 0 \end{pmatrix}.$$

Both representations correspond to an average batch size of ≈ 16.45 customers.

Transitions from state 1 to state 2 or backwards take place independently of the arrival or service events (see Figure 3.6).

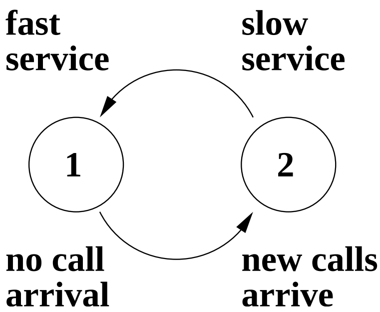

Figure 3.6: The diagram of the system states

The rate matrices of the customer service and the state transitions are the following:

$$C_0 = \begin{pmatrix} 50 & 0 \\ 0 & 5 \end{pmatrix}, \quad C_1 = \begin{pmatrix} 0 & 1 \\ 1 & 0 \end{pmatrix}.$$

Matrix $\mathbf{M}$ is scaled such that various server utilisations are investigated:

$$\mathbf{M} = \begin{pmatrix} 0 & 0 \\ 0 & m \end{pmatrix}.$$

The batch size distribution given that there is no customer in the system is the same as the batch size at other times: $\mathbf{T}' = \mathbf{T}$, $\alpha' = \alpha$, and the batch arrival matrix is also the same: $\mathrm{M}' = \mathrm{M}$.

The calculations were repeated for 9 different average utilisations with hyperexponential and Erlang batch sizes. Table 3.2 compares the mean queue length in the case of batch arrival and in the case of a pure M/M/1 system. The batch arrival pattern leads to increased queue length. It can be seen in Table 3.2 that even a short tailed batch size distribution can significantly increase the queueing. However, the hyperexponential batch size distribution that has much slower decay increase the queueing even more albeit the average batch length is the same.

The numerical examples in the rest of this section are computed with hyperexponential batch size distribution and $m = 1$, thus the average utilisation is 0.3.

Server utilisation	0.1	0.2	0.3	0.4	0.5	0.6	0.7	0.8	0.9
Heavy batch	5.3	12.7	23.1	38.2	60.1	94.6	153.9	275.4	645.2
Erlang batch	3.2	8.0	14.9	25.3	41.0	65.9	109.4	199.0	473.6
M/M/1	0.11	0.25	0.42	0.67	1.0	1.5	2.3	4.0	9.0

Table 3.2: Comparison of the mean queue lengths of M/M/1 and batch arrival systems

Initial matrix	$\mathbf{0}$	$\mathbf{I}$
Iteration steps	5847496	73

Table 3.3: The number of iterations with stopping condition (3.42)

The dimension of the QBD matrices based on (3.16), (3.17) and (3.18) is 26×26. To test the abilities of the numerical methods with a large dimensional problem I did not simplify this QBD representation according to the effective representation, which would result in a smaller dimensional (8×8) matrix. Various solution methods were tested in order to obtain the $\mathbf{G}$ and $\mathbb{G}$ matrices and the stationary distribution.

The $\mathbb{G}$ matrix can be calculated by Equation 3.35 performing iterative substitution:

$$\mathbb{G} = \mathbb{A}_1^{-1} \left(\mathbb{A}_2 + \mathbb{A}_0 \mathbb{G}^2 \right) \ . \tag{3.41}$$

The procedure can be started from the zero matrix and from the identity matrix with the

$$\left| \mathbb{G}_{\text{cur}} - \mathbb{G}_{\text{prev}} \right| < 10^{-8} \tag{3.42}$$

stopping condition.

If the stopping condition is

$$|\mathbb{G}\mathbb{1} - \mathbb{1}| < 10^{-8}, \tag{3.43}$$

and the I start with zero matrix then the algorithm has difficulties because it cannot reach the stopping criteria even after a large number of iterations. The result of the iterative substitution starting from the identity matrix with stopping condition (3.42) “almost satisfies” the stopping condition (3.43) (the $|\mathbb{G}\mathbb{1} - \mathbb{1}|$ error is around $2.8 \cdot 10^{-8}$). If the algorithm is started from the zero matrix using (3.42), then the resulted $\mathbb{G}$ matrix is much worse (the error is around $9.6 \cdot 10^{-3}$).

The modified boundary algorithm (Section 8.3 in Latouche and Ramaswami [34]) is a similar iterative method. It uses stopping condition (3.42) and its main iteration step is

$$\mathbb{G} = (\mathbb{A}_1 + \mathbb{A}_0 \mathbb{G})^{-1} \mathbb{A}_2.$$

Starting from matrix $\mathbf{I}$ the algorithm stopped after 63 iterations. Like in the case of the iterative substitution, the resulting $\mathbb{G}$ matrix “almost satisfies” the stopping condition (3.43) (the error is around $2.8 \cdot 10^{-8}$).

In the case of the logarithmic reduction algorithm (see Section 8.4 in Latouche and Ramaswami [34]) I used the stopping condition (3.42), though Latouche and Ramaswami

[34] propose the stopping condition (3.43). The reason for using the former condition is that in this case the algorithm converged within 25 iteration steps while in the case of latter condition the iteration experienced numerical difficulties.

Although the number of iterations was the smallest with this algorithm for the stopping condition (3.42), the resulting $\mathbb{G}$ was "much worse" than the ones obtained by the previous two algorithms with respect to the $|\mathbb{G}\mathbb{1} - \mathbb{1}|$ error. (It was $8.6 \cdot 10^{-5}$).

The higher order matrix equation can also be solved. For an iterative solution of (3.5) I transformed it to

$$\mathbf{G} = -\mathbf{W_1}^{-1}\left(\mathbf{W_0} + \sum_{i=2}^{c} \mathbf{W_i}\, \mathbf{G}^i\right).$$

I used the initial condition of $\mathbf{G} = \mathbf{0}$ and stopping condition (3.42) applied for $\mathbf{G}$.

This method converges very slowly and the number of operations in one iteration step is large. After 2585156 steps the method converged but the resulting $\mathbf{G}$ matrix has quite "bad quality". The condition (3.43) gives 0.2 that is quite far from the precision of other methods.

Table 3.4 summarizes the number of iteration steps according to (3.40).

Initial matrix	$\mathbf{0}$	$\mathbf{I}$
Iteration steps	11722	50

Table 3.4: The number of iterations with stopping condition (3.40)

Similarly to the previous cases, the number of iterations to reach the respective stopping condition was larger when the initial value of $\mathbf{G}$ was $\mathbf{0}$. Also, the "quality" of matrix $\mathbf{G}$ was worse in this case. The error is $9.99 \cdot 10^{-9}$, while it is $2.7 \cdot 10^{-10}$ with condition (3.43) when I start from the identity matrix.

I denote the size of the original state space by o ($o = |\mathbf{C_0}|$), the size of the state space of the PH batch size by p ($p = |\mathbf{T}|$), and the size of the expanded state space by q ($q = o + 2op$ according to (3.18)). In the present example $o = 2$, $p = 6$ and $q = o + 2op = 26$. The numbers of multiplications needed by the different methods are compared in Table 3.5.

The Table 3.6 shows the values in the present example. The total number of multiplications was computed by multiplying the number of multiplications in an iteration step by the number of iteration steps.

Method	number of multiplications in one iteration
Iterative substitution	$4q^3$
Modified boundary algorithm	$3q^3$
Logarithmic reduction algorithm	$12q^3$
Algorithm on the original state space	$o^3(4p+1) + 4o^2p^2 + 2o^2p + o^2$

Table 3.5: The number of multiplications in one iteration step of four different iteration methods

Method	number of multiplications	
	one step	until convergence
Iterative substitution	$7 \cdot 10^4$	$3 \cdot 10^6$
Modified boundary algorithm	$5 \cdot 10^4$	$3 \cdot 10^6$
Logarithmic reduction algorithm	$2 \cdot 10^5$	$5 \cdot 10^6$
Algorithm on the original state space	10^3	$5 \cdot 10^4$

Table 3.6: The total number of multiplications of four different iteration methods

I concluded that the methods working on the expanded state space have approximately the same complexity while the method working on the original state space has significantly smaller complexity.

I have got two approaches to calculate the stationary probabilities. The first approach operates on the expanded state space while the second one works with the original block size.

The stationary distribution of the expanded QBD process can be computed as $\pi'_n = \pi'_0\mathbb{R}^n$, where $\mathbb{R}$ is given in (3.21).

Here the interesting part of π'_n is the first block $\pi'_{n,0}$. The solution has to be normalized such that $\sum_{n=0}^{\infty} \pi'_{n,0}\mathbb{1} = 1$. The required π'_0 can be obtained by solving the following system of equations:

$$\pi'_0 \left(\mathbb{B} + \mathbb{A}_0\mathbb{G}\right) = \mathbf{0},$$

$$\pi'_0 \left(\mathbb{I} - \mathbb{R}\right)^{-1} \mathbb{1}^* = 1,$$

where $\mathbb{1}^*$ is a column vector with the same dimension as π'_0, whose first $|\pi'_{n,0}|$ block contains ones and the rest of the vector elements are zero. The sub-block structure to calculate $(\mathbb{I} - \mathbb{R})^{-1}$ is provided in (3.22).

Once π'_0 is computed, π'_{n+1} can be obtained in an iterative way from π'_n by $\pi'_{n+1} = \pi'_n\mathbb{R}$. An advantage of this method is that the number of operations needed in one iteration step is independent of n.

Another advantage of the method is that it works with small matrices only. However, the number of operations needed in the iteration step to compute π_n increases with n.

The queue length of an $M/G/1$ type queueing system with power-tailed service time distribution rate has a power-tail. In a queueing system with batch arrival, the batch size plays a similar role, i.e., if the batch size has power-tail, then the queue length also has power-tail. The present example allows for checking this property, although the batch size does not have a proper power-tailed distribution, but it is slowly decaying for several orders of magnitude. Figure 3.3 shows the queue length distribution in log-log scale calculated with the expanded QBD method. The numerical complexity of method based on (3.6) increases with the queue length. It was infeasible to calculate the probability of a queue length larger than 10^3 with this method.

One can see a region in the distribution of both the batch size (Figure 3.5) and the queue length (Figure 3.3) where the decay is almost linear in log-log scale. That is, within this region the distribution functions approximate $c\, n^b$ functions. These regions go though 5 orders of magnitude in both cases. The power of the decay is approximately

$b = -3.5$ for the batch size, and $b = -2.5$ for the queue length distribution as it can be expected from the $M/G/1$ analogy.

The example can be solved numerically using the formulae presented in Section 13.1 in Latouche and Ramaswami [34]. However, the application of this approach needs finite batch sizes. Therefore, the PH distribution represented by the $(\mathbf{T}, \alpha)$ is approximated by a distribution with finite support such that

$$p_n = \frac{P(X = n)}{P(X \leq N)}, \quad 1 \leq n \leq N, \text{ and } p_n = 0, \quad n > N,$$

where X is a $(\alpha, \mathbf{T})$ PH distributed random variable.

Equation 13.10 in Latouche and Ramaswami [34] (similar to (3.4)) was solved by iterative substitution initialised with the identity matrix. The $\mathbf{C_0}$ and $\mathbf{C_1}$ matrices of Latouche and Ramaswami [34] are the same as ours, $\mathbf{C_n} = p_{n-1}\mathbf{M}$ for $2 \leq n \leq N$ and $\mathbf{C_n} = \mathbf{0}$ for $n > N$. The stopping condition of the iteration was (3.42). The number of iteration steps until the solution converged was around 10 for $N = 100$, $N = 1000$ and $N = 100000$. That is, the number of iterations seems to be independent of N. As it can be expected, if N is small, the queue length distribution quickly reaches the geometric tail and if N is larger, it follows the exact distribution longer in Figure 3.4. The conclusion is that in order to approximate larger quantiles of the queue length distribution with this method, the truncation point N has to be chosen to be extremely large (in the order of 10^8 or more). The required number of calculations makes this approximation method to be numerically infeasible because of the running time and the numerical errors.

3.5 Notes

Here I desrcibe the transformation from the matrix based description of DPH distributions (3.1) into their scalar description (3.14). The $a_{j\ell}$ coefficients can be calculated from the Jordan decomposition of $\mathbf{T}$:

$$\mathbf{T} = \Gamma^{-1}\mathbf{D}\Gamma,$$

where $\mathbf{D}$ has the Jordan-block structure $\mathbf{D} = \text{diag}\{\mathbf{D}_j\}$ with

$$\mathbf{D}_j = \begin{pmatrix} \lambda_j & 1 & 0 & \dots & 0 \\ 0 & \lambda_j & \ddots & \ddots & \vdots \\ \vdots & \ddots & \ddots & \ddots & 0 \\ 0 & 0 & \ddots & \lambda_j & 1 \\ 0 & 0 & \dots & 0 & \lambda_j \end{pmatrix}. \tag{3.44}$$

The size of the $\mathbf{D}_j$ Jordan-block is $\#\lambda_j \times \#\lambda_j$, where $\#\lambda_j$ is the multiplicity of the λ_j eigenvalue.

Substituting this form into (3.1) I have

$$p(i) = \alpha\mathbf{T}^{i-1}t = \alpha\Gamma^{-1}\mathbf{D}^{i-1}\Gamma t = \alpha\Gamma^{-1}\text{diag}\{\mathbf{D}_j^{i-1}\}\Gamma t. \tag{3.45}$$

Due to the structure of Jordan-blocks the elements of the $\mathbf{D}_j^{i-1}$ matrix are

$$[\mathbf{D}_j^{i-1}]_{m,m+\ell-1} = \begin{cases} 0 & \text{if } \ell < 1, \\ \binom{i-1}{\ell-1}\lambda_j^{i-\ell} & \text{if } 1 \leq \ell. \end{cases}$$

Therefore, the $a_{j\ell}$ coefficients can be calculated as the coefficients of the $\binom{i-1}{\ell-1}\lambda_j^{i-\ell}$ term in (3.45).

We note that the general results can be obtained using elementary calculus in the special case of a BMAP/M/1 queue with geometrically distributed batch size. The details are discussed in Éltető and Telek [O1].

Chapter 4

Thesis 3: Analysis of MAP/G/∞ queues

4.1 Problem statement

The assumption of the Poisson customer/flow arrival is considerably general since this is the limiting process in telecommunication systems, when arrivals occur from a large population especially in scenarios where there is significant network traffic (see e.g. Cao et al. [15] or Karagiannis et al. [29]). However there are cases, when the arrival is not a Poisson process. This is the case, for example, when the start of a user activity results in the arrival of several flows in a short time. The web browsing is a good example for such correlated connection arrivals since the download of the objects belonging to a web page involves several transfers (for more details see Vidács et al. [C2]).

It is also possible that the starts of the user activities themselves are correlated. Two examples are:

- Many users wish to use a web shop at the same time because there is a price discount available.
- When a cell phone is switched on, it attaches to a GSM network. During the attach procedure, the identity, location and other details are registered in the HLR (Home Location Register). These information are maintained until the cell phone detaches from the network. There is a typical daily pattern of the attaches, that is, more subscribers switch on their phones during the morning hours than during the afternoon or around midnight.

Both examples lead to queueing system models where the arrival is correlated and there are infinitely many servers, that is, the jobs are immediately start their service in the model.

Takács [59] showed that in a stationary M/G/∞ system the number of customers in the system has Poisson distribution that depends on the average arrival rate and average holding time of the calls, but it does not depend on higher moments of the holding time distribution. However, the above examples highlight that there are cases when the arrival is not Poisson process, therefore Takács's insensitivity result does not apply, and there is a need for applicable solution techniques.

The existing matrix geometric approaches of infinite server queueing systems are based on a set of differential equations describing the time dependent moments of the number of customers. This was first presented by Ramaswami and Neuts in [50]. There, the arrival process was a Phase-type renewal process. Masuyama and Takine in [39] generalised the problem to BMAP (Batch Markovian Arrival Process). Assuming Phase-type holding time distribution, the analytical solution for the moments is possible – otherwise the authors refer to the numerical solution of the differential equations. However, the formulae describing the solution become increasingly complex with the higher moments. Also, it can be difficult to obtain the probabilities of the number of customers from the moments (e.g. Rácz et al. [49]).

The approach of Thesis 3 is different from the existing approaches of Masuyama and Takine [39]. The main contribution of Thesis 3 is that it provides a numerical method for approximating the stationary probability distribution without having to evaluate the moments of the number of customers. Bounds on the error of the approximation are presented, therefore it is possible to find the practical tradeoff between the numerical accuracy and the computational complexity. Thesis 3 also shows that the analytical results of Masuyama and Takine [39] can be generalised from the Phase-type holding time distribution to a wider class of distributions in the case of MAP arrivals.

I use the proposed numerical methods to evaluate a specific telecommunication example with special attention on the dependence between the stationary distribution and the correlation in the arrival process. I also briefly investigate the sensitivity of the solution on the distribution of the customer holding time.

4.2 Results

The results are published in [C6].

Thesis 3

In Thesis 3 I propose a numerical solution for a MAP/G/∞ system. The solution does not restrict the service time distribution. The first step of finding the solution is the calculation of the moment-generating function of the stationary number of customers in the MAP/G/∞ system for discrete holding time distributions. Next, I generalise it to continuous time distributions. I show that the formula obtained in this way is in fact a form of the probability generating functional of the MAP point process. I also show some elementary manipulation techniques and numerical bounds that are used in the numerical procedures.

The moment-generating function of the number of arrivals of a MAP with matrices $\mathbf{D_0}$ and $\mathbf{D_1}$ (see Thesis 2 for the definition of MAP) in the $(0, x)$ interval is defined as

$$P_{i,j}(z, x) = E(z^{N(x)}|J(0) = i, J(x) = j)P(J(x) = j|J(0) = i),$$

where $N(x)$ denotes the number of arrivals in $(0, x)$, and $J(x)$ is the state of the background Markov chain at time x. The $\mathbf{P}(z, x) = \{P_{i,j}(z, x)\}$ matrix is given e.g. by Latouche and Ramaswami [34]:

$$\mathbf{P}(z, x) = e^{(\mathbf{D_0}+z\mathbf{D_1})x}.$$

The idea is that the customers at, say, time 0 are those who arrived before and did not leave until that time. This implies that the MAP arrival process should be filtered since only some of the customers are still in the system at time 0. It is possible that from those who have arrived before some are already left the system. The filtration of the MAP process can be described by introducing the time dependent MAP process, that is, the phase transition structure of the arrival process changes over time.

Definition 5. *Let MAP1 and MAP2 be two MAP processes on the same state space. MAP1 is characterized by* $(\mathbf{D_0^{(1)}}, \mathbf{D_1^{(1)}})$ *and MAP2 by* $(\mathbf{D_0^{(2)}}, \mathbf{D_1^{(2)}})$*. In interval* (s,t)*, the arrivals are generated by MAP1, and in interval* (t,u) *the arrivals are generated by MAP2 such that the initial state of MAP2 at* t *is the state of MAP1 at* t*, i.e.,* $J_1(t) = J_2(t)$ *(Figure 4.1).*

In order to handle time dependent MAPs, I introduce the $\mathbf{P}(z,x,y) = \{P(z,x,y)_{i,j}\}$ matrix as the moment-generating function of the number of arrivals in the (x,y) interval, where

$$P_{i,j}(z,x,y) = E(z^{N(x,y)} | J(x) = i, J(y) = j) P(J(y) = j | J(x) = i), \tag{4.1}$$

and $N(x,y)$ denotes the number of arrivals in the (x,y) interval. Using this definition one can investigate the basic properties of piece-wise constant time dependent MAP processes.

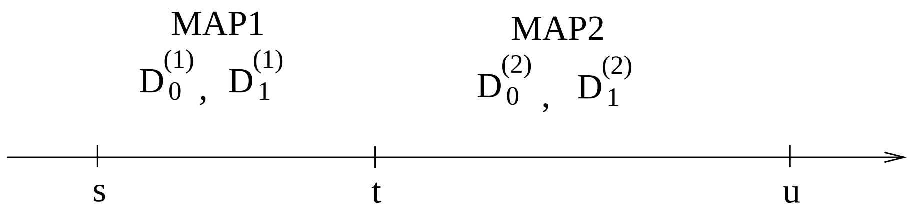

Figure 4.1: Piece-wise constant time dependent MAP

Thesis 3.1

In Thesis 3.1, I derive the moment-generating function of the arrivals of a piece-wise constant time dependent MAP process. Using this expression I calculate the moment-generating function of the number of customers in a MAP/G/∞ system with discrete holding time distribution.

The first step for establishing the moment-generating function of the number of customers in the system is the identification of the moment-generating function of a piece-wise constant time dependent MAP consisting of two pieces.

Theorem 6. *The moment-generating function of the number of arrivals in the* (s,u) *interval is*

$$\mathbf{Z}(z,s,u) = \mathbf{Z_1}(z,s,t) \cdot \mathbf{Z_2}(z,t,u),$$

where $\mathbf{Z_1}(z,s,t) = e^{(\mathbf{D_0^{(1)}} + z\mathbf{D_1^{(1)}})(t-s)}$ *and* $\mathbf{Z_2}(z,t,u) = e^{(\mathbf{D_0^{(2)}} + z\mathbf{D_1^{(2)}})(u-t)}$.

Corollary 7. *Theorem 6 can be generalised to a piece-wise constant time dependent MAP with arbitrary number of pieces.*

I formally state the relation between the piece-wise constant MAPs and the MAP/G/∞ system. Consider an infinite server queueing system where the customers arrive to the system according to a $(\mathbf{D_0}, \mathbf{D_1})$ MAP and stay for a random amount of time X. The service time is a discrete random variable with finite support. Denote the probability distribution by

$$P(X = a_i) = p_i, i = 1, \ldots, n,$$

where $a_1 > a_2 > \ldots > a_n > 0$. For notational convenience I introduce $a_{n+1} = 0$ (Figure 4.2).

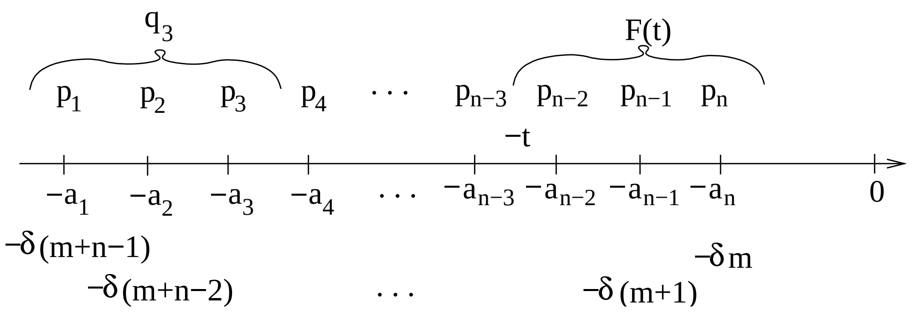

Figure 4.2: Discrete equidistance service time distribution

Some of the customers arriving in the past leave before time 0. Since the goal is to collect those customers, who are still in the system, the past arrival instants have to be filtered by the probability of staying at least until 0. That is, the arrival process of the "oldest" customers (arriving in the $[-a_1, -a_2]$ interval) is $(\mathbf{D_0} + (1 - q_1)\mathbf{D_1}, q_1\mathbf{D_1})$ and so on.

Theorem 8. *The moment-generating function of the stationary number of customers (N) in the system is*

$$E(z^N) = \pi \left(\prod_{i=1}^{n} e^{(\mathbf{D}+(z-1)q_i\mathbf{D_1})(a_i - a_{i+1})} \right) \mathbb{1}, \tag{4.2}$$

where $\mathbf{D} = \mathbf{D_0} + \mathbf{D_1}$*,* π *is the stationary distribution of the CTMC with generator* $\mathbf{D}$*,* $q_i = \sum_{j=1}^{i} p_j$*,* $\mathbb{1}$ *is the column vector of ones, and the product is ordered.*

Thesis 3.2

In Thesis 3.2, I generalise the result obtained for discrete holding time distribution to analyse the MAP/G/∞ queue with continuous time distribution. I show that the expression for the moment-generating function is strongly related to the probability generating functional of the MAP point process. I show that the moment-generating function in the continuous case can be expressed as a product. I show an inverse transformation method obtaining the probabilty distribution of the number of customers in the system.

I show a formula describing the MAP/G/∞ system with discrete holding time distribution. Next, I investigate how this formula changes if the discretisation becomes "infinitely fine", that is, continuous.

Theorem 9. *The moment-generating function of the number of customers in MAP/G/∞ queue with holding time distribution $F(t)$ with support on the (t,T) interval is*

$$\begin{aligned}\mathbf{P}(z,t,T) &= \mathbf{I} + \int_t^T (\mathbf{D} + (z-1)(1-F(y_1))\mathbf{D_1})dy_1 \\ &+ \int_t^T (\mathbf{D} + (z-1)(1-F(y_1))\mathbf{D_1}) \int_t^{y_1} (\mathbf{D} + (z-1)(1-F(y_2))\mathbf{D_1})dy_2 dy_1 \\ &+ \dots\end{aligned} \tag{4.3}$$

This form of the moment-generating function can be rearranged into another form:

$$\begin{aligned}\mathbf{P}(z,t,T) &= e^{\mathbf{D}(T-t)} + (z-1)\int_t^T e^{\mathbf{D}(T-y_1)}(1-F(y_1))\mathbf{D_1}e^{\mathbf{D}(y_1-t)}dy_1 \\ &+(z-1)^2 \int_t^T e^{\mathbf{D}(T-y_1)}(1-F(y_1))\mathbf{D_1}\int_t^{y_1} e^{\mathbf{D}(y_1-y_2)}(1-F(y_2))\mathbf{D_1}e^{\mathbf{D}(y_2-t)}dy_2 dy_1 \\ &+ \dots\end{aligned} \tag{4.4}$$

The significance of this form is that in case of $t=0$, $T=\infty$, I obtain the moment-generating function of the MAP/G/∞ system as the evaluation of the probability generating functional of the MAP point process with the function $1-F(t)$. Section 5.5 of Daley and Vere-Jones [19] proposes the following expansion for the probability generating functional of an arbitrary point process:

$$G[1+\eta] = 1 + \sum_{k=0}^{\infty} \frac{1}{k!} \int_{\mathcal{X}^{(k)}} \eta(x_1)\dots\eta(x_k)M_{[k]}(dx_1 \times \dots \times dx_k),$$

where $M_{[k]}$ is the kth factorial moment measure, and $\eta(\cdot)$ is a bounded Borel measurable $\mathbb{R} \to \mathbb{C}$ function. The measurable space for the kth factorial moment measure in the present case is $\mathbb{R}^k$. In fact, here

$$\eta(x) = -(z-1)(1-F(x)),$$

$$G[1+\eta] = \pi\mathbf{P}(z,0,\infty)\mathbb{1}$$

and

$$M_{[k]}(dx_1 \times \dots \times dx_k) = \pi e^{\mathbf{D}(x_1-0)}\mathbf{D_1}\dots\mathbf{D_1}e^{\mathbf{D}(x_k-x_{k-1})}\mathbf{D_1}e^{\mathbf{D}\infty}\mathbb{1}dx_1 \times \dots \times dx_k,$$

if $x_1 > x_2 > \dots > x_k$. In case one is interested in the first factorial moment measure, that is, the Lebesgue measure multiplied by the average arrival intensity, then the above gives the following expression

$$M_{[1]}(dx) = \pi e^{\mathbf{D}(x-0)}\mathbf{D_1}e^{\mathbf{D}\infty}\mathbb{1}dx = \pi\mathbf{D_1}\mathbb{1}dx$$

that is familiar from the matrix-geometric theory.

The second form (4.4) of the moment-generating function makes it possible to identify a wide class of holding time distributions $F(x)$, for which the integrals can be computed analytically. It is not difficult to see that the elements of the matrix exponential functions have the following general form:

$$\left[e^{\mathbf{D}x}\right]_{i,j} = \sum_{k=1}^{\#\lambda} \sum_{l=1}^{\#\lambda_k} c_{k,l} x^l e^{\lambda_k x},$$

where $\#\lambda$ denotes the number of eigenvalues in matrix $\mathbf{D}$, and $\#\lambda_k$ denotes the multiplicity of the eigenvalue λ_k. If $F(x)$ is a distribution function with the following piece-wise behaviour

$$F(x) = \begin{cases} \sum_{k=1}^{K^{(1)}} \sum_{l=1}^{L_k^{(1)}} c_{k,l}^{(1)} x^l e^{\gamma_k^{(1)} x}, & 0 \leq x < t_1 \\ \sum_{k=1}^{K^{(2)}} \sum_{l=1}^{L_k^{(2)}} c_{k,l}^{(2)} x^l e^{\gamma_k^{(2)} x}, & t_1 \leq x < t_2 \\ \vdots & \\ \sum_{k=1}^{K^{(N)}} \sum_{l=1}^{L_k^{(N)}} c_{k,l}^{(N)} x^l e^{\gamma_k^{(N)} x}, & t_{N-1} \leq x \end{cases} \tag{4.5}$$

then the integral coefficients for any of the powers of $(z-1)$ in (4.4) will have the same general pice-wise form having coefficients that depend on the coefficients of $e^{\mathbf{D}x}$ and $F(x)$ with analytically tractable relations. Note that the class of distributions with structure like (4.5) are called expolynomial distributions. All continuous Phase-type distributions are also expolynomial but there are non-Markovian distributions in the class, e.g. the uniform distribution. It is easy to see that the class of expolynomial distributions is closed to the convolution and probability mixture.

I showed that the moment-generating function of the MAP/G/∞ in the case of discrete service time can be given in a product form. This property remains in the continuous case as well.

Corollary 10. *Due to Theorem 9. and (4.13) the moment-generating function* $\mathbf{P}(z,t,T)$ *can be expressed as the product of "sub moment-generating functions":*

$$\mathbf{P}(z,t,T) = \mathbf{P}(z,t^*,T) \cdot \ \mathbf{P}(z,t,t^*),$$

where $t^* \in (t,T)$.

Corollary 10. can be useful, for example, in such cases when the calculation of the moment-generating function by integrating over an interval (t,T) is difficult, but it is much less difficult over subintervals like (t,t^*) and (t^*,T). This is the case, for example, when the holding time distribution changes at t^*.

The moment-generating function of the number of customers with unbounded positive holding time distribution is obtained as $\mathbf{P}(z,0,\infty) = \lim_{T\to\infty} \mathbf{P}(z,0,T)$. Using the definition of $\mathbf{P}(z,t,T)$, the probability of having n customers in the system, $\mathbf{V}_n(t,T)$, can be obtained by the residue theorem.

Corollary 11. *Since* $\mathbf{P}(z,t,T)$ *is the moment-generating function of* $\mathbf{V_n}(t,T)$, $\mathbf{V_n}(t,T)$ *is the residue of the function* $\frac{1}{z^{n+1}}\mathbf{P}(z,t,T)$ *in* $z=0$.

$$\mathbf{V}_n(t,T) = \frac{1}{2\pi i} \oint \frac{1}{z^{n+1}} \mathbf{P}(z,t,T) dz, \tag{4.6}$$

where $\imath$ is the imaginary unit.

Thesis 3.3

In Thesis 3.3, I define a partial ordering between the distribution functions. I show that the partial ordering of service time distributions is preserved among the the stationary distributions of the number of customers in the MAP/G/∞ systems. These results make it possible to bound the moments and the probability distributions from below and above. The bounds are used in the validation of the numerical approximation of the stationary number of customers.

Since my proposed method for computing the distribution is essentially numerical, I define relations that will be helpful in the error control of the approximations. Let the relation of random variables X and Y, and their moment-generating functions be defined as follows.

Definition 12. *$X \trianglelefteq Y$ iff $P(X \le x) \ge P(Y \le x)$ for $\forall x$ (i.e., $F_X(x) \ge F_Y(x)$) and $X(z) \trianglelefteq Y(z)$ iff $P(X \le x) \ge P(Y \le x)$ for $\forall x$ where $X(z) = E(z^X)$ and $Y(z) = E(z^Y)$ are the moment-generating functions of X and Y, respectively.*

Note that

- $X_1 \trianglelefteq Y_1$ and $X_2 \trianglelefteq Y_2$ imply $X_1 + X_2 \trianglelefteq Y_1 + Y_2$,
- $X_1(z) \trianglelefteq Y_1(z)$ and $X_2(z) \trianglelefteq Y_2(z)$ imply $X_1(z)X_2(z) \trianglelefteq Y_1(z)Y_2(z)$ and
- $X \trianglelefteq Y$ implies that the nth ordinary and the nth factorial moments of X are not greater than the ones of Y, i.e., $E(X^n) \le E(Y^n)$ and $E(X(X-1)\dots(X-n+1)) \le E(Y(Y-1)\dots(Y-n+1))$.

I use this relation of random variables to present the relation of the number of customers in the MAP/G/∞ system with different service time distributions. Let $\mathbf{P}(z,t,T)$ be the generator matrix of the number of customers present in the MAP/G/∞ system at time 0, and arrived in the $(-T,-t)$ interval with arrival process $\mathbf{D_0}, \mathbf{D_1}$, and service time distribution $F(t)$. Similarly let $\mathbf{P}^*(z,t,T)$ be the same generator matrix with arrival process $\mathbf{D_0}, \mathbf{D_1}$, and service time distribution $F^*(t)$.

Theorem 13. *If $F(t) \ge F^*(t)$ then $\mathbf{P}(z,t,T) \trianglelefteq \mathbf{P}^*(z,t,T)$.*

Theorem 13. implies that if $F(t)$ is a continuous distribution function and $\check{F}(t)$, $\hat{F}(t)$ are two discrete distribution functions with finite support, and they bound $F(t)$ from both sides, then there is no need to evaluate any integrals involving $F(t)$ as a function, because the discrete distributions make it possible to use Theorem 8.

Theorem 14. *$\mathbf{P}(z,t,T)$ is bounded by the following integrals of matrix exponential expressions*

$$\underline{\mathbf{P}}(z,t,T) \trianglelefteq \mathbf{P}(z,t,T) \trianglelefteq \overline{\mathbf{P}}(z,t,T), \tag{4.7}$$

where $t = t_0 < t_1 < \ldots < t_{N-1} < t_N = T$

$$\underline{\mathbf{P}}(z,t,T) = \prod_{i=0}^{N} \check{\mathbf{P}}(z,t_{N-i},t_{N-i+1}), \quad \overline{\mathbf{P}}(z,t,T) = \prod_{i=0}^{N} \hat{\mathbf{P}}(z,t_{N-i},t_{N-i+1}),$$

and

$$\check{\mathbf{P}}(z,t_k,t_{k+1}) = e^{\mathbf{D}(t_{k+1}-t_k)} + (z-1)(1-F(t_{k+1}))\int_{t_k}^{t_{k+1}} e^{\mathbf{D}(t_{k+1}-y_1)}\mathbf{D_1}e^{\mathbf{D}(y_1-t_k)}dy_1$$
$$+(z-1)^2(1-F(t_{k+1}))^2\int_{t_k}^{t_{k+1}} e^{\mathbf{D}(t_{k+1}-y_1)}\mathbf{D_1}\int_{t_k}^{y_1} e^{\mathbf{D}(y_1-y_2)}\mathbf{D_1}e^{\mathbf{D}(y_2-t_k)}dy_2dy_1$$
$$+\dots \tag{4.8}$$

$$\hat{\mathbf{P}}(z,t_k,t_{k+1}) = e^{\mathbf{D}(t_{k+1}-t_k)} + (z-1)(1-F(t_k))\int_{t_k}^{t_{k+1}} e^{\mathbf{D}(t_{k+1}-y_1)}\mathbf{D_1}e^{\mathbf{D}(y_1-t_k)}dy_1$$
$$+(z-1)^2(1-F(t_k))^2\int_{t_k}^{t_{k+1}} e^{\mathbf{D}(t_{k+1}-y_1)}\mathbf{D_1}\int_{t_k}^{y_1} e^{\mathbf{D}(y_1-y_2)}\mathbf{D_1}e^{\mathbf{D}(y_2-t_k)}dy_2dy_1$$
$$+\dots \tag{4.9}$$

I note that in the case when $F(t)$ does not have finite support then it is not possible to find a finite discrete distribution function that bounds $F(t)$ above. In this case one should truncate the infinite support. The error of the truncation can be estimated as it is done in Theorem 15.

Theorem 15. *Computing the probability masses with (4.6) the error caused by a finite truncation of the service time distribution at T is bounded by*

$$\|\mathbf{V_n}(0,\infty) - \mathbf{V_n}(0,T)\| \le lD^n\epsilon(z,T), \tag{4.10}$$

where $\epsilon(z,T) = \left(e^{|z-1|\|\mathbf{D_1}\|\int_T^\infty(1-F(y))dy} - 1\right)e^{|z-1|\|\mathbf{D_1}\|E(X)}$, and l is the length of the closed contour around 0 on which the residue is calculated, $1/D$ is the minimum distance of the closed contour from 0. If the residue is calculated on circle with radius r, then $l = 2r\pi$ and $D^n = r^n$.

4.3 Discussion

I begin the discussion with the proofs of the theorems stated in the Thesis.
Proof of Theorem 6: According to its definition the complete moment-generating function is

$$\mathbf{P}_{i,j}(z,s,u) = E(z^{N(s,t)+N(t,u)}|J(s)=i,J(u)=j)P(J(u)=j|J(s)=i)$$
$$= \sum_k E(z^{N(s,t)+N(t,u)}|J(s)=i,J(t)=k,J(u)=j) \tag{4.11}$$
$$\cdot P(J(t)=k|J(s)=i,J(u)=j)\ P(J(u)=j|J(s)=i).$$

Since the $N(s,t)$ and the $N(s,t)$ processes are conditionally independent, the conditional expectation can be broken up as

$$E(z^{N(s,t)+N(t,u)}|J(s)=i,J(t)=k,J(u)=j)$$
$$= E(z^{N(s,t)}|J(s)=i,J(t)=k)\ E(z^{N(t,u)}|J(t)=k,J(u)=j),$$

and using the Markov-property

$$P(J(t) = k|J(s) = i, J(u) = j)\ P(J(u) = j|J(s) = i)$$
$$= P(J(t) = k|J(s) = i)\ P(J(u) = j|J(t) = k),$$

from which the theorem comes. □

Proof of Theorem 8: I evaluate the distribution of customers in this queueing system at time 0. The customers arriving to the system before $-a_1$ leave before 0. The customers arriving in the $(-a_i, -a_{i+1})$ interval are present at time 0 with probability $q_i = \sum_{j=1}^{i} p_j$ and leave before time 0 with probability $1 - q_i$. The customers arrive in the $(-a_n, 0)$ interval are all present at time 0. Note that $q_n = 1$.

Based on the interpretation that the arrivals of the $(-a_i, -a_{i+1})$ interval are filtered out with probability $1 - q_i$, I can generate an equivalent piece-wise constant time dependent MAP, whose number of arrivals in the $(-a_1, 0)$ interval is identical with the number of customers of the considered MAP/D$_n$/∞ queue at time 0.

The equivalent piece-wise constant time dependent MAP is identical with the original one, except that, it takes into consideration the filtering of arrivals. In the $(-a_i, -a_{i+1})$ interval the equivalent MAP is characterized by $(\mathbf{D_0} + (1 - q_1)\mathbf{D_1}, q_1\mathbf{D_1})$, and in the $(-a_n, 0)$ interval it is identical with the original one, i.e. $(\mathbf{D_0}, \mathbf{D_1})$. Figure 4.3 shows the equivalent piece-wise constant time dependent MAP.

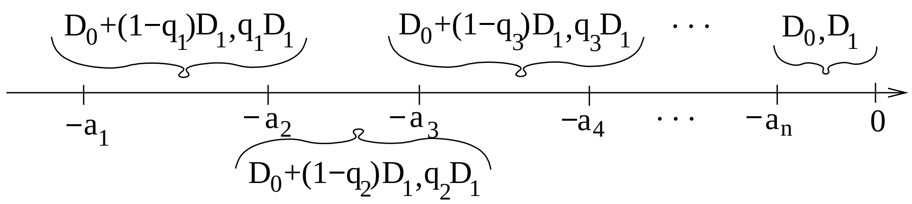

Figure 4.3: The equivalent time dependent MAP

The moment-generating function of the number of arrivals arrived in the $(-a_i, -a_{i+1})$ interval is

$$P_i(z, -a_i, -a_{i+1}) = e^{(\mathbf{D_0}+(1-q_i+zq_i)\mathbf{D_1})(a_i-a_{i+1})}.$$

According to Theorem 6., the moment-generating function of the number of arriving customers of the equivalent MAP in the $(-a_1, 0)$ interval is:

$$\mathbf{P}(z) = \prod_{i=1}^{n} e^{(\mathbf{D_0}+(1-q_i+zq_i)\mathbf{D_1})(a_i-a_{i+1})} = \prod_{i=1}^{n} e^{(\mathbf{D}+(z-1)q_i\mathbf{D_1})(a_i-a_{i+1})}. \tag{4.12}$$

Considering that the background MAP is in steady state at time $-a_1$, this results in the theorem. □

In the special case when the service time is a discrete equidistance distribution between $m\delta$ and $(n + m - 1)\delta$, such that $a_i = (n + m - i)\delta$ (Figure 4.2), I have

$$F(t) = P(X \leq t) = \sum_{j=n+m-\lfloor t/\delta \rfloor}^{n} p_j, \quad q_i = 1 - F((n+m-i-1)\delta),$$

and the matrix of moment-generating function becomes

$$\mathbf{P}(z)=\prod_{i=1}^{n}e^{(\mathbf{D}+(z-1)q_i\mathbf{D_1})\delta}=\prod_{i=1}^{n}e^{(\mathbf{D}+(z-1)(1-F((n+m-i-1)\delta))\mathbf{D_1})\delta}. \tag{4.13}$$

Proof of Theorem 9: This model is already analysed by Masuyama and Takine [39], however, the moment-generating function below can be obtained as a limit of Equation 4.13.

From (4.13) I have the moment-generating function of the number of customers in a MAP/D_n/∞ queue with equidistance discrete distribution. Introducing the

$$\mathbf{M}((n+m-i-1)\delta)=\mathbf{D}+(z-1)q_i\mathbf{D_1}=\mathbf{D}+(z-1)(1-F((n+m-i-1)\delta))\mathbf{D_1}$$

matrix function (4.13) becomes

$$\mathbf{P}(z)=\prod_{i=1}^{n}e^{(\mathbf{D}+(z-1)q_i\mathbf{D_1})\delta}=\prod_{i=1}^{n}e^{\mathbf{M}((n+m-i-1)\delta)\delta}=\prod_{i=1}^{n}\sum_{k=0}^{\infty}\frac{\mathbf{M}((n+m-i-1)\delta)^k\delta^k}{k!}, \tag{4.14}$$

where $\|\mathbf{M}((n+m-i-1)\delta)\|\leq\|\mathbf{D}+\mathbf{D_1}\|$.

I rewrite this product of infinite sums as an infinite sum of finite sums with increasing order. I group elements of the infinite sum and separate them with large brackets:

$$\begin{aligned}\prod_{i=1}^{n}\sum_{k=0}^{\infty}\frac{\mathbf{M}((n+m-i-1)\delta)^k\delta^k}{k!}&=\Big(\mathbf{I}\Big)+\Big(\sum_{i=1}^{n}\mathbf{M}((n+m-i-1)\delta)\delta\Big)\\&+\Big(\sum_{i=1}^{n-1}\mathbf{M}((n+m-i-1)\delta)\delta\sum_{j=i+1}^{n}\mathbf{M}((n+m-j-1)\delta)\delta+\sum_{i=1}^{n}\frac{\mathbf{M}((n+m-i-1)\delta)^2\delta^2}{2!}\Big)\\&+\Big(\sum_{i=1}^{n-2}\mathbf{M}((n+m-i-1)\delta)\delta\sum_{j=i+1}^{n-1}\mathbf{M}((n+m-j-1)\delta)\delta\sum_{k=j+1}^{n}\mathbf{M}((n+m-k-1)\delta)\delta\\&+\sum_{i=1}^{n-1}\frac{\mathbf{M}((n+m-i-1)\delta)^2\delta^2}{2!}\sum_{j=i+1}^{n}\mathbf{M}((n+m-j-1)\delta)\delta\\&+\sum_{i=1}^{n-1}\mathbf{M}((n+m-i-1)\delta)\delta\sum_{j=i+1}^{n}\frac{\mathbf{M}((n+m-j-1)\delta)^2\delta^2}{2!}+\sum_{i=1}^{n}\frac{\mathbf{M}((n+m-i-1)\delta)^3\delta^3}{3!}\Big)\\&+\ldots\end{aligned}$$

Assuming $\mathbf{M}(x)=\mathbf{D}+(z-1)(1-F(x))\mathbf{D_1}$ is a continuous matrix function, $m=t/\delta$, $n+m-1=T/\delta$, and decreasing δ to 0, the first order terms form weighted sums, which approximate integrals. The higher order terms vanish. The remaining significant terms are:

$$\begin{aligned}&\prod_{i=1}^{n}\sum_{k=0}^{\infty}\frac{\mathbf{M}(T-i\delta)^k\delta^k}{k!}\\&=\Big(\mathbf{I}\Big)+\Big(\sum_{i=1}^{n}\mathbf{M}(T-i\delta)\delta\Big)+\Big(\sum_{i=1}^{n-1}\mathbf{M}(T-i\delta)\delta\sum_{j=i+1}^{n}\mathbf{M}(T-j\delta)\delta\Big)\\&+\Big(\sum_{i=1}^{n-2}\mathbf{M}(T-i\delta)\delta\sum_{j=i+1}^{n-1}\mathbf{M}(T-j\delta)\delta\sum_{k=j+1}^{n}\mathbf{M}(T-k\delta)\delta\Big)+\ldots+\sigma(\delta),\end{aligned} \tag{4.15}$$

where $\sigma(\delta) \to 0$ as $\delta \to 0$. Letting $\delta \to 0$ results

$$\begin{aligned}\mathbf{P}(z,t,T) &= \mathbf{I} + \int_0^{T-t} (\mathbf{D} + (z-1)(1-F(T-x_1))\mathbf{D_1})dx_1 \\ &+ \int_0^{T-t} (\mathbf{D} + (z-1)(1-F(T-x_1))\mathbf{D_1}) \int_{x_1}^{T-t} (\mathbf{D} + (z-1)(1-F(T-x_2))\mathbf{D_1})dx_2dx_1 \\ &+ \dots\end{aligned} \tag{4.16}$$

Substituting $y_i = T - x_i$ results the theorem. □

Proof of Theorem 13:

The proof is based on the interpretation that I observe the number of customers in the queueing system at time 0. A customer arriving to the system at time $-x$ is present at time 0, if its service time is greater than t, i.e., it is present with probability $1 - F(x)$ (or $1 - F^*(x)$). Let $\tau_1, \tau_2, \dots, \tau_n$ denote the arrival instances in the $(-T, -t)$ interval, and X_i (X_i^*) ($1 \leq i \leq n$) the binary random variable indicating if the customer arrived at time $-\tau_i$ is present in the system or not. From $F(\tau_i) \geq F^*(\tau_i)$ it follows that $X_i \trianglelefteq X_i^*$. Therefore the number of customers present in the MAP/G/∞ system at time 0 and arrived in the $(-T, -t)$ interval fulfills $\sum_{i=1}^n X_i \trianglelefteq \sum_{i=1}^n X_i^*$. □

Note that Thoerem 13 and its proof is also valid for any stationary arrival process.

Proof of Theorem 14: Based on the service time distribution, $F(x)$, I define the $\check{F}(x)$ and the $\hat{F}(x)$ discrete distributions as follows

$$\check{F}(x) = F(t_{k+1}) \text{ and } \hat{F}(x) = F(t_k) \text{ if } x \in (t_k, t_{k+1}).$$

By this definition $\check{F}(x) \geq F(x) \geq \hat{F}(x)$. Note that $\check{F}(x)$ and $\hat{F}(x)$ are expolynomial as well.

Noting that $\underline{\mathbf{P}}(z,t,T)$ ($\overline{\mathbf{P}}(z,t,T)$) is the moment-generating function of the number of customers at time 0 arrived in the $(-T, -t)$ interval, when the service time distribution is $\check{F}(x)$ ($\hat{F}(x)$), and using Theorem 13. the theorem is given. □

Theorem 14. allows to bound the stationary distribution of the number of customers from both sides, when the service time distribution has a finite support. In case of a service time distribution with infinite support, the theorem can be used to bound the distribution of customers arrived in any finite interval form both sides. The lower bound obtained for a finite interval is a lower bound of the distribution of customers with infinite service time as well, while the upper bound is approximated by Theorem 15.

Lemma 3. *The moment-generating function fulfills the following bound*

$$\|\mathbf{P}(z,t,T)\| \leq e^{|z-1|\|\mathbf{D_1}\| \int_t^T (1-F(y))dy} \tag{4.17}$$

Proof:

$$\begin{aligned}
&\|\mathbf{P}(z,t,T)\| = \\
&\left\| e^{\mathbf{D}(T-t)} \Big[\mathbf{I} + (z-1) \int_0^{T-t} e^{-\mathbf{D}y_1} \left[(1-F(y_1))\mathbf{D_1}\right] e^{\mathbf{D}y_1} dy_1 \right. \\
&\quad \left. + (z-1)^2 \int_0^{T-t} e^{-\mathbf{D}y_1} \left[(1-F(y_1))\mathbf{D_1}\right] e^{\mathbf{D}y_1} \int_0^{y_1} e^{-\mathbf{D}y_2} \left[(1-F(y_2))\mathbf{D_1}\right] e^{\mathbf{D}y_2} dy_2 dy_1 + \dots \Big] \right\| \\
&\leq 1 + |z-1| \frac{\|\mathbf{D_1}\| \int_t^T (1-F(y))dy}{1!} + \dots + \ |z-1|^n \frac{\|\mathbf{D_1}\|^n \left(\int_t^T (1-F(y))dy\right)^n}{n!} + \dots \\
&= e^{|z-1| \|\mathbf{D_1}\| \int_t^T (1-F(y))dy}.
\end{aligned} \tag{4.18}$$

□

Proof of Theorem 15:

First I provide a bound of $\|\mathbf{P}(z,0,\infty) - \mathbf{P}(z,0,T)\|$ using (4.17):

$$\begin{aligned}
&\|\mathbf{P}(z,0,\infty) - \mathbf{P}(z,0,T)\| = \|\mathbf{P}(z,T,\infty)\mathbf{P}(z,0,T) - \mathbf{P}(z,0,T)\| \\
&\leq \|\mathbf{P}(z,T,\infty) - \mathbf{I}\| \, \|\mathbf{P}(z,0,T)\| \leq \left(e^{|z-1| \|\mathbf{D_1}\| \int_T^\infty (1-F(y))dy} - 1 \right) e^{|z-1| \|\mathbf{D_1}\| \int_0^T (1-F(y))dy} \\
&\leq \left(e^{|z-1| \|\mathbf{D_1}\| \int_T^\infty (1-F(y))dy} - 1 \right) e^{|z-1| \|\mathbf{D_1}\| E(X)} = \epsilon(z,T)
\end{aligned} \tag{4.19}$$

Using this I have

$$\begin{aligned}
&\|\mathbf{V_n}(0,\infty) - \mathbf{V_n}(0,T)\| = \left\| \frac{1}{2\pi i} \oint \frac{1}{z^n} \left(\mathbf{P}(z,0,\infty) - \mathbf{P}(z,0,T)\right) dz \right\| \\
&\leq \left\| \frac{1}{2\pi i} \oint \frac{1}{z^n} \left(\left(e^{|z-1| \|\mathbf{D_1}\| \int_T^\infty (1-F(y))dy} - 1 \right) e^{|z-1| \|\mathbf{D_1}\| E(X)} \right) dz \right\| \\
&\leq \left\| \frac{1}{2\pi i} \oint \frac{\epsilon(z,T)}{z^n} dz \right\| \leq l D^n \epsilon(z,T).
\end{aligned} \tag{4.20}$$

□

4.4 Application

Figure 4.4 shows the structure of the Markov Arrival Process. The arrival rate in State A is $\lambda_A = 0.1 \ 1/s$, and in State B is $\lambda_B = 10.0 \ 1/s$. The mean customer holding time is $E(X) = 100s$.

I consider two service time distributions with the same mean. The hyper-exponential distribution demonstrates the accuracy of the results also with respect to the exact factorial moments, which I can calculate in this case. The other distribution belongs to the Weibull family. There are three main reasons for choosing these distributions:

1. The Weibull distribution does not belong to the Phase-type distribution family therefore it seems to be rather difficult to calculate the factorial moments.

2. The asymptotical decay of the chosen Weibull distribution is slower than exponential, that makes it a good candidate to test the numerical accuracy of the proposed technique.

3. The two considerably different distributions highlight the fact that if the arrival process is not Poisson, then the stationary distribution of the system is not insensitive to the holding time.

In the case of the Weibull distribution the resulting stationary distribution is compared with simulation results and the difference of the upper and lower bounds are presented.

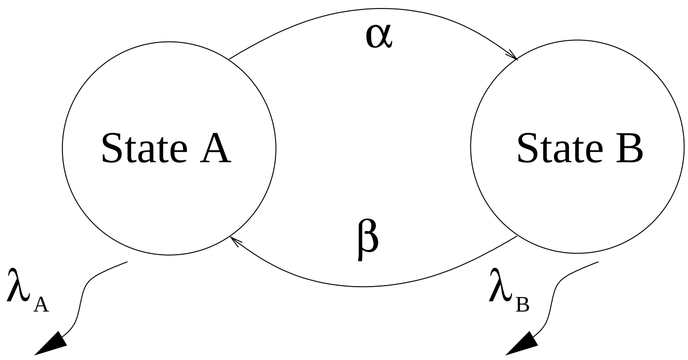

Figure 4.4: The state diagram of the Markov Arrival Process

The exact factorial moments are the integral coefficients in (4.4) that could be formally calculated for expolynomial holding time distributions (e.g. hyperexponetial in the present case) characterised by (4.5). The formal calculations were performed with Maple 5.00. The calculation of the first 20 factorial moments took 24 hours on a SUN Enterprise 420R computer with 450MHz CPU, 2GByte RAM.

The numerical procedure of computing the stationary distribution according to (4.13) is implemented in Octave 2.1.40. It took approximately 15 hours for the numerical calculations to develop the presented results (for hyperexponential and Weibull holding time distributions) on a HP desktop with 2.5 GHz CPU, 1 GByte RAM and Red-Hat linux system. Since the inversion of the generating function could be performed on parallel processors one can reduce the computation time significantly.

The exact moments were not obtained by formal calculations for Weibull distributions that are non-expolynomial. In these cases, the systems were modelled in a tailor-made simulator and the results of the simulations are presented for comparison.

The holding time of the customers is hyper-exponentially distributed with cdf: $F(x) = 1 - \gamma_1 e^{-\mu_1} - \gamma_2 e^{-\mu_2}$, where $1/\mu_1 = 50s$, $\gamma_1 = 0.947$, $1/\mu_2 = 1000s$, $\gamma_2 = 0.053$. Figure 6.3 shows the stationary probability distributions of the number of customers in the system.

In order to validate the numerical computation method, Table 4.1 compares some of the factorial moments obtained from the lower and upper bound calculation of the probability mass function with the direct analysis of factorial moments. The exact moments are always bounded numerically with relative errors of at most 5-6%.

Figures 4.5 and 4.6 present the distribution of the number of customers with Weibull distributed customer holding time: $F(x) = 1 - e^{-(x/\theta)^\eta}$. The parameters were chosen so that the average holding time would approximate the average of the hyperexponential distribution (cca. 100), that is, $\eta = 0.986$, $\theta = 94.8$. The asymptotic decay is slightly sub-exponential. Figures 4.5 and 4.6 present the numerical and discrete event simulation results.

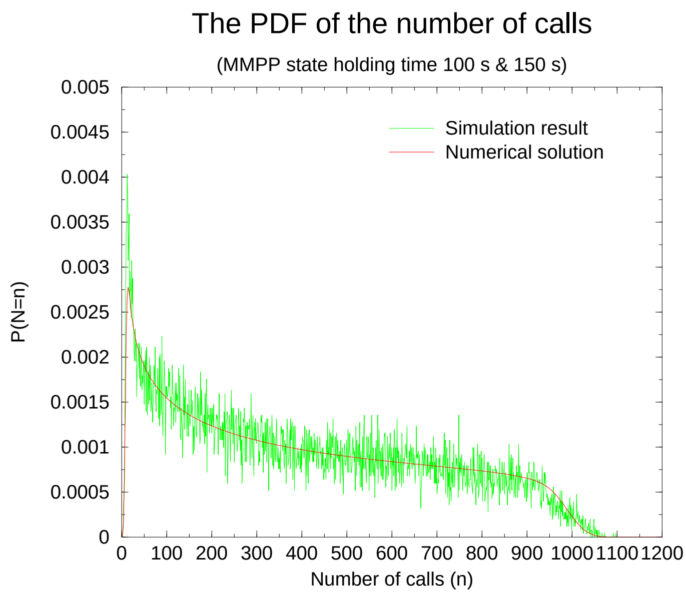

Figure 4.5: The distributions of the number of calls with Weibull service time distribution $(1/\beta = 100, 1/\alpha = 150)$

It worth noting that one can see significant differences between Figure 6.3 c) and Figure 4.6, though the average holding times are approximately the same (cca. 100) and the arrival processes are exactly the same in both cases. The case with hyper-exponential holding time shows that the periods with high and low arrival intensities are much less separated than in the Weibull case. Although there are bi-modal distributions in both cases, the pdf is rather different from the mixture of two Poisson distributions with hyper-exponential holding time than with Weibull holding time.

The numerical estimation procedure involve three types of approximations.

- The infinite support of the holding time is not feasible for the numerical calculations. If the support is truncated, the distribution of the number of customers in the system changes.
- Theorem 13 proves that a continouous time distribution with finite support can be substituted with two discrete distributions in a way that the resulting cumulative distribution functions of the number of customers in the system under- and overestimate the cdf corresponding to the continuous time distribution.

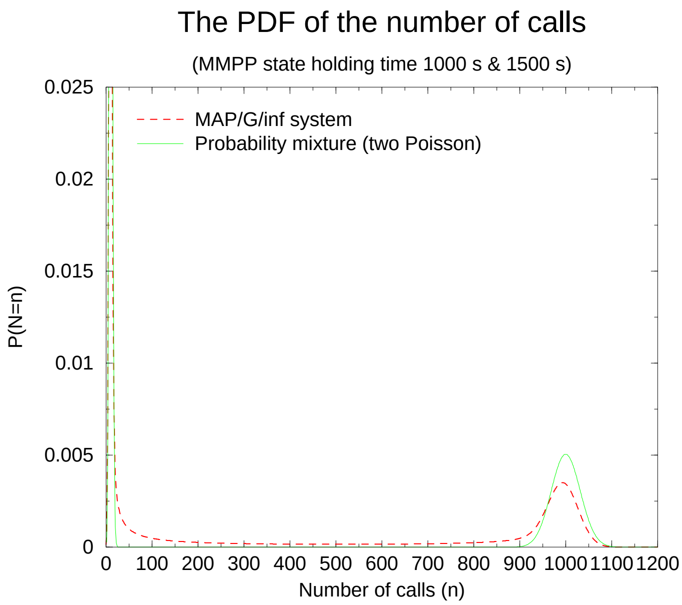

Figure 4.6: The distributions of the number of calls with Weibull service time distribution $(1/\beta = 1000, 1/\alpha = 1500)$

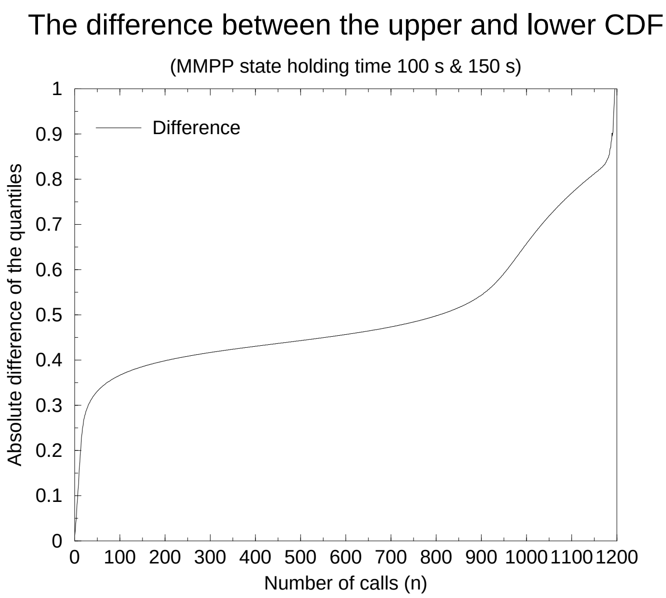

Figure 4.7: The difference of bounds with Weibull service time distribution $(1/\beta = 100, 1/\alpha = 150)$

- The calculation of the distribution function of the number of custormers given a discrete holding time involves numerical integration on a closed contour in the complex plane.

The error analysis resulted in a fairly low error of the approximation. Theorem 15 gives an upper bound for the error, when the the infinite support of the holding time distribution is truncated at a finite point T

$$\|\mathbf{V_n}(0,\infty) - \mathbf{V_n}(0,T)\| \leq lD^n\epsilon(z,T),$$

In the present case $D = 1$ and $l = 2\pi$. If T is chosen to be 465000 seconds then the bound on the overall error ($lD^n\epsilon(z,T)$) is in the order of 10^{-19} for arbitrary $\mathbf{V}_n$. That is, effect of the truncation in the estimated $\mathbf{V_n}$ probability distribution is under control.

The over- and underestimation of the exact distribution due to discretisation does not need to be controlled since the difference between the upper and lower bound provides the error estimation. The probability distribution is discretised into 45000 points. 40000 are distributed in an equi-probabilistic way, that is, the neighbouring $F(t_{k+1}) - F(t_k)$ probabilities (see Theorem 14.) are equal. The remaining 5000 points are spaced evenly between $1337s$ and $100000s$, except that the last point is 465000 seconds. The discrete $\check{F}(x)$ and $\hat{F}(x)$ distributions bound $F(x)$ above and below in the $[0, 465000]$ interval.

The closed contour of the numerical integration is chosen to be the unit circle. The residue integral is approximated by the trapezodial-rule using 1000 evenly placed samples starting at $z = 1$.

The quality of the numerical estimation depends on three main factors:

- the trunctation point T of the holding time distribution,
- the number and location of the points of the discretisation,
- the number and location of the points of the numerical integration in the complex plane.

If T is increased, the error due to the truncation decreases but the size of the support of the distribution becomes larger that should be covered by the discretisation.

The comutational complexity of the numerical method depends linearly on the number of discretisation points. The difference between the upper and lower bounding distributions can be descreased by increasing the number of discretisation points. The difference can also be descreased by choosing appropriate locations of the points without impact on the number of calculations.

The comutational complexity of the numerical method depends linearly on the number of points of the numerical integration. The error of the numerical integration can be decreased by increasing the number of integration points. This error can also be decreased by choosing appropriate numerical integration method that can increase the computational complexity.

As it was described above, the discretisation step leads to an upper and lower bound for the cumulative density function of the number of customers in the system. In the case of hyper-exponential distribution the factorial moments can be compared to the exact calculation as it is done in Table 4.1. However, for Weibull holding time distribution the exact calculation of the moments was not possible. In this case, the quality of the numerical approximation can be evaluated by calculating the difference between the upper and lower bounds obtained from the discretisation.

When the cumulative distribution function of the lower bound is substracted from the cdf of the upper bound, then the scale of the difference is so small that it is difficult to compare it to any of the original functions and the evaluation of the difference (whether it is large or not) is also difficult.

Therefore, the differences between the quantiles corresponding to the same probability is calculated. Figure 4.7 shows this difference. The difference of cca. 0.45 corresponding to 500 calls means the following. Denote the value of the lower bound cdf by $p_{\text{lower},500}$ at 500,

$$p_{\text{lower},500} = P(N_{\text{lower}} <= 500) \approx 0.631.$$

In this case, the $p_{\text{lower},500}$ quantile of the upper bound cdf if 500.45. That is for the value of the upper bound cdf $p_{\text{upper},501}$ at 501,

$$p_{\text{upper},501} = P(N_{\text{upper}} <= 501) \approx 0.632,$$

we have

$$p_{\text{lower},500} \leq p_{\text{exact},500} \leq p_{\text{exact},501} \leq p_{\text{upper},501}.$$

In simple words, compared to the lower bound cdf the upper bound cdf is shifted to right by less than 1. That is either the upper or lower bound effectively estimates the exact distribution of the number of customers in the system up to 1200 calls.

	lower b.	exact.	upper b.
n	$1/\beta = 1s, 1/\alpha = 1.5s$		
1	$4.06 \cdot 10^{2}$	$4.07 \cdot 10^{2}$	$4.09 \cdot 10^{2}$
2	$1.66 \cdot 10^{5}$	$1.67 \cdot 10^{5}$	$1.68 \cdot 10^{5}$
10	$1.51 \cdot 10^{26}$	$1.56 \cdot 10^{27}$	$1.60 \cdot 10^{26}$
15	$2.19 \cdot 10^{39}$	$2.30 \cdot 10^{39}$	$2.39 \cdot 10^{39}$
20	$3.54 \cdot 10^{52}$	$3.76 \cdot 10^{52}$	$3.97 \cdot 10^{52}$

	lower b.	exact.	upper b.
n	$1/\beta = 10s, 1/\alpha = 15s$		
1	$4.06 \cdot 10^{2}$	$4.07 \cdot 10^{2}$	$4.09 \cdot 10^{2}$
2	$1.73 \cdot 10^{5}$	$1.73 \cdot 10^{5}$	$1.74 \cdot 10^{5}$
10	$5.78 \cdot 10^{26}$	$5.91 \cdot 10^{26}$	$6.05 \cdot 10^{26}$
15	$3.21 \cdot 10^{40}$	$3.31 \cdot 10^{40}$	$3.41 \cdot 10^{40}$
20	$2.39 \cdot 10^{54}$	$2.49 \cdot 10^{54}$	$2.59 \cdot 10^{54}$

	lower b.	exact.	upper b.
n	$1/\beta = 100s, 1/\alpha = 150s$		
1	$4.06 \cdot 10^{2}$	$4.07 \cdot 10^{2}$	$4.09 \cdot 10^{2}$
2	$2.07 \cdot 10^{5}$	$2.08 \cdot 10^{5}$	$2.09 \cdot 10^{5}$
10	$9.71 \cdot 10^{27}$	$9.87 \cdot 10^{27}$	$1.00 \cdot 10^{28}$
15	$2.48 \cdot 10^{42}$	$2.54 \cdot 10^{42}$	$2.61 \cdot 10^{42}$
20	$7.53 \cdot 10^{56}$	$7.78 \cdot 10^{56}$	$8.06 \cdot 10^{56}$

	lower b.	exact.	upper b.
n	$1/\beta = 1000s, 1/\alpha = 1500s$		
1	$4.06 \cdot 10^{2}$	$4.07 \cdot 10^{2}$	$4.09 \cdot 10^{2}$
2	$2.86 \cdot 10^{5}$	$2.87 \cdot 10^{5}$	$2.88 \cdot 10^{5}$
10	$1.04 \cdot 10^{29}$	$1.06 \cdot 10^{29}$	$1.08 \cdot 10^{29}$
15	$7.50 \cdot 10^{43}$	$7.71 \cdot 10^{43}$	$7.93 \cdot 10^{43}$
20	$5.88 \cdot 10^{58}$	$6.10 \cdot 10^{58}$	$6.34 \cdot 10^{58}$

Table 4.1: Comparison of the first 20 factorial moments from exact and numerical calculation in the case of hyper-exponential holding time distribution

Chapter 5

Thesis 4: Modelling of TCP Flows

5.1 Problem statement

The majority of current Internet traffic is carried by the Transmission Control Protocol (TCP). The central role of TCP called for intensive research on understanding TCP dynamics and developing planning and dimensioning methods for TCP networks. Most of these studies investigating the performance of TCP networks are using the assumption of persistent sources, which always have data to send. However, the most popular application in the current Internet is the World Wide Web (WWW). The WWW is based on the HTTP protocol that mainly uses non-persistent file transfers to retrieve Web pages. Therefore, there is a need for an analysis framework including also non-persistent TCP sources.

The subject of Thesis 4 is the study the traffic of a limited number of TCP connections from access network's perspectice. The goal is to assess the throughput performance of the TCP connections and the queueing behaviour. My choice of subject is based on the following observations.

Observation 1,
In the backbone, the aggregation level makes it worthless to allow increasing queues when the rate of the input traffic exceeds the link capacity (e.g. Kantawala and Turner [28] argue for short buffers in the WAN routers). In cases when core link utilisation is high, it is the packet loss and not the increased round-trip delay that signs this situation to the endhosts, who reduce their sending rate according to e.g. the TCP protocol. This is particularly the case in core networks with high bandwidth-delay product. The reason for this might be that the number of flows can be very large (e.g. Barakat et al. [7] present statistics that at average there are cca. 300 new flows starting in a backbone link in each second). Indeed, when it comes to the study of core networks, the traffic modelling theory considers larger concepts than a single TCP connection. For example, Ben Fredj et al. [21] define the traffic flows as a group of TCP connections in their notion of modelling, while Barakat et al. [7] choose either a flow definition based on 5 tuples (e.g. a TCP connection) or the common 24 bit prefixes in the IP address fields. My main conclusion from these is that the packet loss probability in the backbone is determined by a large number of flows.

Observation 2,
In contrast to the backbone networks, the reduced aggregation makes it possible to allocate large enough buffers in the access networks to handle temporal traffic bursts. I have two conclusions here. On the one hand, due to the relatively large buffer space, the access networks are transparent from packet loss point of view. On the other hand, the queueing delay in this case depends very much on the individual traffic flows (e.g. TCP connections), unlike the packet loss in the backbone network that depends on the aggregate behaviour of the large amount of traffic flows.

Though my choice of subject is rather limited in terms of data volume, number of packets and queue lengths, it is still too complex to approach by a single modelling technique. For example, in theory it might be possible to represent the whole system with a Markov chain with a detailed state space, that accounts for all the building blocks of the queueing system like

- the number of packets in all the queues,
- the internal state variables of all the TCP connections and
- the states of the higher level protocols e.g. HTTP or the individuals using the Internet.

However, even the description of such a Markov chain might be of overwhelming difficulty, not to mention the problem of finding a stationary solution of the Markov chain.

In my view, the main problem is the desire for a uniform description of events operating over significantly different time-scales. I can identify at least three different time-scales. I list them in the order of granularity.

1. The packet level queueing operates in the order of the service time of a packet (i.e. in the order of microseconds).
2. The TCP feedback mechanism operates in the order of the round-trip time of a packet (i.e. in the order of milliseconds).
3. The higher layer protocols such as HTTP or humans operate on human sensible time-scales (i.e. in the order of seconds or above).

In Thesis 4, I attempt to tackle the problem by decomposition according to the three time-scales into three subproblems. I try to answer the question whether it is possible to find relations between the different time-scales. The feedback mechanism of TCP makes this somewhat non-trivial, since the queueing is determined by the rates at which the TCP sources send packets. Furthermore, these rates are partly determined by the queueing delays and packet losses in the network.

There are several related papers in the field of modelling and performance analysis of the TCP protocol. The basic model of the TCP was developed and the well-known inverse square root law was investigated e.g. by Mathis et al. [40] or Padhye et al. [45]. A number of variants of these basic models were also developed by relaxing several assumptions of the original scenario, e.g. in Cardwell [17]. The scope of Thesis 4 is not finding another simplified model of the TCP protocol, but to incorporate them into a modelling framework. The proposed framework is established in such a way that any of these developments can serve as an input for the analysis of the TCP traffic on the time scale of queueing.

The open-loop methodology in the queueing analysis of TCP traffic was shown to be inadequate for proper TCP modelling without extensions taking into consideration the adaptivity of TCP (see e.g. Arvidsson and Karlsson [3]).

One modelling approach, which takes into consideration the closed-loop nature of TCP is the fixed-pont method. It consists of two main iteration steps. One iteration step calculates the TCP throughput and congestion-window size as a function of the network conditions. The other iteration step calculates the average queue lengths, packet losses and other network conditions given the traffic input determined by the TCP protocol.

Some related papers that use the fixed-point methods are Alessio et al. [1], Arvidsson and Krzesinski [4], Bu and Towsley [14], Roughan et al. [53] or De Vendictis et al. [61]. For example, Bu and Towsley [14] consider the TCP flow behaviour with active queue management. Roughan et al. [53] present similar results for TCP network performance.

The fixed point approach makes it possible to treat arbitrary topology networks. However, it is difficult to prove either the existence or the uniqueness of a fixed point in the iteration. The rate of convergence is also a less known issue. Therefore, it is important to find an alternative approach modelling the queueing of TCP without these drawbacks.

In contrast to the earlier studies I deal with *closed-loop modelling principle*. This princple considers a closed-queueing network where neither packets arrive nor leave. Instead, a fixed number of packets are circulating in the network.

Heyman et al. [25] consider a scenario that is somewhat similar to the subject of this work. However, in Heyman [25] there is only one buffer that is filled up when its server utilisation approaches 100%, while the closed-loop modelling or fixed point iterations do not assume bottleneck links a priori. Heyman et al. [25] consider the number of TCP flows describing in this way a coarse time-scale in their model, though a bit unwittingly, since they do not discuss this in detail. Other possibility for improvement is their flow level model, because their desciption is based on the Engset model. Its beautiful feature is that it is insensitive, but there are practical scenarios where the assumptions e.g. on the finite population and independent off-times might not be applicable.

There are another models that obtain more detailed results on the number of parallel connections (Ben Fredj et al. [21]). However, in Ben Fredj [21] the goal is to study the bandwidth sharing. The packet level queueing performance is not dealt with. Both Heyman [25] and Ben Fredj [21] consider particular network topologies and I think that the extention of the modelling presented in these papers to more general topologies is at least not straightforward.

5.2 Results

The results are published in [C4].

Thesis 4

I define an analysis framework outlined in Figure 5.1, describing the traffic of non-persistent TCP connections in access networks that arrive according to a MAP, which is independent of the packet loss and round-trip delay in the network. The proposed framework decomposes the the system into three different time-scales represented by three submodels.

In the network sumbodel, I describe the average queue lengths and average TCP throughputs using the Mean-Value Analysis (MVA). In the flow submodel, I describe the number of parallel TCP connections as a Markov chain. The TCP connections using the same path in the network are grouped in the flow submodel.

I validate the proposed framework in a particular network scenario by comparing the predictions to simulation results. Application level performance descriptors such as average download time can also be obtained.

My proposed analysis framework for TCP network performance analysis has the following main features:

1. it has a *TCP submodel* which can incorporate any of the advanced TCP models;
2. it has a *network submodel* which is based on a closed-loop modelling principle and uses MVA;
3. it has a *flow submodel* which captures the dynamics of parallel non-persistent TCP sources based on a Markov chain;
4. it does not assume any particular network topology;
5. it can provide both average performance descriptors (e.g. queue length, round-trip time, throughput, download time, etc.) and detailed flow level traffic and performance characteristics (e.g. approximate distributions of the above listed characteristics).

The summary of Figure 5.1 is the following. The TCP submodel provides input for both the network and flow submodel. The network submodel provides input for the flow submodel. The flow submodel computes the distribution of the number of TCPs. Finally, the average descriptors are obtained by deconditioning. The following paragraphs describe these in more detail.

The *TCP submodel* describes the TCP's response given certain network conditions. The input parameters here are the usual parameters needed in models describing the TCP protocol, such as the maximum segment size, the advertised window, the acknowledgement strategy, the packet loss probability etc. The output is the average number of packets kept in the network by one TCP connection and the average download time in round-trip units. I note that my modelling framework splits the operation of TCP in some sense. For the packet level traffic of TCP connections, I use the theory of closed-queueing networks.

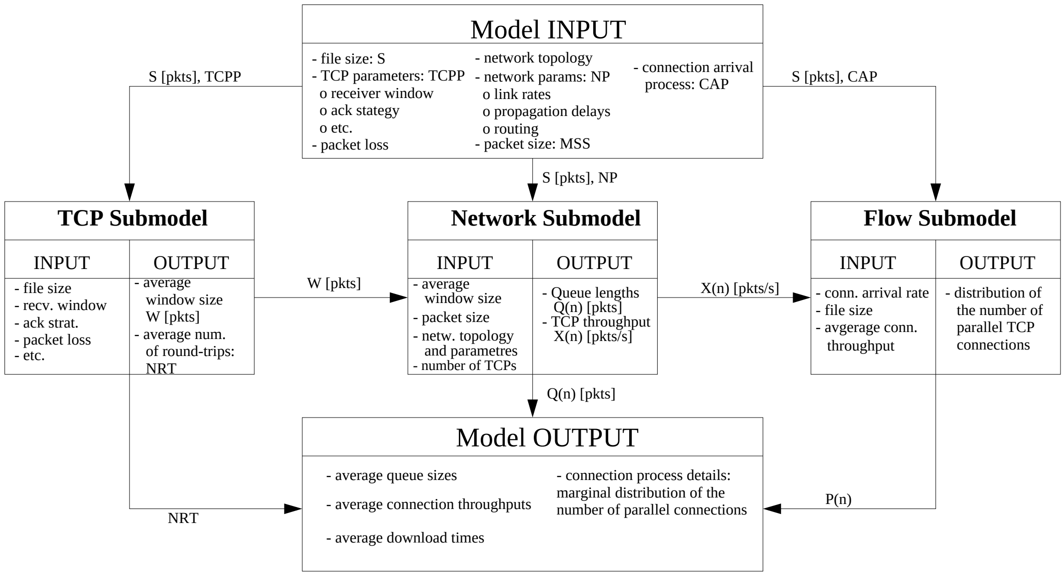

Figure 5.1: The analysis framework

The TCP flavour (and implementation), and the response of the TCP protocol to the packet loss is taken into consideration in the *TCP submodel*, where I use available results for calculating the descriptors of a TCP connection.

The *network submodel* computes the network performance, given an offered load for arbitrary topology. The input of this submodel is the number of packets circulating in the network, the link rates, propagation delays and routing. The outputs are the average queue lengths (in packets) and connection throughputs (in pkts/s) in a closed-loop network with the given parameters. The calculations can be done by using fixed-point iterations (first calculate the round-trip time (RTT) depending on the throughput, second calculate the throughput depending on the RTT), as it is done by Arvidsson and Krzesinski [4]. In order to overcome the drawbacks of the fixed-point method that are related to its convergence properties, I propose to use the analysis of closed-queueing networks by mean-value analysis (MVA). I note that the possibility of using the MVA was already suggested, but Roughan et al. [53] do not pursue this idea further.

The approach can handle theoretically arbitrary topology networks, and is able to obtain not only average performance descriptors, but also more detailed results (e.g. distributions). Nevertheless, I note that a more complex network topology may imply increased computational requirements determined by the MVA solution technique.

The *flow submodel* deals with the dynamics of the network by modelling the constantly changing offered load according to a Markovian process. The input of this model is the connection arrival process, the average file size and the conditional average connection throughputs. The output of the model is the distribution of the number of parallel TCPs. The calculations assume that the number of packets transmitted in a TCP connection has geometric distribution. The arrival of TCP connections into a group – i.e. a set of connections running along the same path in the network – is assumed to be a Poisson process. Although both assumptions seem to be rather restrictive these are not real limitations. The distribution of the file sizes can be generalised to have Phase-type distribution and the arrivals can be generalised to be a MAP. These generalisations can still be fitted into a Markov chain of the flow submodel. I had two main reasons for the assumptions on the file size distribution and arrival process.

- These assumptions made the demonstrative calculations to be much more simple and easy to follow.

- The assumptions were motivated by measurement experience.

The number of groups is the same as the number of paths being actually used in the network. The states of the Markov chain are vectors containing the number of ongoing TCP connections in all possible groups. The comparison is done for 10 input parameter settings resulting in different bottleneck queues in the network.

The analysis framework is tested on an example network with 10 different parameter settings. The results are shown in Table 5.1. The simulated and calculated performance descriptors of interest match each-other with 5% - 15% tolerance.

	Source A	Comm. queue	Source B	RTT A	RTT B	Source A	Comm. queue	Source B	RTT A	RTT B
	Test 1					Test 6				
comp.	8.4	4.2	12.9	1.6	2.3	15.2	3.7	10.9	2.5	2.0
exp.	10.6	2.8	12.3	1.8	2.1	14.7	2.6	12.4	2.4	2.1
real	9.5	0.76	12.9	1.6	2.1	15.0	0.8	12.0	2.3	2.0
	Test 2					Test 7				
comp.	7.0	13.6	8.3	2.1	2.3	25.6	3.5	11.3	3.9	2.0
exp.	9.3	7.8	10.4	2.0	2.2	33.2	2.5	11.5	4.8	2.0
real	9.7	10.0	5.6	2.2	1.8	37.4	0.8	11.4	5.3	1.9
	Test 3					Test 8				
comp.	6.8	22.0	6.7	2.7	2.8	9.0	3.3	20.0	1.7	3.5
exp.	9.4	14.7	9.7	2.5	2.6	10.2	2.4	20.3	1.7	3.5
real	7.8	11.4	10.8	2.1	2.6	10.6	0.8	19.0	1.7	3.2
	Test 4					Test 9				
comp.	6.6	35.0	5.4	3.7	3.6	9.2	3.0	24.6	1.7	4.3
exp.	8.3	25.6	9.0	3.2	3.4	10.3	2.1	25.0	1.7	4.4
real	8.0	25.2	7.8	3.1	3.2	10.6	0.8	35.5	1.7	5.9
	Test 5					Test 10				
comp.	5.35	69.0	3.7	6.2	6.1	9.2	2.8	37.2	1.6	6.6
exp.	8.1	96.7	5.2	8.6	8.3	11.0	2.2	36.7	1.8	6.5
real	6.7	43.8	5.7	4.5	4.4	10.1	0.8	31.5	1.6	5.6

Table 5.1: Comparing computed and simulated average queue lengths (in packets and round-trip times) using the exponential and realistic packet size models

5.3 Discussion

The subject of Thesis 4 is the study of the traffic of the queueing behaviour of a limited number of TCP flows in an access network. I assume that there is a limited effect of individual TCP connections on the packet loss, because as I pointed out in Observation 1, the packet loss rate does not change if the TCP throughputs of a few flows change. Nevertheless, I note that from global network perspective the long-term average packet loss rate changes on a large time-scale, but this is above the coarsest time-scale considered in Thesis 4.

I note in Observation 2 that one TCP connection can have significant effect on the queueing delay in the access network, that is why the round-trip delay is not an external factor for the TCP connections.

In the following I describe my analytic framework (see Figure 5.1). The main performance descriptors of interest here are the average queue lengths and the average round-trip times (RTTs). Application level performance descriptors, like average download time or average throughput, can be obtained directly from the average RTT using recent results, e.g. Alessio et al. [1], Arvidsson and Krzesinski [4], Roughan et al. [53] for short and persistent TCP connections.

As it was described in Thesis 4, the model consists of three submodels, the first of which is responsible for the TCP behaviour, the second one describes the network response and the third one deals with the dynamics in the system on flow level. Next, the three submodels are explained.

TCP submodel

The TCP submodel provides the average offered load to the system, given the RTT, the packet loss probability and other parameters. Several publications revealed that the average window size of a TCP source is proportional to the inverse square root of the loss probability e.g. in Padhye [45]. This *inverse square root law* was first proved for the case, where some restrictive assumptions hold (e.g. low loss rate, persistent sources, neglecting slow-start, etc.). Further research demonstrated that the relaxation of these assumptions makes the exact formula more complex, but the inverse square root law still holds. The appropriate TCP model can be chosen from these results depending on the investigated scenario (e.g. I chose the one developed by Cardwell et al. [17]). The TCP Reno version was used in the analysis and in the simulations.

The application level performance descriptors, like the file download time, can be obtained using the output of the TCP submodel and the average RTT, that is the final output of the present method. The TCP model gives the average number of round-trip times needed to download a file. The average download time is simply the product of the number of round-trip units and the average RTT. Finally, the throughputs of the persitent TCP connections are the side-results of the method.

Network submodel

The *network submodel* consists of a closed-queueing network of IP packets with arbitrary network topology analysed by the MVA (Mean Value Analysis, see Reiser and Lavenberg [51], Lazowska et al. [35]). The motivation why MVA was chosen for the network submodel is that it can model appropriately the self-clocking mechanism of TCP without the need for any fixed-point technique. The MVA method is a finite number of iterations of equations on the average waiting time in queues (average response time), the average throughput and the average queue length. The input of this submodel is the average window size (W [packets]), network parameters and the number of parallel TCP connections. The network submodel computes the conditional average performance descriptors based on the above input parameters.

Denote by n the number of parallel connections in the system. The method below is performed on a set of possible values for n. The number of packets circulating in the closed-loop system is $n \cdot W$ packets. Denote $R_k(n \cdot W)$ the average waiting time upon a packet arrival in queue k. $R_k(n \cdot W)$ is related to the average queue length with one less packet in the system $Q_k(n \cdot W - 1)$. If the service center is not a FIFO queue but a propagation delay, then the response time is simply $R_k(i) = D_k$, where D_k denotes the average delay. (The theoretical explanation can be found e.g. in Reiser and Lavenberg [51].)

$$R_k(n \cdot W) = S_k(1 + Q_k(n \cdot W - 1)), \tag{5.1}$$

where S_k is the average service demand of one packet. If all the average response times are given, then the average throughput $X(i)$ is

$$X(n \cdot W) = \frac{n \cdot W}{\sum_k R_k(n \cdot W)}. \tag{5.2}$$

The average queue lengths can be computed from the average response time and the average throughput by

$$Q_k(n \cdot W) = X(n \cdot W) R_k(n \cdot W). \tag{5.3}$$

If the number of flows is large, then the original MVA method does not scale well. However, there exist approximate MVA algorithms that provide good estimations with significantly reduced computational complexity (see Lazowska et al. [35]).

Since MVA is developed for Jackson networks, this is a limitation of the proposed modelling approach without the need for fixed-point iterations. However, if it turns out that for some reason this limitation is too restrictive to be used for a specific problem, one can substitute MVA with a better suited queueing network model and a fixed-point iteration to control TCP throughput and RTT toghether. For example, according to the TCP, many packets are sent in pairs, triples or even larges batches instead of individual packet emissions. This can happen when TCP's congestion window increases upon the arrival of an acknowledgement, or when the ack covers more than one packet. In this case a general queueing model is beneficial, like the one I have proposed in Chapter 3, where I considered a case of a FIFO queue with considerably general packet arrival (allowing batch arrivals also) and service time distribution.

Flow submodel

My *flow submodel* describes the changing number of TCP connections in progress. The model consists of a Markov chain which is an embedded Markov chain at packet departure instants, where the states are the number of parallel TCPs. It can be seen that being the last packet at a departure instant is an independent event having the same probability for all states ($p = 1 - e^{-1/S}$), if the file size is geometric (with average S packets). The TCP connection arrivals are modelled by the Poisson arrival process, and the expected time between two consecutive packet departures from a certain service point is

$$E(T_n) = \frac{1}{X(n \cdot W)}, \tag{5.4}$$

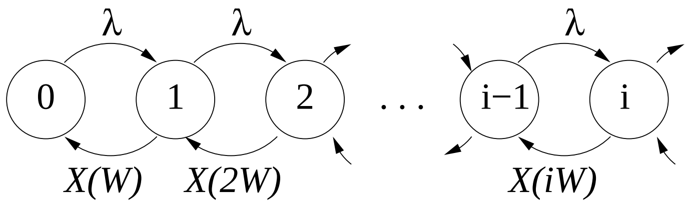

Figure 5.2: The Markov chain describing the flow model

where n is the number of TCPs and $X(n)$ is the conditional average throughput obtained from the network submodel. The probability that j new TCPs arrive given n ongoing TCPs is

$$p(n,j) = \frac{(\lambda E(T_n))^j}{j!} e^{-\lambda E(T_n)}, \tag{5.5}$$

where λ is the connection arrival rate. Figure 5.2 shows the simple Markov chain of my present example. It is shown in Figure 5.2 that the connection departure rates are in fact the TCP throughputs obtained in the network submodel.

Stationary probabilities of the Markov chain can be computed by various Markov chain solution techniques (e.g. Stewart [58]).

I note that the changing number of TCP connections can sometimes be well described by finite or infinite server queueing systems. The customers in this imagined queueing system are the TCP connections and the service is the data transfer through the network. I obtain

- **an infinite server queueing system**, if the probability of keeping any of the links permanently saturated is small, here the system seldom reaches the region where the $X(i \cdot W)$ departure rate approach its maximum,

- **a finite server queueing system**, when the saturation occurs more frequently, and when it occurs, then the TCP throughput $X(i \cdot W)$ equals to the service rate of the bottleneck buffer.

Chapter 3 can be used for solving problems in finite server queueing systems, while in Chapter 4 I propose a Markov chain solution for a class of infinite server systems with correlated customer arrivals in both cases. I note that the correlations in the arrival process makes the infinite server system to be sensitive on the customer holding time distribution, as it is shown in Chapter 4.

Therefore the modelling technique proposed in this chapter can be used in such cases when techniques e.g. in Ben Fredj [21] or Heyman [25] based on the insensitivity are not feasible.

Finally the average queue lengths can be obtained from the conditional averages by taking their weighted sum with the steady-state probabilities as weights.

$$Q_k = \sum_{n=0}^{\infty} Q_k(n) P(n). \tag{5.6}$$

Note that though the properties of the Poisson flow arrival process were used here, there are results e.g. by Nuzman et al. [44] showing that this is not always in line with actual measurements. However, the arrival process can be generalised to a Markov-Modulated Poisson Process by extending the state space of the above Markov chain by taking into consideration the state transitions of the MMPP together with the transitions related to TCP arrivals/departures.

The validation of the analytical results was done by simulations of the example network. The simulation tool was the IP version of the Plasma platform (Planning Algorithms and Simulation for Network Management, for details see Haraszti et al. [24]). Plasma IP is a packet-level simulation tool including an implementation of the the Reno version of the TCP protocol, developed by the HSN Lab at Budapest University of Technology and Economics and Ericsson Traffic Lab.

The topology in my example network contains three FIFO queues and a packet delay. There are two traffic flows shaped by queue A and B, and multiplexed in a common queue (see Figure 5.3). The TCP connections arrive and depart randomly, so the number of parallel TCP connections changes over the time.

The traffic flows contain two types of TCP transfers, where the connections of the same type have common sources and destinations. The goal of the proposed method is to predict the average queue lengths and average packet round-trip times that develop in the IP network.

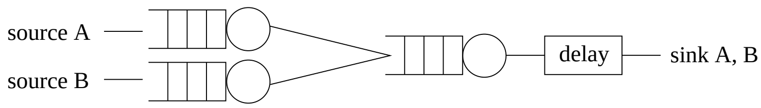

Figure 5.3: Network topology example

The connection arrival intensities and the average file sizes are different for flows A and B. The connection arrival process is a Poisson process in the present network example. Although there are results showing that the Poisson model for connection-level arrival process is not always appropriate, see e.g. Nuzman [44]. This was used for the sake of computational simplicity, nevertheless this is not a critical assumption, as it was discussed in the network submodel. The file sizes are assumed to be exponential. Contrary to the fact that a number of papers showed that these distributions have heavy-tails, see e.g. Paxson [47], my modelling approach is that the body of a file size distribution can be approximated by the mixture of exponential distributions. In fact, by using the mixture of exponential distributions, even a polynomial decrease can be followed by several orders of magnitude. On the other hand, and the files in the far end tail (the extremely large files) can be simply considered as persistent file transfers.

The simulations were repeated with different server utilisation levels. The parameters of the investigated network were the following:

- The bandwidth of the common link was 144 x 1/utilisation kbps[1], the bandwidth of

[1]For example, in the case of 0.63, 0.73, 0.64 server utilisations, the corresponding link rates were 230, 110, 100 kbps.

source A's link was 80 x 1/util. kbps, and the bandwidth of source B's link was 64 x 1/util. kbps,

- 0.5 s fixed packet delay,
- the packet size was 1500 bytes,
- the agent used TCP Reno with 10 packets receiver window. No Nagle algorithm and no delayed acknowledgement were used.

The average file sizes in flows A and B were 20 and 40 kbyte, respectively. The offered load of the TCP traffic was generated with Poisson connection arrivals. The resulting offered rates were 80 and 64 kbps.

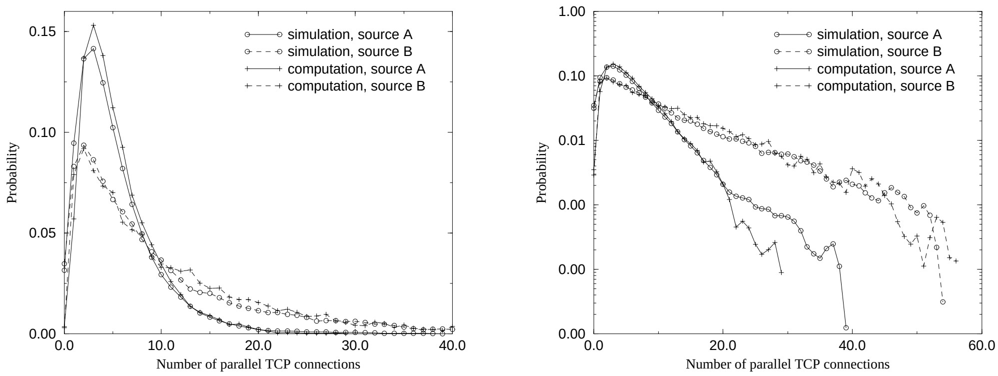

Figure 5.4: The distributions of the number of parallel TCP connections (lin-lin and lin-log scale)

Figure 5.4 shows the distributions of the number of parallel TCP connections according to the equilibrium distribution of the Markov chain of the flow submodel. A good agreement can be observed in Figure 5.4 between the distributions computed by my method and the distributions obtained from the simulations.

To give a more comprehensive validation, two performance descriptors were computed and logged in simulations in 10 test cases:

- the packet round-trip delays on the routes of the two source-sink pairs (route A and B),
- the file download times of the files transmitted between the source-sink pairs.

Table 5.2 shows the parameter set on which the comparison was done. Table 5.1 compares the average queue lengths and round-trip time results from computations and simulations. Table 5.3 compares the computed average download times and the results of the simulations. The reason for not testing the framework for higher utilisation levels is twofold. On one hand, the operating region of the utilisation of a "healthy" network rarely goes above 90%. On the other hand, both the TCP submodel and the network submodel assumes "averge behaviour" in the sense, that second order effects due to the heavy load are not considered.

Test	1	2	3	4	5	6	7	8	9	10
Utilisation in queue A	0.73	0.73	0.73	0.73	0.73	0.80	0.85	0.73	0.73	0.73
Utilisation in queue B	0.64	0.64	0.64	0.64	0.64	0.64	0.64	0.75	0.80	0.85
Utilisation in queue AB	0.63	0.75	0.80	0.85	0.90	0.63	0.63	0.63	0.63	0.63

Table 5.2: The utilisations in the three servers in 10 test cases

The download times in Table 5.3 are computed by two different ways:

- the average round-trip times were multiplied by the average download time in round-trip units: $T_d^{A,B}$ in Table 5.3,
- the average download times were also logged directly in the simulations: $\widehat{T}_d^{A,B}$.

	T_d^A [s]	$\widehat{T}_d^A$ [s]	Err. +/- [s]	T_d^B [s]	$\widehat{T}_d^B$ [s]	Err. +/- [s]	T_d^A [s]	$\widehat{T}_d^A$ [s]	Err. +/- [s]	T_d^B [s]	$\widehat{T}_d^B$ [s]	Err. +/- [s]
Test 1							Test 6					
calc.	9.3	-	-	15.2	-	-	14.5	-	-	13.2	-	-
exp	10.4	10.3	0.1	13.9	16.3	0.3	13.9	14.3	0.1	13.9	13.9	0.2
det	9.3	10.7	0.2	13.9	15.0	0.3	13.3	13.3	0.2	13.2	13.9	0.3
Test 2							Test 7					
calc.	12.1	-	-	15.2	-	-	22.5	-	-	13.2	-	-
exp	11.6	13.5	0.1	14.5	16.2	0.2	27.7	26.5	0.3	13.2	14.8	0.2
det	12.7	11.5	0.1	11.9	14.3	0.2	30.6	27.7	0.5	12.5	14.3	0.2
Test 3							Test 8					
calc.	15.6	-	-	18.5	-	-	9.8	-	-	23.1	-	-
exp	14.5	13.5	0.1	17.2	14.9	0.2	9.8	10.7	0.1	23.1	22.6	0.4
det	12.1	15.9	0.2	17.2	22.2	0.4	9.8	10.6	0.1	21.1	26.5	0.5
Test 4							Test 9					
calc.	21.4	-	-	21.4	-	-	9.8	-	-	28.4	-	-
exp	18.5	20.5	0.2	22.4	26.0	0.5	9.8	11.6	0.1	29.0	29.9	0.5
det	17.9	18.2	0.2	17.9	23.0	0.4	9.8	11.1	0.1	38.9	27.8	0.5
Test 5							Test 10					
calc.	35.8	-	-	40.3	-	-	9.3	-	-	43.6	-	-
exp	49.7	44.1	0.5	54.8	55.5	1.0	10.4	10.5	0.1	42.9	54.3	1.0
det	26.0	30.4	0.3	29.0	39.4	0.7	9.3	9.8	0.1	37.0	33.8	0.6

Table 5.3: Comparison of the computed and simulated average download times in seconds. The column "Err." shows the 95% confindence interval of the simulation statistics expressed in seconds

Two different models were used in the simulations. The first one assumes exponential packet sizes (the model is strongly related to a BCMP-type network). The second case uses the packet sizes determined by the TCP stack. It can be seen that the computations well approximate the exponential model. The last columns of the tables show the average round-trip times. The simulated queue lengths were sampled in equal time intervals.

Larger differences occur when the utilisation becomes large on the links, which might be due to the high variance of the queue length and TCP effects (e.g. repeated retransmission timeout events). These effects were not studied in detail, as my scope was to investigate the ordinary TCP behaviour. The average round-trip time predictions therefore estimate the simulated averages with mostly less than 5 %-15 % error.

5.4 Notes

Mean-Value Analysis (Reiser and Lavenberg [51]) is a numerical method that provides exact solution for product-form closed-loop packet switched networks. In Section 5.4, I show that IP networks, where the TCP generates traffic, can be modelled as closed-loop networks.

Consider a network with persistent TCP connections with small receiver window sizes and assume that there is no random packet loss in the system. After a short initial transient, the congestion windows (cwnd) of all TCP connections reach their limit. The number of circulating packets will stay fixed due to the self-clocking mechanism. If I assume additionally that the packet sizes are exponentially distributed, then I obtain a product-form closed-queueing network.

These assumptions can be relaxed without seriously degrading the quality of the MVA approximation:

- If the exponential assumption on the packet size can be generalised to a bounded packet size distribution, the predictions of MVA will be mostly pessimistic. This is because of the small coefficent of variance of the bounded distributions that implies smaller average queue lengths.

- If packet loss is introduced, then the cwnds of the individual TCPs will fluctuate around their expected value, which can be computed by the *inverse square root law* of Padhye et al. [45]. The lost packets can be included in the MVA method as packets that are delayed until their retransmission. This involves an “artificial” service center only. The system is approximated assuming a fixed $E(N)$ number of packets. In reality, the cases when $N < E(N)$ are balanced by the cases when $N > E(N)$.

- The assumption on persistent connections can be relaxed to randomly arriving and departing connections, similarly to the previous step. The high variation in the number of packets in the system is decreased by conditioning on the number of parallel connections, which is handled as a random process. Then the system is analysed in each case, given the same number of connections when the number of packets is almost the same.

Chapter 6

Extension of results: the critical time-scale

One of my research experiences so far is that if a model yearns for a broad scope and exact description at the same time then the price it has to pay is its analytical and/or numerical complexity. In my opinion, it is generally better to direct the modelling efforts towards breaking down a difficult problem into simple parts instead of trying to establish a single and general model. As an application of my results, this section demonstrates this principle in the case of traffic modelling.

The application example of Thesis 3 shows two MAP/G/∞ queueing systems. The difference between the two systems is the arrival model. In one case, the correlations in the arrival process are in the order of the holding time, while in the other case changes in the arrival process occur seldom compared to the holding time. This difference is reflected in the distribution of the number of customers. When the changes are slow, the distribution looks like it was obtained by the mixture of two distributions as I show in Section 6.1.

In Thesis 4, I show a case study where the performance of a TCP/IP traffic scenario is approximated by numerical calculations using simple queueing models. A few performance descriptors of the example scenario are obtained from repeated simulations where the parameters of the TCP/IP traffic are varied. The quality of the approximation is evaluated by comparing the simulated performance descriptors to their predictions. I think the promising results of the validation are not just because of the providential choice of the network scenario. In Section 6.2, I discuss when and why good quality approximations made by the modelling framework of Thesis 4 can be expected.

In fact, the discussions both in Section 6.1 and Section 6.2 are based on the fact that effects can be found that operate on different time-scales and these can be analysed independently of each other. The significance of the time-scale where a queueing model operates has been recognised, and the term "critical time-scale" has been introduced by Ryu et al. in [54]. They argue that in finite single server queueing systems the correlation in the arrival process (e.g. packets, cells arrival) is important in the time-scale of queueing and the correlation above this time-scale does not affect the network performance significantly.

The concept of critical time-scale has been extended to infinite server queueing systems by Grossglauser [23] in a measurement-based admission control context. In that paper Grossglauser argues that a measurement-based admission control algorithm could take into consideration slow changes in the traffic, while fast changes can be dealt with using overprovisioning. In an infinite server system the time-scale of interest is a function of the holding time of the customers.

In Section 6.1 the critical time-scale is determined by the call holding time distribution while in Section 6.2 the critical time-scale is determined by the distribution of the queue length and the service time.

If the range of the correlations exceeds the critical time-scale, a quasi stationary equilibrium develops in the queueing systems. This quasi stationary equilibrium changes slowly following the change on the coarser time-scales. It depends on short-range effects only, therefore it can be calculated using the solution methods of Thesis 3 in the case of MAP/G/∞ systems and MVA, or Thesis 2 in the case of access buffers. The "global" stationary equilibrium is obtained as a probability mixture of the "local" quasi stationary equilibria.

6.1 Critical time-scale in a MAP/G/∞ system

The concept of the critical time-scale is presented via two example network scenarios. In the examples, the arrival process is a variable rate Poisson process. Both examples model a system, where voice (video, etc.) calls are routed through an egress node. The arrival of the calls is modulated by some external effects.

It will be shown that if the time-scale of the call arrival rate change is below the holding time of the calls, the correlations should be taken into consideration, i.e., the system cannot be decomposed into subsystems. However, if the routing changes happen above the range of call durations, the system can be approximated by a mixture of subsystems with tolerable approximation error. Moreover, it will be shown that the distribution of the call holding time changes the critical time-scale.

The first example is a multiservice system focusing on the traffic of voice calls. Normally, all calls are allowed and routed towards a switch, but sometimes a few new calls are allowed and the others are blocked. The decision is made in a filter depending on the available resources to set up new calls. An assumption here is that the resources available for the call setup are independent of the number of ongoing calls. The time-scale of the decision changes is assumed to be in the order of a few seconds at most.

In the second example, two areas are interconnected via a microwave link that transmits the calls. However, this microwave link might become unavailable due to environmental conditions in which case a backup satellite link is used. The gray arrow represents this link in Figure 6.1. The calls are rerouted to the satellite link, but only a few new call setups are allowed. In this case, the time-scale of interest can be in the order of 100s-1000s of seconds. In fact, the proposed model here is the same, but the parameters are, of course, different.

Figure 6.1 shows the structure of the call arrivals. The calls from Area A always arrive to the switch according to a constant rate Poisson process. Area B also generates calls according to a constant rate Poisson process, but these calls are occasionally blocked by the filter. The blocking decision is modelled by a two-state Markov chain representing the admission and blocking decisions (see Figure 6.2). The arrival rate from Area A is $\lambda_A = 0.1\ 1/s$ and from Area B is $\lambda_B = 9.9\ 1/s$. The mean call holding time is $E(X) = 100s$.

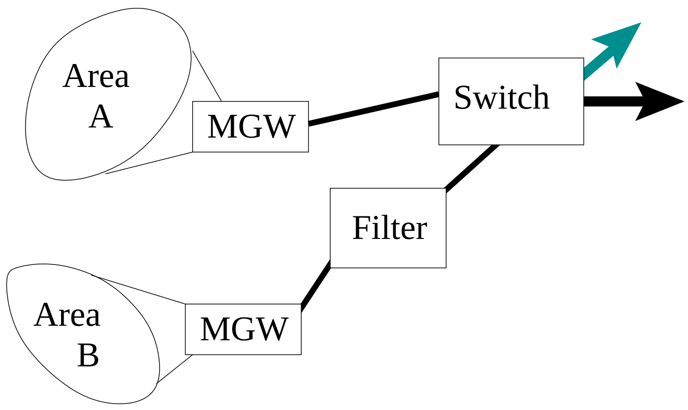

Figure 6.1: The routes of the calls in the two examples

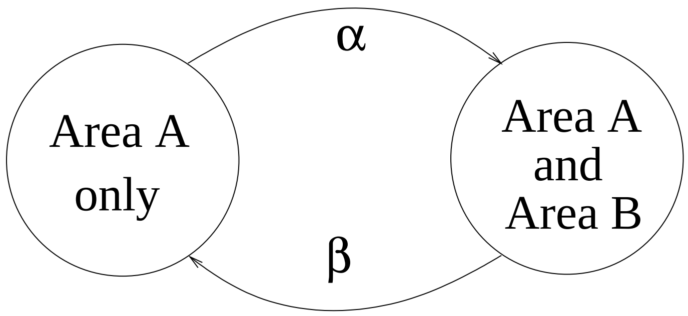

Figure 6.2: The routed areas to Egress node 1 in the different MMPP states

6.1.1 Hyper-exponential service time distribution

The holding time of the calls is hyper-exponentially distributed with cdf:

$$F(x) = 1 - \gamma_1 e^{-\mu_1} - \gamma_2 e^{-\mu_2},$$

where $1/\mu_1 = 50s$, $\gamma_1 = 0.947$, $1/\mu_2 = 1000s$, $\gamma_1 = 0.053$. The results shown in Figures 6.3 a), b), c) and d) are calculated by the numerical method of Thesis 3. The figures show the stationary probability distributions of the number of calls in the system. The holding times of the two-state Markov chain representing the filtering decisions varied from $1/\beta = 1s$ to $10000s$ when both areas access the switch and $1/\alpha = 1.5s$ to $15000s$ when only Area A can access the switch. When the arrival rate changes very frequently, i.e. in the order of seconds, see Figure 6.3 a), the range of correlations of the

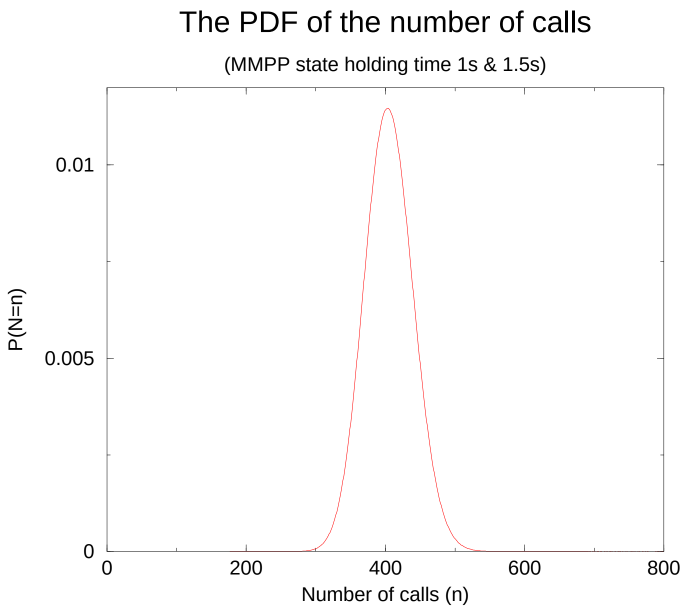

$(1/\beta = 1s, 1/\alpha = 1.5s)$

Figure 6.3: a) The distribution of the number of calls with different parameters

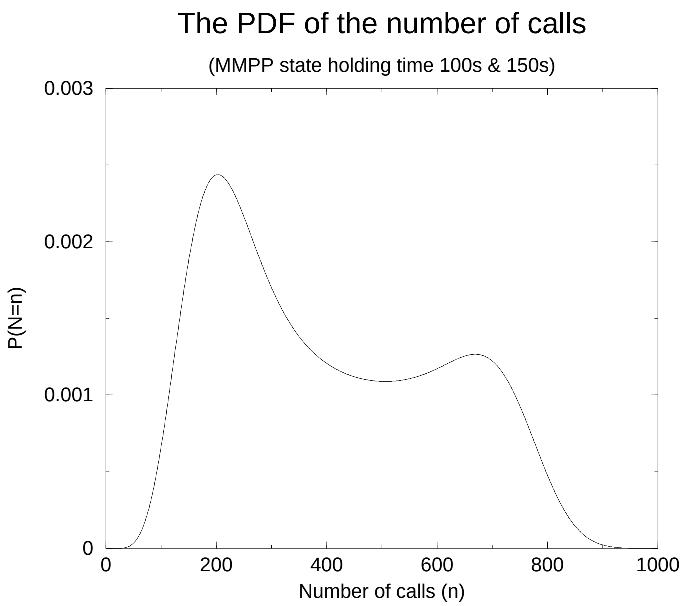

$(1/\beta = 100s, 1/\alpha = 150s)$

Figure 6.3: b) The distribution of the number of calls with different parameters

arrival process is very short and a unimodal distribution develops. The arrival process as well as the distribution of customers are not Poisson, but as the frequency of routing changes increases to infinity, the resulting arrival process and the distribution of customers tend to Poisson.

As the rate changes become less frequent, see Figure 6.3 b) and c), the correlations of

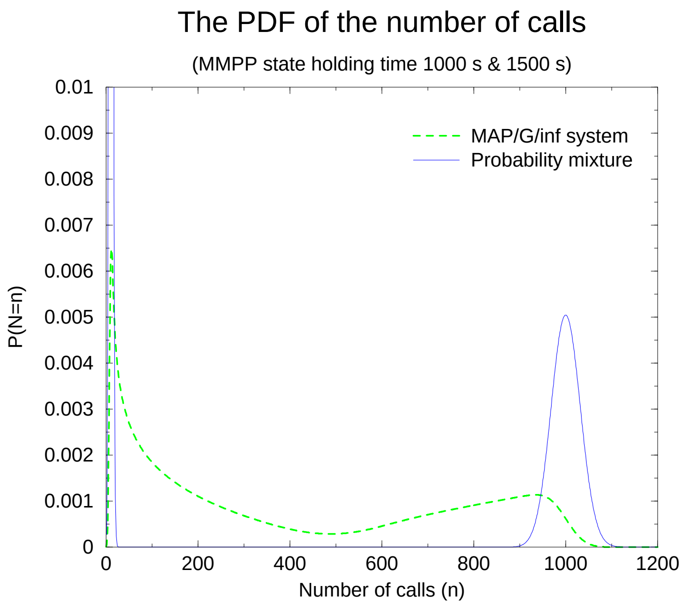

$(1/\beta = 1000s, 1/\alpha = 1500s)$

Figure 6.3: c) The distribution of the number of calls with different parameters

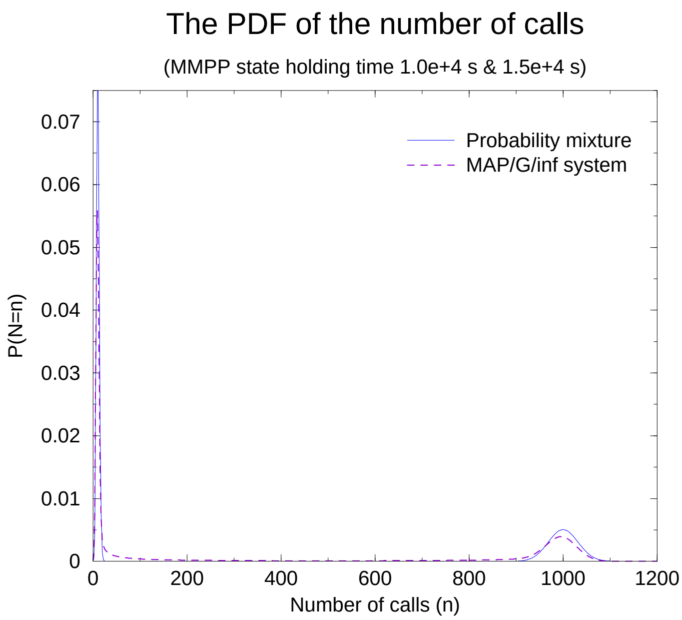

$(1/\beta = 10000s, 1/\alpha = 15000s)$

Figure 6.3: d) The distribution of the number of calls with different parameters

the arrival process start to have effects, and a bi-modal distribution develops.

When the correlations are in the order of the holding time of the calls (the average is $100s$ with a $1000s$ component in the hyper-exponential distribution), it would lead to significant errors if this system was approximated by two independent subsystems: one where the calls arrive only from Area A, and one where the calls arrive both from Area A and Area B. This error is represented in Figure 6.3 c), where the resulting bi-modal distribution is compared with the mixture of two Poisson distributions obtained by the analysis of the two subsystems (which are M/G/∞ queues in this case). In these scenarios one should care the correlations in the arrival process.

Figure 6.3 d) shows a scenario in which the range of the correlations is well above the range of the call holding time: $1/\beta = 10000s, 1/\alpha = 15000s$. The distribution can indeed be separated into two components, which come from two M/G/∞ subsystems with Poisson arrival processes with rates $\lambda_A = 0.1\ 1/s$ and $\lambda_A + \lambda_B = 10\ 1/s$.

My conclusion from these examples is that in infinite server queues the long-range correlation of the arrival process needs not necessarily be considered. It is enough to substitute the model with long-range dependence with subsystems having only short-range dependence, which can be described by smaller MAP/G/∞ models and the final result can be obtained as the probability mixture of the subsystems' distribution.

6.2 Critical time-scale in a closed-queueing system

It was shown by Ryu et al. in [54] that the critical time-scale in a finite single server queueing system is approximately the size of the buffer multiplied by the service time, that is, the maximum queueing delay.

In my examples the buffers are assumed to be large in order to avoid packet loss in the access network, but due to the closed-loop nature of TCP and the limited level of aggregation, the variation in the number of packets in the buffers cannot be arbitrarly large. That is, the concepts of Ryu [54] can be applied.

The following simulated network example consists of a FIFO queue, random packet drop and a packet delay object. The TCP connections arrive according to a Poisson process with rate 0.2 1/s and the size of the transmitted data is exponential with the mean of 40 kbyte. The link rate is 100 kbps, therefore the long-term average link utilisation is 0.64. The packet delay is 0.5s and the Maximum Transmission Unit (MTU) is 1500 bytes.

The range of the queueing delay is 2.25s with 150 packets in the queue, that is, approximately this is the critical time-scale. Since the arrival rate of the TCP connections is 0.2 1/s, the average time between the arrival of two TCP connections is 5s.

The average time between the arrival of two TCP connections is larger than the critical time-scale of the system, therefore the number of TCP connections change slowly compared to the time-scale of queueing in the FIFO queue.

Using the TCP submodel of Thesis 4, the average size of the congestion window is obtained (it is 5.4 packets per connection). The network is analysed by MVA, which analysis is repeated 45 times using different number of packets. On the other hand, the queue length and the number of TCP connections were sampled in the simulation experiment. A series of conditional averages of the queue length was computed given the number of ongoing TCP connections. Figure 6.4 compares the results[1] of the average queue lengths provided by the MVA and the experimental series. Since the MVA computes not only the average queue length but also the average throughput, the experiment

[1]The number of packets can be calculated as 5.4 times the number of TCP flows in Figure 6.4.

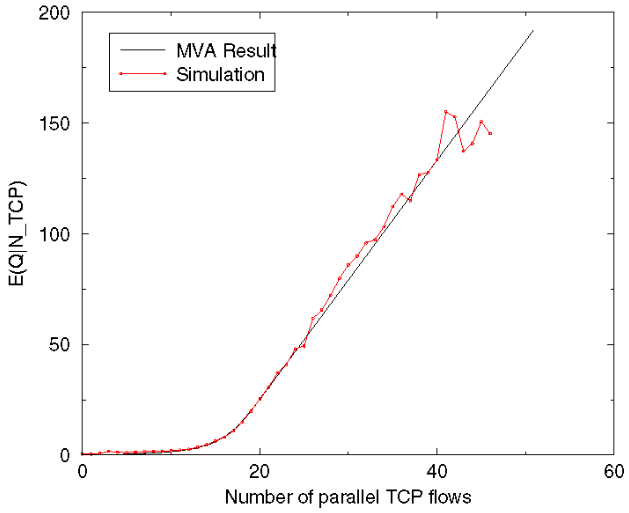

Figure 6.4: Conditional average queue length in simulation and computed by MVA

was repeated with the throughput samples. The same level of agreement is found for the average utilisations and throughputs like the one we can see in Figure 6.4, therefore it is omitted.

Though the values of the queueing delay and TCP connection arrival rate change from one network scenario to another, the ratio between the queueing delay and the average connection interarrival time remain if a moderate long-term average link utilisation is assumed. Therefore, in these cases the correlations in the packet arrival process due to the changing number of TCP connections can be neglected in the calculation of a quasi stationary equilibrium. The quality of the performance predictions in these cases relies on the quality of the approximations of the packet level queueing models of the traffic of a fixed number of TCP connections.

Chapter 7

Bibliography

[1] E. Alessio, M. Garetto, R. Lo Cigno, M. Meo, M. Ajmone Marsan, *Analytical Estimation of Completion Times of Mixed NewReno and Tahoe TCP Connections over Single and Multiple Bottleneck Networks*, Proceedings of IEEE Globecom 2001, San Antonio, Texas, USA, 2001.

[2] J. Andrén, M. Hilding, D. Veitch, *Understanding End-to-End Internet Traffic Dynamics*, Globecom'98, Sydney, v. 2, pp.1118-1122, 1998.

[3] A. Arvidsson and P. Karlsson, *On traffic models for TCP/IP*, Proceedings of ITC16, Edinburgh, U.K., 1999.

[4] A. Arvidsson, A. Krzesinski, *A Model of a TCP Link*, Proceedings of 15th ITC Specialist Seminar, Internet Traffic Engineering and Traffic Management, Wuerzburg, Germany 2002.

[5] S. Asmussen, G. Koole, *Marked Point Processes as Limits of Markovian Arrival Streams*, Journal of Applied Probability, v. 30, pp. 365-372, 1993.

[6] Dieter Baum, *Convolution Algorithms for BMAP/G/1-Queues*, Universität Trier, Mathematik/Informatik, Forschungsbericht 96-22, 1996.

[7] C. Barakat, P. Thiran, G. Iannaccone, C. Diot, P. Owezarski, *A flow-based model for Internet backbone traffic*, IMW '02: Proceedings of the 2nd ACM SIGCOMM Workshop on Internet measurement, 2002.

[8] V. Benes, *General Stochastic Processes in the Theory of Queues*, Addison-Wesley, Reading, MA, 1963.

[9] D. A. Bini, B. Meini, *Using displacement structure for solving Non-Skip-Free M/G/1 type Markov chains. In Advances in Matrix Analytic Methods for Stochastic Models*, Proceedings of the 2nd international conference on Matrix Analytic Methods, pp. 17-37, Notable Publications Inc., 1998.

[10] D. A. Bini, G. Latouche, B. Meini, *Numerical Solution for Structured Markov Chains*, Oxford University Press, Clarendon, 2005.

[11] J. Bolot, *Characterizing End-to-End Packet Delay and Loss in the Internet*, Journal of High-Speed Networks, v. 2, no. 3, pp. 305-323, 1993.

[12] M. S. Borella, S. Uludag, G. B. Brewster, I. Sidhu, *Self-Similarity of Internet Packet Delay*, ICC'97, pp. 513-517, 1997.

[13] M. S. Borella, G. B. Brewster, *Measurement and analysis of long-range dependent behavior of internet packet delay*, in Proceedings of IEEE INFOCOM, v. 2, pp. 497-504, 1998.

[14] T. Bu, D. Towsley, *Fixed Point Approximations for TCP Behaviour in AQM Network*, Proc. of ACM SIGMETRICS, June 16-20, Cambridge, USA, 2001.

[15] J. Cao, W. S. Cleveland, D. Lin, D. X. Sun, *On the Nonstationarity of Internet Traffic*, ACM SIGMETRICS Performance Evaluation Review, v. 29, n.1, p.102-112, June 2001.

[16] J. Cao, K. Ramanan, *A Poisson Limit for Buffer Overflow Probabilities*, Proceedings of IEEE Infocom, 2002.

[17] N. Cardwell, S. Savage, T. Anderson, *Modeling TCP Latency*, Proceedings of Infocom 2000, Tel-Aviv, Israel, 2000.

[18] M. Csörgő, L. Horváth, *Invariance Principles for Changepoint Problems*, Journal of Multivariate Analysis, 27, pp. 151-168., 1988

[19] D. J. Daley, D. Vere-Jones, *An Introduction to the Theory of Point Processes*, Springer-Verlag, New York, 1988.

[20] K. Fall, S. Floyd, *Simulation-based Comparisons of Tahoe, Reno, and SACK TCP*, Computer Communications Review, 1996.

[21] S. Ben Fredj, T. Bonalds, A. Prutiere, G. Gegnie, J. Roberts, *Statistical bandwidth sharing: a study of congestion at Flow level*, In Proceedings of ACM SIGCOMM 2001, San Diego, California, USA, 2001.

[22] M. Garetto, R. Lo Cigno, M. Meo, M. A. Marsan, *A Detailed and Accurate Closed Queuing Network Model of Many Interacting TCP Flows*, Proceedings of Infocom 2001, Anchorage, Alaska, USA, April 22-26, 2001.

[23] M. Grossglauser, *A Time-scale Decomposition Approach to Measurement-based Admission Control*, IEEE/ACM Transaction on Networking, v. 11/4, 2003.

[24] Z. Haraszti, I. Dahlqvist, A. Faragó, T. Henk, *PLASMA - A Tool for ATM Network Operations*, Proceedings of the 15th International Switching Symposium (ISS), Berlin, 1995.

[25] D. P. Heyman, T. V. Lakshman, A. L. Neidhardt, *A new method for analysing feedback-based protocols with applications to engineering Web traffic over the Internet*, ACM Sigmetrics 1997, Seattle, Washington, USA, 1997.

[26] A. Horváth and M. Telek, *Approximating Heavy Tailed Behaviour with Phase Type Distributions*, Advances in algorithmic methods for stochastic models, MAM3, (G. Latouche and P. Taylor, eds.), pp. 191-214, Notable Publications Inc., 2000.

[27] P. E. Jackson, C. D. Stubbs, *A Study of Multiaccess Computer Communications*, Proceedings of the Spring 1969 AFIPS Conference, v. 34, 1969.

[28] A. Kantawala, J. Turner, *Queue Management for Short-Lived TCP Flows in Backbone Routers*, High Speed Symposium, IEEE Globecom, Taipei, Taiwan, 2002.

[29] M. F. T. Karagiannis, M. Molle, A. Broido, *A Nonstationary Poisson View of Internet Traffic*, Proceedings of IEEE INFOCOM, 2004.

[30] D. G. Kendall, *Stochastic Process occurring in the theory of queues and their analysis by the method of imbedded Markov Chain*, Annals of Mathematical Statistics 24, 338-354, 1953.

[31] M. Kendall, A. Stewart, *The Advanced Theory of Statistics*, Charles Griffin London, 1966.

[32] R. El Abdouni Khayari, R. Sadre, B. R. Haverkort, *A Validation of the Pseudo Self-Similar Traffic Model*, International Conference on Dependable Systems and Networks (DSN'02), June, Washington D.C., USA, 2002.

[33] L. Kleinrock, *Queueing Systems*, v. 1-2. Theory, Wiley Interscience, New York, 1975-1976.

[34] G. Latouche, V. Ramaswami, *Introduction to Matrix-Analytic Methods in Stochastic Modeling*. Series on Statistics and Applied Probability, ASA-SIAM, 1999.

[35] E. D. Lazowska, J. Zahorjan, G. S. Graham, K. C. Sevcik, *Quantitative System Performance Computer System Analysis Using Queueing Network Models*, Prentice-Hall, Inc., 1984.

[36] D. V. Lindley, *The Theory of Queues with a Single Server*, Proceedings of the Cambridge Philosophical Society, v. 48, pp. 277-289, 1952.

[37] J. D. C. Little, *A Proof for the Queuing Formula: L=lW*, Operations Research, 9, Is. 3, pp. 383-387, 1961.

[38] L. Liu, J. G. C. Templeton, *The* $GR^{X_n}/G_n/\infty$ *system: system size*, Queueing Systems 8, 323-356, 1991.

[39] H. Masuyama, T. Takine, *Analysis of an Infinite-Server Queue with Batch Markovian Arrival Streams*, Queueing Systems, v. 42, no.3, pp. 269-296, 2002.

[40] M. Mathis, J. Semke, J. Mahdavi, T. Ott. *The Macroscopic Behaviour of the TCP Congestion Avoidance Algorithm*, Computer Communication Review, v. 27, pp. 67-82, 1997.

[41] B. Meini, *Solving M/G/1 type Markov Chains: Recent Advances and Applications*, Comm. Statist. Stochastic Models, 14, pp. 479-496, 1998.

[42] M.F. Neuts, *Matrix Geometric Solutions in Stochastic Models*, Johns Hopkins University Press, Baltimore, 1981.

[43] M.F. Neuts, *Structured Stochastic Matrices of M/G/1 Type and their Applications*, Marcel Dekker, 1989.

[44] C. Nuzman, W. Sweldens, A. Weiss, *A Compound Model for TCP Connection Arrivals: Empirical Study with a General Framework*, Proceedings of ITC 2001, Brazil, 2001.

[45] J. Padhye, V. Firoiu, D. Towsley, J. Kurose, *Modeling TCP throughput: A Simple Model and its Empirical Validation*, ACM Computer Communication Review, 28(4), pp. 303-314, 1998.

[46] E. Parzen, *Nonparametric Statistical Data Modeling*, Journal of the American Statistical Association, pp. 105-126, 1979.

[47] V. Paxson, S. Floyd, *Wide-area traffic: The failure of Poisson modeling*, IEEE/ACM Transaction on Networking, 3(3), pp. 226-255, 1995.

[48] V. Paxson, S. Floyd, *Why We Don't Know How to Simulate the Internet?*, Winter Simulation Conference, 1997.

[49] S. Rácz, A. Tari, M. Telek, *A Moment-based Distribution Bounding Method*, Computers and Mathematics with Applications, 2005.

[50] V. Ramaswami, M. Neuts, *Some Explicit Formulas and Computational Methods for Infinite-server Queues with Phase-type Arrival*, Journal of Applied Probability, v. 17, pp. 498-514, 1980.

[51] M. Reiser, S. S. Lavenberg, *Mean-Value Analysis of Closed Multichain Queueing Networks*, Journal of the ACM, v. 27, no. 2, pp. 313-322, 1980.

[52] A. Riska, E. Smirni, *Exact Aggregate Solutions for M/G/1-type Markov Processes*, Proceedings of ACM SIGMETRICS'02, pp. 86-89, Marina Del Rey, CA, 2002.

[53] M. Roughan, A. Erramilli, D. Veitch, *Network Performance for TCP Networks Part I: Persistent Sources*, Proceedings of ITC'17, Brasil, 2001.

[54] B. K. Ryu, A. Elwalid, *The Importance of Long-range Dependence of VBR Video Traffic in ATM Traffic Engineering: Myths and Realities*, SIGCOMM'96, 1996.

[55] D. Sanghi, A. K. Agrawala, O. Gudmundsson, B. N. Jain, *Experimental Assessment of End-to-end Behaviour on Internet*, INFOCOM'93, 1993.

[56] W. R. Stevens, *TCP/IP Illustrated*, Volume 1, Addison-Wesley, 1995.

[57] W. Smith, *On the Distribution of Queueing Times*, Proceedings of the Cambridge Philosophical Society, v. 49, pp. 449-461, 1953.

[58] W. J. Stewart, *Introduction to the Numerical Solution of Markov Chains*, Princeton University Press, 1994.

[59] L. Takács, *On Erlang's formula*, Annals of Mathematical Statistics, v. 40, pp. 71-78, 1969.

[60] K. Thompson, G. J. Miller, R. Wilder, *Wide-Area Internet Traffic Patterns and Characteristics*, IEEE Network, November-December, 1997.

[61] A. De Vendictis, A. Baiocchi, A. Monticelli, *Simple Models and their Limits for TCP/IP Network Analysis and Dimensioning*, in Proc. of IEEE ICC2002, 2002.

[62] A. Veres, Zs. Kenesi, S. Molnár, G. Vattay, *On the Propagation of Long-Range Dependence in the Internet*, ACM Computer Communication Review, v. 30, No.4, pp. 243-254, October, 2000.

[63] R. W. Wolff, *Poisson Arrivals See Time Averages*, Operations Research, v. 30, pp. 223-231, 1982.

[64] G. Wolfner and M. Telek, *Analysis of Queues with Batch Arrivals*, Performance Evaluation, v. 41, pp. 179-194, 2000.

Publications

Journal papers

[J1] G. Seres, T. Éltető, A. Oláh, *Measurement-based Simulation Model for TCP over ATM*, Annals of Telecommunications, pp. 278-287, no. 5-6, 2000.

[J2] T. Éltető, M. Telek, *Numerical analysis of M/G/1 type queueing systems with Phase type transition structure*, Journal of Computational and Applied Mathematics, submitted to publication, 2005.

[J3] T. Éltető, *Why certain discrete phase type representations have numerically stable spectral decomposition?*, Periodica Mathematica Hungarica, accepted to publication, 2006.

Conference and workshop papers

[C1] T. Éltető, S. Molnár, *On the Distribution of Round-trip Delays in TCP/IP Networks*, LCN'99, Boston, MA, USA, 1999.

[C2] A. Vidács, J. Barta, Zs. Kenesi, T. Éltető, *Measurement-Based WWW User Traffic Model for Radio Access Networks*, 7th International Workshop on Mobile Multimedia Communications (MoMuC2000), Tokyo, Japan, 2000.

[C3] T. Éltető, P. Benkő, *Measurement-based TCP Models*, LCN'00, Tampa, FL, USA, 2000.

[C4] T. Éltető, P. Vaderna, S. Molnár, *Performance Analysis of TCP Networks Loaded by Web Traffic*, ITC'18, Berlin, Germany, 2003.

[C5] P. Vaderna, E. Stromberg, T. Éltető, *Modelling Performance of HTTP/1.1*, GLOBECOM'03, San Francisco, CA, 2003.

[C6] T. Éltető, M. Telek, *Numerical Analysis of Infinite Server Queues with Correlated Arrivals* ITC'19, Beijing, China, 2005.

[C7] P. Vaderna, T. Éltető, *Transient Analysis of a Queuing System with Matrix-Geometric Methods*, NEW2AN'06, Sankt Petersburg, Russia, 2006.

Other

[O1] T. Éltető, M. Telek, *Batch Markov Arrival Process with Phase-type Distributed Batch Size*, `http:\\www.cs.bme.hu\˜eltetot`